

ABSTRACT

Title of Document: BIOMETHANOL CONVERSION FROM SUGAR BEET PULP

Quanzeng Wang, Master of Science, 2006

Directed By: Professor Nam Sun Wang, Dept. of Chemical & Biomolecular Engineering

Conversion of renewable biomethanol was studied from sugar beet pulp with pectin methyl esterases (PMEs). An analytical method for methanol and PME activity was developed based on potassium permanganate assay. Results showed that this method was sensitive, accurate and stable. Two PMEs, natural and mutated, were then produced and characterized. The kinetics parameters of Michaelis-Menten model and thermal deactivation model were determined. Based on the characterization results of PMEs, the methanol conversion from beet pulp was further studied and the effects of organisms, pH values, pulp size, and temperature were evaluated. After this, methods for separation and concentration of methanol from water, including stripping, distillation and pervaporation, were studied and a model for the recovery of methanol from beet pulp after reaction was developed. Finally, the whole methanol conversion process was designed. The economic cost based on this design was estimated.

**BIOMETHANOL CONVERSION FROM SUGAR BEET PULP
WITH PECTIN METHYL ESTERASE**

By

Quanzeng Wang

Thesis submitted to the Faculty of the Graduate School of the
University of Maryland, College Park, in partial fulfillment
of the requirements for the degree of
Master of Science
2006

Advisory Committee:
Professor Nam Sun Wang, Chair
Professor Catherine Fenselau
Professor William E. Bentley
Professor Raymond A. Adomaitis

© Copyright by
Quanzeng Wang
2006

Acknowledgements

During my study here, I feel grateful to my advisor, Dr. Nam Sun Wang. Many thanks to him for the help, not only in my research but also in my life. I got pieces of constructive advice from him for my research. I would also like to thank our sponsors of *the Maryland Industrial Partnerships Program* and *Atlantic Biomass Conversions, Inc.*

My committee was quite helpful. I learned a lot in the field of biochemistry from Dr. Catherine Fenselau. She has always been glad to help. Dr. William E. Bentley serves as a committee member to tons of students. It is my honor to have him on my committee.

Thanks to the BSF (Bioprocess Scale-Up Facility) lab. Ben Woodark was so kind to allow me to use the instruments in BSF. Thanks are also given to Dr. Timothy A. Barbari's lab. They were so generous to let me use their pervaporation equipment. Juchen Guo, a good friend from Dr Barbari's group, gave me a lot of help for the pervaporation experiments. Thanks to Dr. John Fisher for allowing me to use the distillation tower. I also want to acknowledge Dr. Panagiotis Dimitrakopoulos, Dr. Evangelos Zafiriou, Dr. Richard V. Calabrese, and Dr. Raymond A. Adomaitis. They gave me useful advice in my research.

I would like to thank Pegah Parvini and Matthew Dowling. They were involved in the project with great enthusiasm during their short stay in the lab. I also want to thank Jun Li, she helped me a lot for SDS-PAGE. Thanks are also given to my colleagues, Paul Shriner, Yingli Fu, Patricia A. Gonzales, YueSheng Ye, Stephanie H. Kim, Jonghoon Choi, Halima Namatovu, Harin Kanani, et al. Mr. Paul Higgins gave me great help on editing my thesis.

Finally, I wish to thank my parents for fostering and encouraging my interest in science. Special thanks are given to my wife. She is the best I have got in my life.

Table of Contents

Acknowledgements.....	ii
Table of Contents.....	iii
List of Tables.....	v
List of Figures.....	vi
Chapter 1: Introduction.....	1
1.1 Energy shortage and renewable energy.....	1
1.2 Bioenergy and methanol.....	2
1.3 Pectins, pectin methyl esterases (PMEs), and sugar beet pulp.....	4
1.4 Introduction to the project.....	6
1.5 Introduction to the genetically optimizing of bacterial.....	7
Chapter 2: Quantitative Analysis of Methanol.....	8
2.1 Introduction.....	8
2.2 Potassium permanganate assay.....	11
2.2.1 Reagents and procedure of potassium permanganate assay.....	12
2.2.2 Interferences of the impurities in the sample.....	14
2.2.3 The length of oxidation.....	15
Chapter 3: Methods for Measuring PME Activity.....	18
3.1 Introduction.....	18
3.2 Qualitative analysis of PME activity—ruthenium red method.....	19
3.3 Quantitative analysis of PME activity.....	21
3.3.1 The substrate type and concentration.....	22
3.3.2 The ratio of substrate to PME, and the reaction time.....	23
3.3.3 The cation concentration.....	27
3.3.4 The proper pH value.....	28
3.3.5 Discussion.....	30
3.4 Conclusions and discussion.....	32
Chapter 4: PME Production and Characterization.....	33
4.1 Introduction.....	33
4.2 PME production.....	33
4.3 Molecular weight and concentration of PME.....	37
4.4 Michaelis-Menten kinetics of PME.....	39
4.5 Effect of temperature on the activity of PME.....	44
4.5.1 The kinetics of thermal deactivation of PME.....	44
4.5.2 The optimum reaction temperature.....	49
4.6 PME stability during storage.....	52
Chapter 5: Produce Methanol from Beet Pulp.....	54
5.1 Introduction.....	54
5.2 Characterization of pectin in sugar beet pulp.....	54
5.2.1 Extraction of pectin from sugar beet pulp.....	54
5.2.2 Measurement of methoxyl group content in sugar beet pectin.....	56
5.3 Effects of pH value on methanol production from sugar beet pulp.....	57
5.4 Effects of organisms on the methanol production.....	61
5.4.1 Effect of sodium azide on potassium permanganate assay.....	61

5.4.2	Effect of sodium azide on PME activity	62
5.4.3	Effect of organisms on methanol production.....	63
5.5	Effects of temperature on the methanol production.....	65
5.6	Inhibition of PME activity	67
5.6.1	Effect of methanol on the PME activity	67
5.6.2	Inhibition of the PME activity by foreign matter in pulp	68
5.7	Methods to help the PME access to the methoxyl groups in pulp.....	70
5.8	Modeling the methanol production from pulp	72
5.9	Conclusions and discussion	74
Chapter 6:	Methanol Separation	75
6.1	Introduction.....	75
6.2	Modeling of methanol stripping	75
6.2.1	Methanol stripping after reaction.....	75
6.2.2	Methanol stripping during reaction	81
6.3	Distillation	82
6.4	Pervaporation	84
6.5	Conclusions and discussion	89
Chapter 7:	Methanol Recovery from Sugar Beet Pulp	91
7.1	Introduction.....	91
7.2	Wash pulp by direct rinse	92
7.3	Wash pulp by counter-current flow	94
7.4	Compare the k values from direct rinse and counter-current flow	98
Chapter 8:	Process Design and Economic Estimation.....	100
8.1	Introduction.....	100
8.2	Simulation of reactor	102
8.2.1	Theoretical equations for the calculation of volume and residence time	102
8.2.2	Cost estimation of CSTR.....	103
8.3	Simulation of flash.....	107
8.4	Cost estimation of distillation tower.....	108
8.4.1	Simulation of distillation by a shortcut.....	109
8.4.2	Tower height and diameter	112
8.4.3	The optimum reflux ratio and annual cost of distillation tower	113
8.5	Conclusions and discussion	114
References	116

List of Tables

Table 4.4-1 V_m , K_m , and k_2 for CC4 and CC7 at different temperature	42
Table 4.5-1 The Arrhenius equation parameters of CC4 and CC7.....	47
Table 4.5-2 The Arrhenius equation parameters of CC4 and CC7.....	52
Table 5.2-1 Results of AIR extraction	55
Table 5.2-2 Results of pectin extraction from AIR	56
Table 5.6-1 Experiments compositions	69
Table 5.8-1 Reaction time and enzyme amount needed to obtain 100% methanol.....	73
Table 6.3-1 Experiments and simulation results.....	84
Table 6.4-1 Refractive index of methanol-water mixture at 20°C.....	86
Table 8.2-1 Volume calculation of the reactor	106
Table 8.2-2 Cost estimation of the reactor.....	107
Table 8.3-1 Parameters during simulation of flash and reactor	108
Table 8.3-2 Compositions of streams in simulation of flash and reactor	108
Table 8.4-1 Parameters during simulation of distillation tower	109
Table 8.4-2 Compositions of streams in simulation of distillation tower.....	110
Table 8.4-3 Compositions of streams in simulation of distillation tower.....	110
Table 8.4-4 Annual cost of distillation tower	114

List of Figures

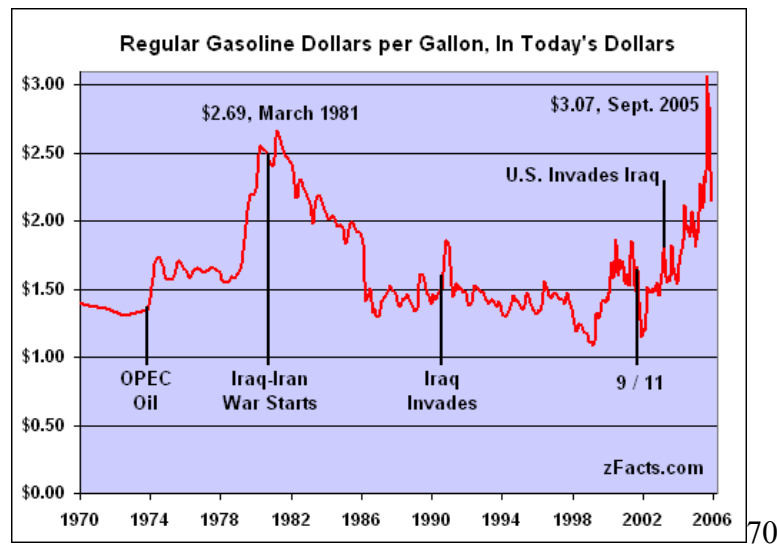
Fig. 1.1-1 Historical gasoline price.....	1
Fig. 1.2-1 Direct methanol fuel cell from ToShiba.....	3
Fig. 1.3-1 Dominant structure of pectins	5
Fig. 1.4-1 Flow sheet of methanol production.....	6
Fig. 2.2-1 Effect of 0.05% sodium azide on the standard curve.....	14
Fig. 2.2-2 Effect of 0.1% pectin on the standard curve	15
Fig. 2.2-3 Effect of oxidation time on the standard curve	16
Fig. 2.2-4 Effect of oxidation time on the standard curve with the test tubes open	17
Fig. 3.2-1 Ruthenium red method using different pectin.....	21
Fig. 3.3-1 PME activity at 30°C with different pectin as substrate	23
Fig. 3.3-2 PME activity at 30°C with different volume ratio of 0.2% pectin to PME.....	26
Fig. 3.3-3 Effect of sodium cation concentration on PME activity	27
Fig. 3.3-4 PME activity at 30°C at different pH value	28
Fig. 3.3-5 Pectin hydrolysis at different pH value.....	29
Fig. 3.3-6 Pectin hydrolysis at different pH value.....	30
Fig. 3.3-7 pH change during the PME activity measurement at 30°C with different volume ratio of 0.2% pectin to PME.....	31
Fig. 4.2-1 The PME production after induction by ruthenium red method.....	34
Fig. 4.2-2 PME production with BioFlo 3000® bench-top fermentor	35
Fig. 4.2-3 Harvest PMEs with Pellicon™ cassette filters.....	36
Fig. 4.2-4 Flow sheet of PMEs harvest with Pellicon™ cassette filters.....	36
Fig. 4.2-5 PME activities of fractions of culture mixture.....	37
Fig. 4.3-1 SDS-PAGE of PME	38
Fig. 4.4-1 Lineweaver-Burk plot of CC4 and CC7 at 30°C.....	41
Fig. 4.4-2 Lineweaver-Burk plot of CC4 and CC7 at 45°C.....	41
Fig. 4.4-3 Lineweaver-Burk plot of CC4 and CC7 at 54°C.....	42
Fig. 4.4-4 Reaction rate versus pectin concentration under the catalysis of CC4	43
Fig. 4.4-5 Reaction rate versus pectin concentration under the catalysis of CC7	43
Fig. 4.5-1 Thermostability of PME at 45°C.....	45
Fig. 4.5-2 Thermostability of PME at 54 °C	45
Fig. 4.5-3 Thermostability of PME at 60 °C	46
Fig. 4.5-4 Residual activity as a function of time at 54°C (Simulation).....	48
Fig. 4.5-5 Residual activity as a function of time at 54°C (Experiments).....	48
Fig. 4.5-6 Effect of temperature on the activity of PME	49
Fig. 4.5-7 Average reaction rate as a function of temperature	51
Fig. 4.5-8 Optimal temperature as a function of sampling time	52
Fig. 4.6-1 PME stability during storage.....	53
Fig. 5.3-1 Pectin hydrolysis at different temperatures and pH values.....	58
Fig. 5.3-2 Hydrolysis of pulp at pH 7~7.5 at 54°C	58
Fig. 5.3-3 Produce methanol from pulp at 54°C	59
Fig. 5.3-4 PME activity versus time at 54°C.....	60
Fig. 5.4-1 Effect of sodium azide on the methanol assay	62

Fig. 5.4-2 Effect of sodium azide on PME activity at 30°C	63
Fig. 5.4-3 Effect of sodium azide on PME activity at 54°C	63
Fig. 5.4-4 Effect of organisms on methanol production from pulp at 54°C	64
Fig. 5.4-5 Methanol produced by organisms	65
Fig. 5.5-1 Thermal hydrolysis of pulp	66
Fig. 5.6-1 Methanol inhibition on PME activity at 54°C	68
Fig. 5.6-2 Inhibition of PME activity from pulp.....	69
Fig. 5.6-3 Inhibition of PME activity from pulp steep	70
Fig. 5.7-1 Produce methanol from pulp at 54°C	71
Fig. 5.8-1 Produce methanol at different temperature	72
Fig. 6.2-1 Methanol stripping from the reactor	76
Fig. 6.2-2 Simulation result of methanol stripping.....	80
Fig. 6.2-3 Experiment results of methanol stripping	81
Fig. 6.2-4 Simulation result of methanol stripping from a continuous reactor.....	82
Fig. 6.3-1 Distillation tower.....	83
Fig. 6.4-1 Pervaporation setup (Right figure was the membrane chamber).....	85
Fig. 6.4-2 The sketch map of pervaporation.....	86
Fig. 6.4-3 Standard curve of refractive index versus methanol concentration at 20°C	87
Fig. 6.4-4 Standard curve of refractive index versus methanol concentration (0-40%) at 20°C	87
Fig. 6.4-5 Permeate concentration versus feed concentration	88
Fig. 6.4-6 Permeate flux versus feed concentration.....	88
Fig. 6.4-7 Separation factor versus feed concentration	89
Fig. 7.1-1 Wash pulp by direct rinse.....	91
Fig. 7.1-2 Wash pulp by counter-current flow.....	92
Fig. 7.2-1 Rinse beet pulp with water continuously	92
Fig. 7.2-2 Methanol concentration in beet pulp as a function of time.....	93
Fig. 7.3-1 Schematics of methanol concentration change in a screw machine	94
Fig. 7.3-2 Schematic of pulp washing by counter-current flow	95
Fig. 7.3-3 Screw machine model	98
Fig. 8.1-1 Flow sheet of sugar production	101
Fig. 8.1-2 Flow sheet of methanol production.....	101
Fig. 8.2-1 Reaction equation for reactor simulation.....	105
Fig. 8.3-1 Simulation of flash after reactor.....	108
Fig. 8.4-1 Simulation of distillation tower.....	109
Fig. 8.4-2 Heat exchange as a function of reflux ratio	111
Fig. 8.4-3 Number of stages as a function of reflux ratio.....	111
Fig. 8.4-4 Annual cost as a function of reflux ratio.....	114

Chapter 1: Introduction

1.1 Energy shortage and renewable energy

The price for gasoline has been rocketing in the past several years. Global demand for petroleum will remain strong and may be increasing. It is understandable for people to worry about the cost of energy for the future. The fact is the price of gasoline has climbed to the historically highest level and the tendency will continue in the long term (Fig. 1.1-1). Granted, it is nearly impossible to accurately project future energy supplies and prices.



(<http://zfacts.com/p/35.html>, accessed September 26, 2005)

Fig. 1.1-1 Historical gasoline price

There is no doubt that the global supply can expand to meet the demand in the near future. The fact is that the fossil fuels, mainly crude oil, natural gas, and coal, will deplete one day since they are non-renewable energy sources. “World oil production will decrease first..... Very soon the increasing demand cannot be met any more. The prices will increase further. It is not unrealistic to assume that we are already at the beginning of this phase.” (Lieberman, 2005)

To meet the energy demand, we have to turn to renewable energy. Renewable energy is 'energy obtained from the continuous or repetitive currents of energy recurring in the natural environment' (Twidell and Weir, 1986). It includes solar energy, wind energy, bioenergy, hydroelectricity, wave energy, tidal power and geothermal energy. The sun is the ultimate source of most of our renewable energy supplies. Bioenergy, hydroelectricity, wind energy and wave energy are indirect solar energy since they come originally from solar radiation.

1.2 Bioenergy and methanol

Bioenergy comes directly from biomass, a renewable energy resource derived from the carbonaceous waste of various human and natural activities, such as dead trees, left-over crops, by-products from agriculture industry, and major parts of household waste. The most popular way of using biomass is burning, like cooking and heating. As the largest U.S. renewable energy source every year since 2000, biomass also provides the only renewable alternative for liquid transportation fuel (U.S. Department of Energy, 2005). The most useful products from biomass include methane, methanol, ethanol and other biofuels. Among them, methanol can be used to make countless industrial and consumer products such as synthetic textiles, recyclable plastics, and biodiesel. It can also be used as fuel to drive a cell phone, MP3 player, car, and so on. New applications for methanol are being found all the time.

Nowadays, the direct use of alcohol for fuel cells, named direct alcohol fuel cells (DAFC), becomes a hot topic. "A fuel cell is a device that uses hydrogen (or hydrogen-rich fuel) and oxygen to create electricity by an electrochemical process. Most fuel cells are powered by hydrogen, which can be fed to the fuel cell system directly or can be generated within the fuel cell system by reforming hydrogen-rich fuels such as methanol, ethanol, and hydrocarbon fuels."(U.S. Department of Energy, 2005). DAFC does not need to be recharged, as long as oxygen and fuel are supplied to the fuel cell.

Therefore, DAFC is ideal for space-limited portable applications, like MP3 player, video camera, or laptop computer. The advantages of alcohols over hydrogen for fuel cells are: 1) alcohols have a higher energy density than hydrogen, which means longer operating time; 2) alcohols are easier to transport and supply to the public since it is a liquid, like gasoline; 3) the operating temperature is low; 4) alcohols are inexpensive and readily available.

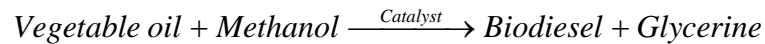
A DAFC with methanol or ethanol as the fuel is called a direct methanol fuel cell (DMFC) or direct ethanol fuel cell (DEFC) accordingly. Presently the power density of the DEFC is only 50% of the DMFC (Wiens, 2005). Since the ratio of hydrogen to carbon in methanol is higher than that in ethanol, DMFC release less carbon monoxide or carbon dioxide. “Tests performed on a fuel cell bus, fueled by methanol, showed zero emissions of particulate matter and hydrocarbons, and near-zero emissions of carbon monoxide and nitrous oxides – levels far below the 1998 emission standard for buses. (Rose, 2003)” Another advantage of DMFC over DEFC is the catalyst for DMFC is cheaper than that for DEFC. Some wonderful commercial products have been developed. Toshiba have announced the world’s smallest direct methanol fuel cell with energy output of 100 milliwatts (Fig. 1.2-1).



Fig. 1.2-1 Direct methanol fuel cell from ToShiba

Methanol can also be used to produce biodiesel. Biodiesel or alkyl ester is an alternative fuel produced from methanol and biomass such as soybean. It is made through

a chemical process called transesterification whereby the glycerin is removed from the vegetable oil or fat. The reaction can be depicted as



Biodiesel can be blended at any level with petroleum diesel to be used in compression-ignition (diesel) engines. It is nontoxic, biodegradable, and essentially free of sulfur and aromatics. The production and use of biodiesel, compared to petroleum diesel, resulted in a 78.5% reduction in carbon dioxide emissions (<http://www.biodiesel.org>).

A big potential market for methanol is right here in at least two fields, fuel cell and biodiesel. What we should do is to find a new way to produce methanol. Currently, methanol is mainly made from natural gas. In 1997, 86% of methanol was produced from natural gas (Ohlström et al., 2001). As mentioned before, natural gas is non-renewable. Methanol made from biomass, however, can be available forever if only the sun is shining. Even more, using methanol produced from biomass can reduce our yearly addition of more fossil carbon to the atmosphere, slowing the increase in global warming. The production of methanol from biomass represents a more broadly applicable and environmentally clean approach to generate power.

1.3 Pectins, pectin methyl esterases (PMEs), and sugar beet pulp

Among numerous biomasses, pectin is one of the best for methanol production. Pectin is a grouping of closely associated polysaccharides from the primary cell walls and intercellular regions, found in higher plants. It is abundant in fruit and vegetable. Apple, plum, grape, peach, currant, citrus, et al. are especially high in pectin. “The dominant feature of pectins is a linear chain of α -(1,4)-linked D-galacturonic acid units in which varying proportions of the acid groups are present as methoxyl (methyl) esters.” (Stephen, 1995) Generally speaking, galacturonic acid units compose more than 65% of pectins structure. An important structure characteristic of pectins is the esterification of galacturonic acid residues with methanol and/or ethanol. The percentage of carboxyl

groups esterified with methanol is called degree of methylation (DM). If DM is higher than 50%, the pectins are called high-methoxyl (HM) pectins. Other wise, the pectins are called low-methoxyl (LM) pectins. Since pectins are abundant in methoxyl side groups, they can be deesterified to produce methanol.

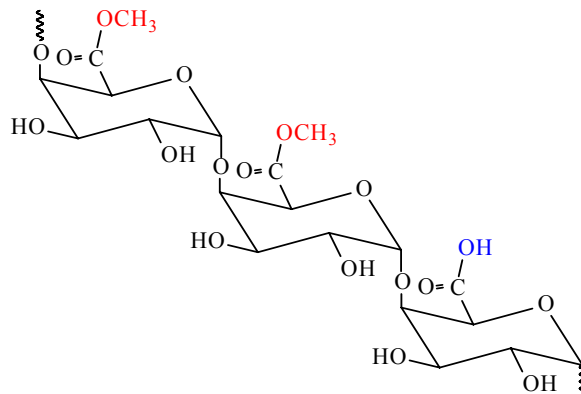


Fig. 1.3-1 Dominant structure of pectins

Deesterification of pectins can be carried out by a chemical method.

Hydrolyzation of methoxyl side groups with the catalysis of acid or base is a widely used chemical method. However, these old technologies are already fully developed with little room for further cost saving. On the other hand, hydrolyzation catalyzed by enzyme can be thousands of times faster than that by acid or base. Enzyme is specific for reactions. Those can deesterify the pectins are called pectin methyl esterases (PME). The fast and high specific catalysis of PME make them the most economically promising alternative for hydrolyzation.

Sugar beet pulp is a by-product of sugar factory which is usually used as animal feed. Dry sugar beet pulp contains 55%~62% of pectin which in turn contains 9%~10% of methyl side group. The methyl side groups are esterified with carboxylic acid groups in pectin. Therefore, Hydrolysis of the ester group yield methanol. Since a huge amount of sugar beet pulp is produced in sugar factory, it is a good bio resource for methanol production with PEM.

1.4 Introduction to the project

Atlantic Biomass Conversions Inc. is a pioneer in developing renewable biofuels from leftover, low value agricultural wastes. Producing methanol from biomass, especially from low value sugar beet pulp is the main project supported by the company. The overall objective of the project is to develop an economical turn-key process of methanol production by converting the waste pulp in sugar beet processing. The company wishes to establish a patentable bioreactor system to maximize production of fuel-cell-quality methanol from sugar beet pulp.

The whole project was carrying on with the cooperation of two research groups. Dr. Craig S. Laufer, Department of Biology, was the lead researcher at Hood College, and Dr. Nam Sung Wang, Department of Chemical Engineering, was the lead researcher at University of Maryland at College Park. Scientists at Hood College genetically optimized a bacterium which can produce PME by directed evolution techniques. Researchers at the University of Maryland focused on the characterization of PME and refining of the entire bacterial conversion process so that this process would be integrated into existing sugar beet processing plants. The flow sheet of the whole process follows.

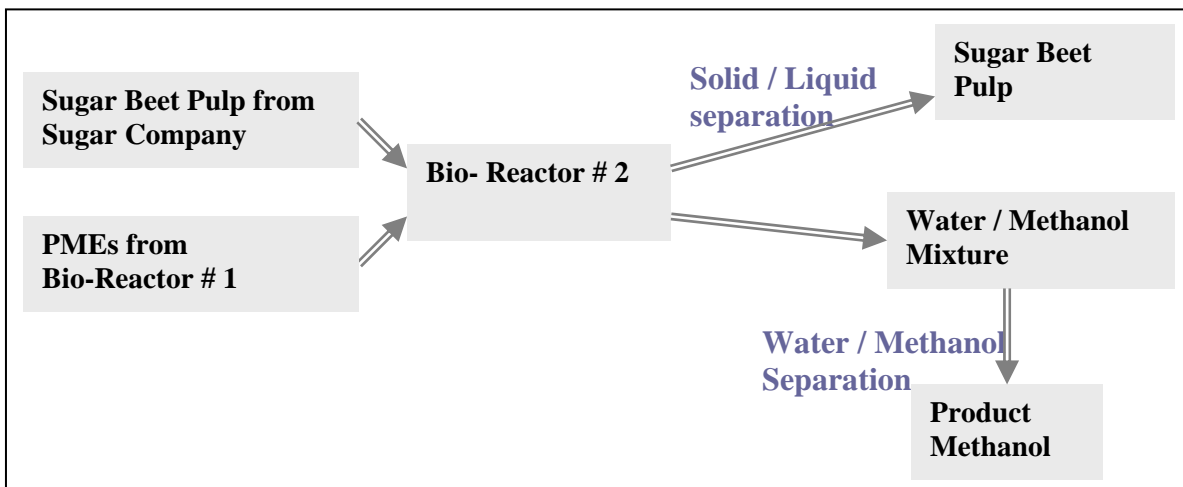


Fig. 1.4-1 Flow sheet of methanol production

1.5 Introduction to the genetically optimizing of bacterial

A well studied pectin methyl esterase (PME) is produced by *Erwinia chrysanthemi* B374. The nucleotide sequence of the PME gene of *Erwinia chrysanthemi* B374 is already known (Plastow, 1988). However, PME from this gene can not bear high temperature. Since our reaction could be carried out at 60°C and higher, mutants that can work at such a high temperature should be obtained. Dr. Craig S. Laufer's research group engaged in the work of mutating and selecting for desirable mutants. The main tools they used were pBAD/TOPO ThioFusion Expression Kit from Invitrogen. The PME gene from *Erwinia chrysanthemi* was first transferred into *E.coli* by pBAD/TOPO ThioFusion Expression Kit to obtain a beginning bacterium CC4. From CC4, several mutants were then obtained. CC7, which came from a point mutation of CC4, was the best one among them.

Chapter 2: Quantitative Analysis of Methanol

2.1 Introduction

Finding an accurate method to quantify methanol was an essential part in my project. Since methanol was produced from sugar beet pulp under high temperature, the sample composition from reaction was complex. With the degradation of all kinds of polysaccharides and proteins, there could be thousands of compositions in the sample. Therefore, to measure the methanol concentration in such a sample is a challenge. So far the analysis methods for methanol as recorded include High Performance Liquid Chromatography (HPLC), Gas Chromatography (GC), Near-Infrared Spectroscopy, Chemical Assay, and Enzymatic Assay.

HPLC is a common technique to quantify methanol. To determine the degree of methylation and acetylation of pectins, Voragen, Schols, and Pilnik (1986) analyzed the supernatant by HPLC after the pectin was saponified and precipitated. Drawbacks of the HPLC method are that it needs a large amount of materials, the method is time consuming and pectins sometimes form a gel in column (Huisman, Oosterveld and Schols, 2004). The analysis of methanol in Chinese liquor medicine by HPLC was reported (Kuo, Wen, Huang, and Wu, 2002). Before analysis, the derivatization of methanol by 4-[N-methyl, N-(1-naphthylmethyl)]-amina-4-oxobutanoic acid (NAOB) was carried out. The reaction required several hours.

GC is also a popular technique for quantitative analysis. Quantification of methanol in alcoholic beverage with a wax capillary column was ever reported (Wang, Wang & Choong, 2004). In this report, simultaneous quantification of methanol and ethanol in alcoholic beverage using a rapid gas chromatographic method coupling with dual internal standards was carried out. The sample with the added internal standard was directly injected into the column. The compositions in the sample included methanol,

ethanol, acetonitrile, 1-propanol, isobutanol, 2-pentanol, isoamyl alcohol, amyl alcohol, and tert-butanol. All of these compositions are volatile small molecules.

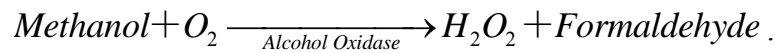
However, GC encountered problems with my samples. First, more than 99% of my sample was water, which can damage most capillary columns for GC except several wax ones. Second, there were not only volatile small molecules in my samples, but also many non-volatile big molecules. As we know, about half of the dry beet is pectin, which is composed of anhydrogalacturonic acid, neutral sugars (rhamnose, fructose, arabinose, xylose, mannose, galactose, glucose), feruloyl ester groups, methyl ester groups, and acetyl ester groups (Rombouts and Thibault, 1986). Beside pectin, there are all kinds of proteins and other polysaccharide in it. During reaction, all these components could degrade into hundreds of smaller non-volatile molecules.

Adding a protection column before the analysis column can trap these non-volatile molecules. However, the protection column should be changed frequently since the sample is dirty, which will increase the cost. Also, leak at the joint of protection column and analysis column is a problem sometime. Another method is to use head-space GC. The head-space sampling is useful for the analysis of volatiles, especially where the sample matrix is dirty. In head-space sampling, the sample is placed into a vial which is inserted into a thermostatted sleeve. The sample is then heated for several minutes and the volatiles are injected to the column. Savary and Nunez (2003) developed a gas chromatography-mass spectrometry method for determining the methanol and acetic acid contents of pectin using headspace solid-phase microextraction and stable isotope dilution. Huisman, Oosterveld, and Schols (2004) used head-space GC to determine the degree of methyl esterification. However, these methods were complex and instrument-dependent.

Although not popular, near-infrared spectroscopy is also a technique to analyze methanol. This technique was used in the distillation industry by Van den Berg, Van Osenbruggen, and Smilde (1997). Again, the sample from the distillation industry was

simpler than mine. A NIRSystem (Foss Inc., Silver Spring, MD) was used to measure methanol concentration in our lab. The results showed that this system could work well for simple water-methanol mixture at higher concentration (>1%). For complex sample and low concentration, it was difficult to measure. Besides, this system highly depends on both the instrument and the mathematics methods in the software.

Enzymatic assay is a relatively new technique. The basic reaction for this assay is that methanol is oxidized to formaldehyde by alcohol oxidase under the existence of oxygen. The reaction is described as



After the reaction, there are two methods to continue the measurement. The first one is to react formaldehyde with 2,4-pentanedione to yield the colored product 3,5-diacetyl-1,4-dihydro-2,6-dimethylpyridine (Klavons, & Bennett, 1986). The optical density is then measured at 412nm. The second method is to use a biochemistry analyzer. The probe signal current rises when the hydrogen peroxide diffuses toward the platinum anode in the probe assembly. The shortcoming of enzymatic assay is that the enzyme is expensive and unstable. A biochemistry analyzer (Model 2700 select; Yellow Spring Instrument Co., Inc, Yellow Springs, Ohio) in our lab showed an error of more than 50 percent sometimes.

The last method, which is also the oldest method, to quantify methanol is by chemical assay. The methanol is analyzed via the oxidation of methanol to formaldehyde with potassium permanganate, followed by condensation with 2,4-pentanedione to yield the colored product 3,5-diacetyl-1,4-dihydro-2,6-dimethylpyridine (Wood & Siddiqui, 1971). There were seldom papers like the one by Wood & Siddiqui, which had been cited 197 times by the end of 2005 (from *Web of Science*). Researchers never stop using this method although there are also several other methods available. Two samples are Brummell et al used this method to analyze the samples of acetone-insoluble cell walls

(Brummell, Cin, Crisosto & Labavitch, 2004) and Ovodova et al used this method to analyse the structure of pectin from marsh cinquefoil *Comarum palustre* L. (Ovodova, Bushneva & Shashkov, 2005). One disadvantage of this method is that some chemicals are toxic. However, this is not a problem if the lab rules are strictly followed. Another disadvantage of this method is that it is laborious. The whole process for one sample needs two hours. However, it will be a good method if this problem can be solved. The details of the potassium permanganate assay will be discussed below.

2.2 Potassium permanganate assay

The potassium permanganate assay is a classic chemical method for methanol analysis. This method is sensitive, accurate and stable. The minimum methanol needed for one sample is only 2 micrograms. The standard error of results is small and the results are repeatable. An excellent paper to describe this assay was by Wood and Siddiqui (Wood & Siddiqui, 1971). However, this method is not perfect for my project.

As mentioned above, the potassium permanganate assay is time consuming. It needs two hours for one sample with this method. If we can measure a batch of samples simultaneously, this shortcoming can be overcome. However, the problem for batch assay is that not all of these samples can be ready at the same time. For example, samples will be taken at a different time if one wants to follow the methanol concentration change during a reaction. One solution to this problem is to freeze the samples at first and then assay them together later. However, during the process of freezing and melting, the enzyme will still be active which will bring large error to the results. In this chapter, the potassium permanganate was developed to isolate this problem.

Another possible problem of applying the potassium permanganate methods to my project is from the interferences of thousands of impurities. In Wood's paper, the interferences of some chemicals were studied. However, the results in this paper are not enough for my project since there are much more chemicals in my samples.

2.2.1 Reagents and procedure of potassium permanganate assay

The potassium permanganate assay was based on Wood's paper (Wood & Siddiqui, 1971) except several details were modified. In this method, three reagents, potassium permanganate, sodium arsenite, and pentane-2,4-dione were used. Among them, potassium permanganate was an oxidant which oxidized methanol to formaldehyde, sodium arsenite a reducing agent that reduced the excessive potassium permanganate to colorless Mn^{2+} , pentane-2,4-dione an agent that reacted with formaldehyde to yield the colored product 3,5-diacetyl-1,4-dihydro-2,6-dimethylpyridine. The reagent preparation and assay procedure are shown bellow.

Reagents

A: 2%(w/v) aqueous potassium permanganate

Modification: In Wood's paper, the solution was prepared and filtered through medium-porosity sintered glass which had been cleaned with chromic acid, water, dilute potassium permanganate, and water again. Our results showed that the filtration was not necessary. The potassium permanganate(Sigma, Cat. # 207985) solution in D.I. water was used directly. And the solution could be kept for at least 2 weeks.

B: 0.5 M sodium arsenite in 0.12 N H_2SO_4

Note: The solution was stable for more than half a year.

C: 0.02 M pentane-2,4-dione dissolved in a solution containing ammonium acetate (2.0M) and acetic acid (0.05 M)

Modification: In Wood's paper, the pentane-2,4-dione should be freshly distilled. In my experiment, solution containing ammonium acetate (2.0M) and acetic acid (0.05 M), which could be preserved more than half a year, was prepared at first. The pentane-2,4-dione (Sigma, Cat. # P7754) was added before use. The final solution could be kept for more than 2 weeks.

Procedure

(1) Aliquots (1mL) of unknown or methanol standards (2-40 μg) in 1.0N H_2SO_4 were cooled in test tubes in an ice-water bath.

Note: This step was to make sure the following reaction was at low temperature.

(2) Reagent A (0.2 mL) was added, taking care that the sides of the tubes were not splashed. The solution was mixed by gentle swirling and the tubes held in the ice-water bath for 15 min.

Note: In this step, methanol was oxidized to formaldehyde with potassium permanganate in acidic condition. Under alkaline environment, the formaldehyde would be continuously oxidized to formic acid, which caused error in further steps.



(3) Reagent B (0.2 mL) was then added, followed by water (0.6mL), and the thoroughly mixed solution left for 1 hr at room temperature.

Note: In this step, excessive potassium permanganate was reduced to colorless Mn^{2+} by sodium arsenite.

(4) Reagent C (2 mL) was then added and, after shaking, the tubes were closed with marbles, heated at 59°C for 15 min, and cooled to room temperature.

Note: In this step, formaldehyde reacted with 2,4-pentanedione to yield the colored product 3,5-diacetyl-1,4-dihydro-2,6-dimethylpyridine.

(5) Optical densities were read at 412 nm using blank water as reference.

(6) The standard solutions were prepared and measured following the same procedure as above. The standard curve was drawn. The methanol mass of sample was calculated from the trendline equation of a standard curve.

2.2.2 Interferences of the impurities in the sample

The potassium permanganate assay is robust. In Wood's paper, the interferences of ethylenediaminetetraacetic acid (EDTA), hydroxymethylfurfural (HMF), ethanol, galactose, arabinose, glucose, and galacturonic acid were studied. The results showed that these chemicals interfered only slightly or not at all. For example, the optical density of 20 microgram methanol was 0.461 while the optical density of 500 microgram ethanol was only 0.061.

In my research, the interferences by sodium azide and pectin were also studied. Sodium azide was used to inhibit the bacterial in sugar beet pulp in my experiments. The effect of 0.05% sodium azide to the standard curve is shown in Fig. 2.2-1. Pectin solution was used to measure the PME activity in my research. The interference of 0.1% pectin on the standard curve is shown in Fig. 2.2-2. These figures shows that 0.05% sodium azide and 0.1% pectin came very near but did not affect the standard curve.

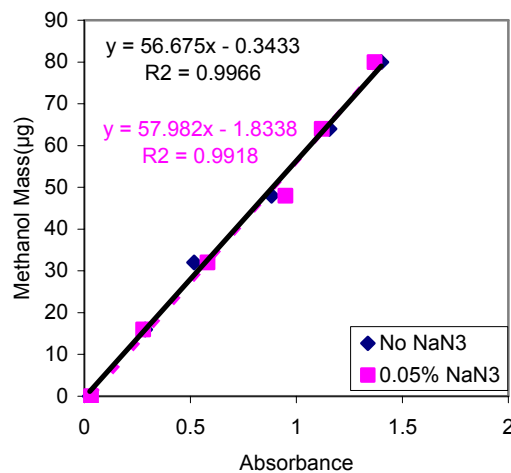


Fig. 2.2-1 Effect of 0.05% sodium azide on the standard curve

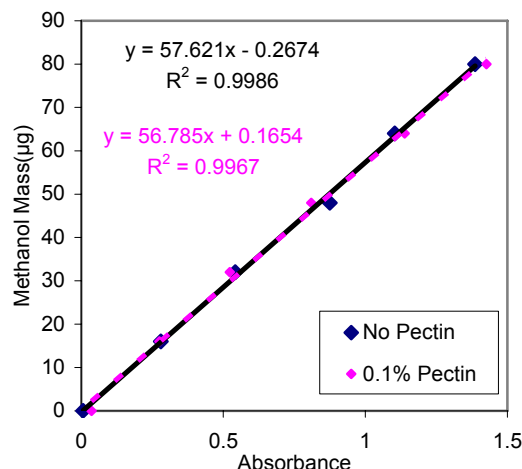


Fig. 2.2-2 Effect of 0.1% pectin on the standard curve

Although some of the most important impurities have been studied, thousands of them are still left. It is impossible to study every impurity. To solve this problem, a good idea is to use the same background as the samples for the standard curve. The control experiments were always carried out whenever the potassium permanganate was used. In this way, whatever impurities in the sample will affect the standard curve in the same way. Therefore, we can make sure our results are always reliable.

2.2.3 The length of oxidation

A shortcoming of the potassium permanganate assay is that it is time consuming. The assay of one sample needs two hours. Solution to this is to assay a batch of samples at the same time. The problem of batch assay is that not all the samples can be ready at the same time. For the reaction under the catalysis of enzyme, the reaction can still continue if it is not assayed right away after the sample is taken. A solution to this is to add extra chemicals to deactivate the enzyme right after the sample is taken. However, new chemicals make the assay method more complex. If the enzyme can be deactivated by the chemical in the assay, this problem is solved.

In this section, the potassium permanganate assay was developed. The procedure of the assay was modified so that a batch of samples could be assayed simultaneously with no new chemical added.

The key issue to measure batch samples was to synchronize the assays of different samples at the time reagent B was added. The oxidant, Reagent A could be added right after the sample was taken. Reagent A was added at a different time if samples were taken at a different time. However, Reagent B could be added at the same time for all the samples. This means the oxidation time for a different sample was different.

It was claimed that the optimal conditions for oxidation by 2% permanganate were at 0°C for 15 min (Wood & Siddiqui, 1971). Then what if the oxidation time is longer? To answer this question, six series of experiments were carried out following the similar procedure discussed in section 2.2.1. In each experiment, a standard curve was obtained. The only difference between each series of experiments was the oxidation time. Methanol was oxidized for 15min, 35min, 60min, 80min, 105min and 135min, respectively. The results are shown in the following figure.

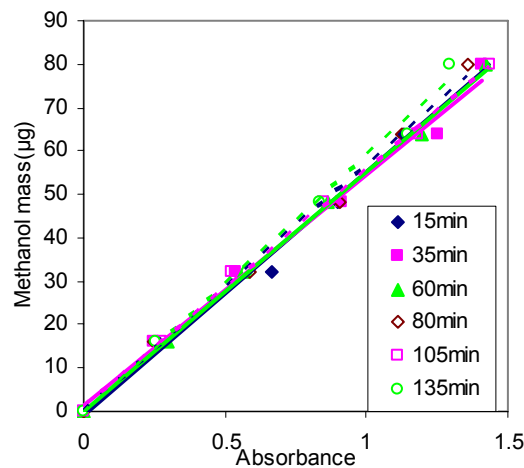


Fig. 2.2-3 Effect of oxidation time on the standard curve

From the above figure, the trendlines of standard curves with different oxidation times are almost overlapped. That means the oxidation time ranging from 15 min to 135min did not affect the assay results.

The critical point in the experiments is that the test tube should be sealed. Three series of experiments with different oxidation times were carried out with the test tubes open. As shown in the following figure, the trendlines were totally different although the initial samples were the same. That is because more formaldehyde was evaporated for a longer oxidation time so the final absorbance decreased.

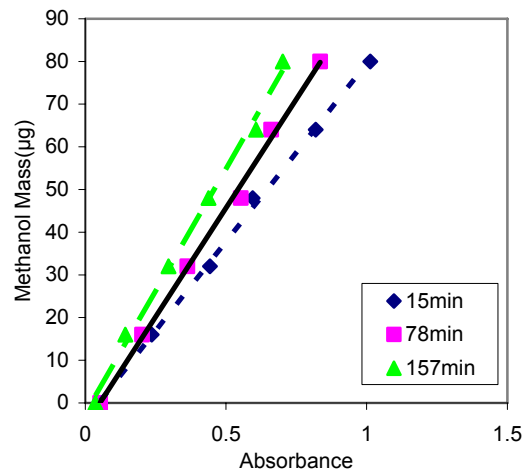


Fig. 2.2-4 Effect of oxidation time on the standard curve with the test tubes open

Chapter 3: Methods for Measuring PME Activity

3.1 Introduction

In this chapter, two methods specifically for measuring our PME activity were established. One was for the qualitative analysis of PME activity and the other was for the quantitative analysis of the PME activity. These methods were used through the whole project so that the results obtained at different times or by different operators could be compared.

Compared with other chemicals, enzyme is special. It is difficult to describe enzymes in a way that chemicals are described. The most important character for an enzyme is its activity. Enzyme activity is usually measured in the terms of the activity unit (U). One unit is equal to the amount of enzyme which will catalyze the transformation of 1 micromole of the substrate per minute under standard conditions. Unfortunately, the so called 'standard conditions' is often defined in different ways. Many commercial enzyme suppliers define the enzyme activity differently in terms of the factors like the substrate type and concentration, temperature, pH value, cation concentration and reaction time. These factors have impacts on the measured enzyme units. This can be seen from the mechanistic model for simple enzyme kinetics, which is $v = \frac{V_m[S]}{K_m + [S]}$ (Shuler & Kargi, 2002). Assume the amount of enzyme in the reaction is fixed. If K_m is a small value, say 0.1mM, the assay carried out at 1 mM substrate will give almost twice the number of units as the assay carried out at 0.1 mM substrate. Also, a vial of 500 units of an enzyme measured at relatively low temperature may actually give more units than that measured at a relatively high temperature.

Activity value is quoted as units per ml. Two vials of enzyme can contain the same number of units in total but their activities may be different if they have different

volume. In storage, some activity may suffer a loss so it is sensible to confirm the actual activity at the time the experiment is carried out.

Specific activity value is quoted as units per mg. It is the number of enzyme units per ml divided by the concentration of protein in mg/ml. Specific activity value is less important than activity value since the amount of substrate converted is just determined by the number of enzyme units in the reaction. It is impossible to calculate the volume of enzyme required for an assay from the specific activity alone. However, specific activity is an important measure of enzyme purity and quality. Different batches of enzyme with the same purity should exhibit the same activity value.

3.2 Qualitative analysis of PME activity—ruthenium red method

Ruthenium red is a dye that can selectively bind to the carboxyl groups of polysaccharide. The crystal structure of ruthenium red and stereochemistry of its pectic stain was studied by Sterling whose results showed that there would be [n-2] staining sites for ruthenium red if there were [n] monomer of anhydrogalacturonide units in the pectin polysaccharide (Sterling, 1970). As early as 1964, ruthenium red had been used showing the decomposition of cellulose (Babel, 1964). Iwai and his/her cooperators stained the cell walls in carrot embryogenic callus (EC) and non-embryogenic callus (NC) to compare their composition difference (Iwai, 1999).

Pectins, like other polysaccharide, can be stained by ruthenium red. Ruthenium red solution has been used to stain gel slice containing pectin (Chang, 1998) and even to stain pectin solution directly (Hou, 1999). A qualitative plate assay was used to screen the presence of the enzyme activity during purification or deactivation (Pitkänen, 1992). In this assay, enzyme samples of 2 μ l were applied into wells made in agar [1% (w/v) agarose, 0.5% (w/v) pectin, 1.5 mM CaCl₂ 50mM Tris-HCl, pH8.6]. After incubation for 30 min at 37°C, the enzyme activity was revealed by staining the gels with 0.05%

ruthenium red. A darker-stained area on a reddish background was observed if the enzyme samples had activity.

The technique of the qualitative plate assay is easy, fast and sensitive. The exact composition of the gel is not important. The main points are that there should be pectin and agar in the gel and the pH should be near neutral. In order to compare our results with our collaborator, Dr. Craig S. Laufer's research group at Hood College, the same composition developed by them was used in my experiments. The Petri-Dish consisted of 0.25% (w/v) pectin, 1.5% (w/v) agar, 75% M9 minimal salts, and 25% water. The assay included several steps: 1) Dispense 4 μ L of sample on top of Petri-dish; 2) Incubate the Petri-dish for 20min at 37°C; 3) Rinse the dish with D.I. water; 4) Stain the dish with fresh ruthenium red (0.05%) for 5min; 5) Rinse the dish to remove excess ruthenium red. If the enzyme has activity, free carboxyl groups will be released by enzyme, which will combine the ruthenium red and show a deeper color. The background will be stained a weak pink color, depending on the degree of esterification (DE) of the pectin used.

The pectin can come from citrus, apple or beet pulp. Our PME enzyme can hydrolyze all of them to release free carboxyl groups. Fig. 3.2-1 shows the comparison of the ruthenium red method using these pectins. Twenty different enzyme samples were applied on three Petri-dishes made of citrus pectin, apple pectin and beet pectin. The same sample was dropped at the same position on each dish. From the figures, three dishes show the similar results. If the enzyme work on one dish, it will also works on the other two. The only difference between dishes is the result shown by the beet pectin dish is not as clear as that shown by the other two. The reason is the methoxyl group content in beet pectin is not as abundant as that in citrus pectin and apple pectin.

Since beet pectin is not commercially available in America, we will not use it in the ruthenium red methods. On the other hand, both citrus pectin and apple pectin have abundant methoxyl groups and are commercial available. Since the price of citrus pectin is much cheaper, it is chosen for the quantitative analysis.

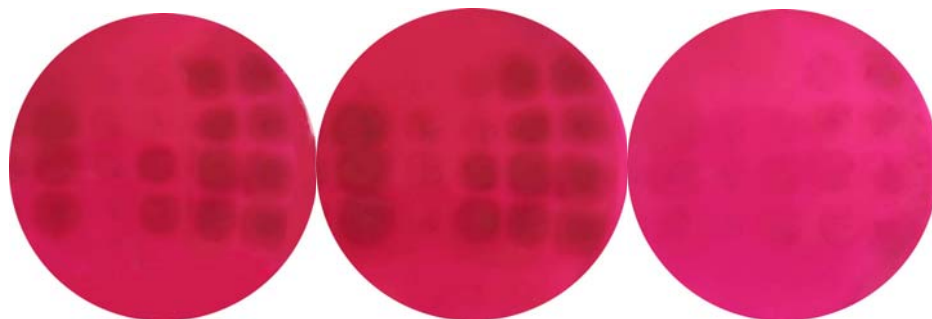


**Fig. 3.2-1 Ruthenium red method using different pectin
(From left to right: citrus pectin, apple pectin, beet pectin)**

3.3 Quantitative analysis of PME activity

The ruthenium red method is fast and sensitive for the qualitative analysis of PME. However, this method can only tell us if the sample has activity. It can not tell the exact activity value. Although theoretically the color intensity for different samples should be different, it is difficult to identify the difference by eyes in most conditions. Therefore, a method for quantitative analysis of PME activity should be established.

Since the potassium permanganate assay is the most sensitive method to analyze the methanol concentration in the methods I have tried, the quantitative analysis of PME activity will be based on this method. The main task in this section is to define the reaction conditions. As discussed above, there are several factors that need to be determined: substrate type and concentration, temperature, pH, cation concentration, the ratio of substrate to PME, and reaction time.

Enzyme will be deactivated faster at a higher temperature. On the other hand, the reaction rate is higher at a higher temperature. So at what temperature should the assay be carried on? Since *Sigma* is well known, the activity of my PME was measured at the same temperature as *Sigma*, **30°C**. Other factors will be figured out in the following sections.

3.3.1 The substrate type and concentration

From the ruthenium red method, PME can catalyze the reaction of both citrus pectin and sugar beet pectin. For a qualitative method, this reason is sufficient for choosing citrus pectin as the substrate. For a quantitative method, however, this is not enough.

PME catalysis depends on the pectin structure. Since the structure of citrus pectin and beet pectin is different, it is possible that the PME can strip off all the methoxyl groups in citrus pectin while only part of the methoxyl groups in beet pectin can be stripped off, and vice versa. Quantitative experiment should be carried on to make sure that PME can strip off all the methoxyl groups in both citrus pectin and beet pectin.

With citrus pectin and beet pectin as substrate respectively, two experiments were carried out in the same way. In every experiment, 5mL of 0.2% pectin and 0.4mL of PME were mixed at pH 7.5 under 30 °C. The released methanol as a function of time was measured. The methanol mass was expressed as a percentage. The theoretically maximum methanol production for citrus pectin and pulp pectin was 87 microgram methanol per gram of citrus pectin and 19 microgram methanol per gram of pulp pectin respectively (from the hydrolysis results by sodium hydroxide in chapter 5). The results are shown in following figure.

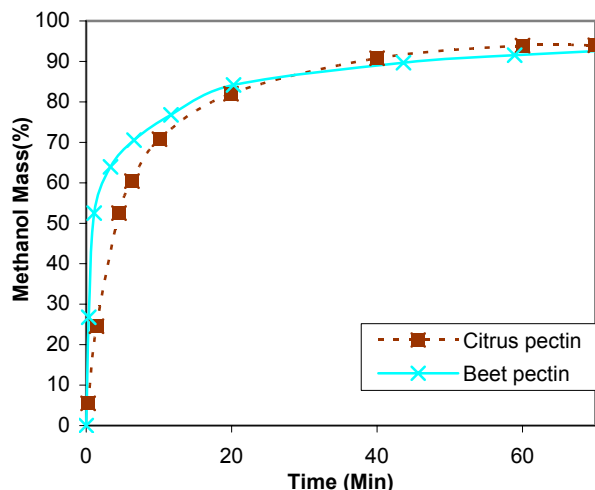


Fig. 3.3-1 PME activity at 30°C with different pectin as substrate

From the above figure, PME can hydrolyze all the methoxyl groups on both citrus pectin and pulp pectin. That means citrus pectin and pulp pectin have similar structure. Therefore, citrus pectin is chosen for the quantitative assay.

Higher concentration is better for the assay since it will decrease slower during the reaction so that the reaction rate is only a function of enzyme activity. Nevertheless, the solubility of pectin in water and the accuracy of the potassium permanganate must be considered. If the concentration of pectin is too high, viscosity of the liquid mixture in potassium permanganate will be high and the accuracy will be low. Depending on the experiments, 0.2% pectin is a proper concentration.

3.3.2 The ratio of substrate to PME, and the reaction time

Other factors that need to be determined include the pH value of the reactants, the ratio of 0.2% citrus pectin to PME and the proper reaction time for the quantitative measurement of PME activity. In this section, the ratio of 0.2% citrus pectin to PME and the proper reaction time will be determined.

As we know, the reaction rate will decrease with the consumption of substrate. For a quantitative analysis of PME activity, the ratio of substrate concentration to PME concentration should be high. The enzyme activity should be measured at the beginning

of the reaction where the reaction rate is constant with the product concentration increasing linearly, and where the rate of production is proportional to the amount of enzyme used.

To do the experiments, the pH value for the reaction should be set at first. PME has a big family. Every member in this family has its own optimum catalysis conditions. The citrus PME were usually assayed at pH 7.5 (Anthon and Barrett, 2003; Mangos and Haas, 2003). Hasunuma measured PME activity from tobacco cells at pH 5 (Hasunuma et al., 2003). PME from *Erwinia chrysanthemi* was assayed at neutral pH (Pitkanen et al., 1992). The PME in my research was also from *Erwinia chrysanthemi*. With reference to these papers, the pH value was set at 7.5 at first. After the ratio of substrate to PME and the reaction time were established, this value was validated again in the next section.

In order to determine the proper reaction time and the ratio of substrate to PME, several parallel experiments were carried out. The ratio of substrate to PME was different in every experiment. In every experiment, samples were taken at intervals and their methanol concentration was measured by potassium permanganate assay. The experiments included two parts, the reaction and the methanol assay. The procedure was as following. The results were shown in Fig. 3.3-2.

Reaction

- (1) Distribute 0.2% pectin solution to several aliquots in test tubes (named reaction tubes), 5mL for each. Each tube was for one substrate to PME ratio.
- (2) Put the reaction tubes into the 30°C incubator. Also, put the PME to be added to the reaction tubes into the incubator. Wait for 30 min. At the same time, prepare the potassium permanganate assay tubes (see the procedure followed).
- (3) Adjust the solution's pH in reaction tubes to 7.5 with 0.25 M Na₂HPO₄ (The initial pH of 0.2% pectin solution was about 3.7. Approximately 31µL of 0.25 M Na₂HPO₄ was added to 1mL of 0.2% pectin solution).

- (4) Add 1mL of PME and water mixture to each reaction tube. The ratios of PME to water were 1:9, 2:8, 3:7, 4:6, and 7:3 (the ratio can be changed depending on the design).
- (5) Take samples, 0.6mL each, from every test tube in intervals. Each sample was added to a ready potassium permanganate assay tube to measure the methanol concentration.

Potassium permanganate assay

- (1) Prepare assay tubes for standard solution.
- Add 310 μL D.I. water, 182 μL H_2SO_4 (5.5N), 8 μL standard solution, and 500 μL 0.2% citrus pectin solution to each tube.
 - The concentrations of standard solution added to each tube were 0%, 0.2%, 0.4%, 0.6%, 0.8% and 1% respectively.
- (2) Prepare assay tubes for samples.
- Several series of assay tubes were prepared. Each series was for one reaction tube. The number of tubes in each series depended on the number of samples to be taken from each reaction tube.
 - Add 218 μL D.I. water and 182 μL H_2SO_4 (5.5N) to each tube.
- (3) Add 0.2 mL reagent A (see potassium permanganate assay in Chapter 2) to each assay tube. Then put all the tubes into ice-water bath.
- (4) Take samples, 0.6mL each, from every test tube in intervals. Each sample was added to an assay tube to measure the methanol concentration.
- (5) Once all the samples had been taken, follow step (2) in the standard procedure of potassium permanganate assay in Chapter 2 to finish the assay.

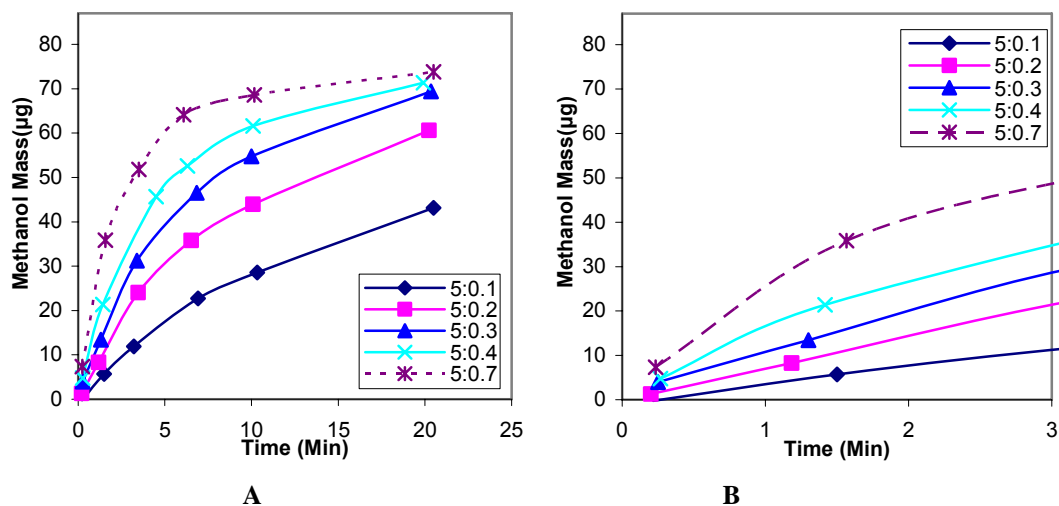


Fig. 3.3-2 PME activity at 30°C with different volume ratio of 0.2% pectin to PME (B is the enlargement of A at the beginning of reaction.)

From Fig.3.3-2 A, the methanol produced was not proportional to the reaction time in a 20min reaction, especially for the reaction with more PME. This was because the reaction decreased once the concentration of pectin decreased significantly. For the enzyme assay, the reaction rate should be constant and be proportional to the enzyme concentration. From Fig. 3.3-2 B, when the reaction time was 3min and when the volume ratios of 0.2% pectin to PME were 5:0.1, 5:0.2 and 5:0.3, these two requirements were satisfied. However, the amount of PME should be defined in a scientific manner. Just the volume of enzyme gives little information.

As mentioned before, one unit of enzyme is equal to the amount of enzyme which will catalyze the transformation of 1 micromole of the substrate per minute under standard conditions. Accordingly, one unit of PME is defined as the amount of PME which will catalyze the hydrolysis of 1 micromole of methoxyl groups per minute in pectin solution at 30°C. From the experiment results, the pectin concentration was 0.17 % (dilute 5mL 0.2% pectin to 6mL). The reaction time was 3min. The activity of added PME was about 10 units per mL. Therefore, the enzyme concentration in reaction for the activity assay should range from 0.17 to 0.5 units per mL.

3.3.3 The cation concentration

The mono- and divalent cation concentration can markedly affect the PME activity (MacDonnell, Jasen, & Lineweaver, 1945; Nakagawa, Yanagawa & Takehana, 1970; Lineweaver & Ballou, 1945; Van Buren, Moyer & Bobinson, 1962; Slezárik & Rexová, 1967; Lee & Macmillan, 1968; Fish & Dustman, 1945; Collins, 1970; Glasziou, 1959; McColloch & Kertesz, 1946; Wang & Pinckard, 1971; Bateman 1963; Manabe, 1973; Kimura, Uchino & Mizushima, 1973; Endo, 1964). Since the PME was obtained by culturing organism in LB media which contain sodium chloride, the effect of sodium cation on PME activity was studied.

The optimum Na^+ concentration was obtained by maintaining pH values around 7.5 and changing the sodium cation concentration from 15mM to 170mM with 1.711M sodium chloride. The following figure shows the relative activities of CC4 and CC7 with the LB as control.

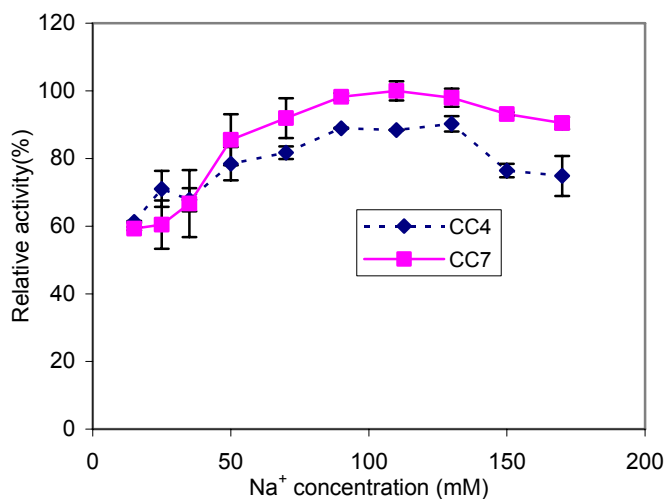


Fig. 3.3-3 Effect of sodium cation concentration on PME activity

From the above figure, the optimum sodium cation concentration ranged from 50mM to 130mM. When the concentration was higher than 50mM, the activity did not change much. Therefore, the concentration of sodium cation in the activity assay was set as 50mM.

3.3.4 The proper pH value

The pH value in the activity assay was set at 7.5 in former experiments. This value resulted from papers about PME. However, my PME is not exactly the same as those in papers. Therefore, this pH value should be validated.

To validate the proper pH value for assay, a series of reaction tubes were prepared with 5 mL of 0.2% citrus pectin in each one. The pH was adjusted to 3.3, 6.5, 7.1, 7.8 and 10.8 respectively and the sodium cation was adjusted to 50mM by 1.711M sodium chloride solution. The enzyme activity in each tube was 0.5 units per minute. The final volume was adjusted to 6mL. The results are shown in the following figure.

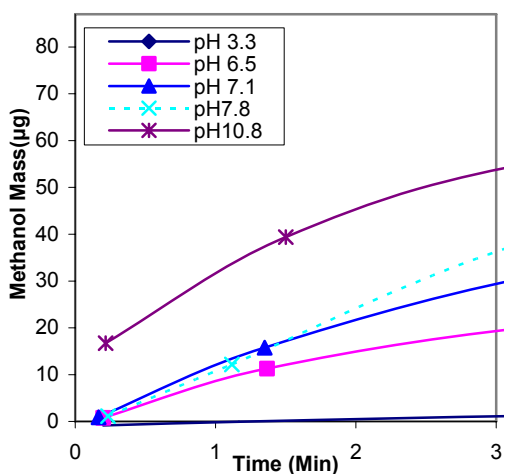


Fig. 3.3-4 PME activity at 30°C at different pH value

The reaction rate can be determined from the slope of the curve. From Fig. 3.3-4, the slopes at pH 7.1 and 7.8 are similar. The curve for pH 10.8 is quite different from others in that the starting point is not zero. This should come from the alkaline deesterification of pectin before the PME was added. To verify it, a similar series of experiments were carried out. This time, no PME was added in each tube. The pH value in the reaction tubes were 3.3, 6.5, 7.1, 7.5, 7.8, 8.9, and 10.4 respectively. The results are shown in Fig. 3.3-5.

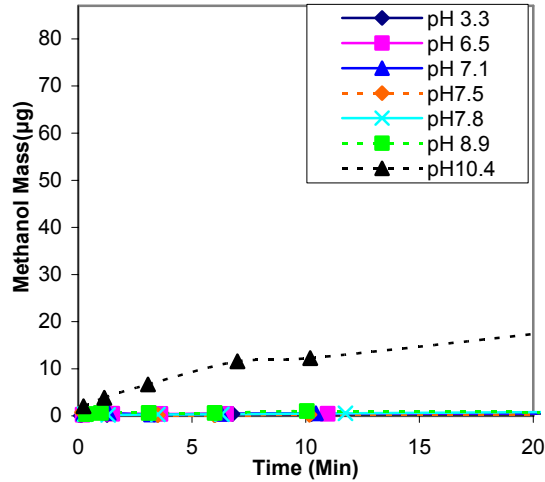


Fig. 3.3-5 Pectin hydrolysis at different pH value

From Fig. 3.3-5, the hydrolysis happened when the pH value was around 10. However, there was almost no hydrolysis when the pH was lower than 9. The measurement of PME activity at high pH is subject to error since alkaline deesterification could affect the enzymatic reaction (Pitkänen, 1992). Therefore, the pH value for the assay should be less than 9.

Further experiments were carried out to find out the optimum pH value for the PME activity assay. In these experiments, the activities of CC4 and CC7 were measured at a different pH value. The pH values were adjusted by 0.25M sodium phosphate buffer. The sodium cation concentration in every experiment was adjusted to 50mM by 1.711M sodium chloride solution. The activities of CC4 and CC7 were relative activities with LB as reference. The results were shown as relative values with the highest activity as 100%. The following figure shows the results.

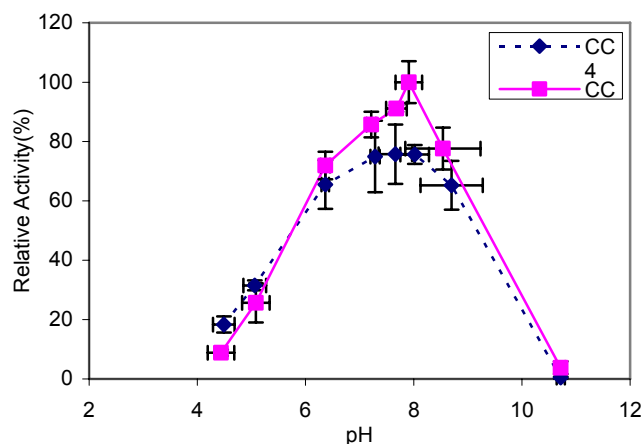


Fig. 3.3-6 Pectin hydrolysis at different pH value

The above figure shows that the optimum pH range for CC4 and CC7 is between 6.4 and 8.8. These results prove that pH 7.5 is a good value for the PME activity assay.

3.3.5 Discussion

Till now, all the factors necessary for the quantitative analysis of PME activity have been determined. For a batch of samples, this quantitative assay is accurate, sensitive and fast. Another advantage of this assay is that its operating volume is small. A 10mL test tube is enough for the assay.

Although similar methods were also reported, most of them maintained the pH value with sodium hydroxide with the aid of an automatic titrator (Collins, 1970; Fish & Dustman, 1945; Lee & Macmillan, 1968; Slezárik & Rexová, 1967; Van Buren, Moyer & Robinson, 1962; Lineweaver & Ballou, 1945; MacDonnell, Jansen and Lineweaver, 1945; Nakagawa, Yanagawa & Takehana, 1969). There are three shortcomings for using the automatic titrator. First, it was not convenient since a titrator must be used. Second, the volume of the reaction mixture was big since two tips should be dipped into the mixture, one for measuring pH and another for titration. Lastly, the cation concentration was changing because of the continuous adding of sodium hydroxide. In fact, in most of those papers, the effects of cations on PME activity were also studied and the optimal

cation concentration was found. Therefore, it was not strict to find the optimal pH value with the cation concentration changing.

Compared with the automatic titration, adding the buffer may have one disadvantage. The automatic titration can control the pH value better while the pH value may change during the reaction if only the buffer is added. However, it depends on how much the pH value changes. From Fig. 3.3-6, a small change does not affect the PME activity. To figure out the pH change, the same experiments as in section 3.3.2 were carried out. Instead of methanol concentration, the pH value was monitored this time. The experiments results are shown in the following figure.

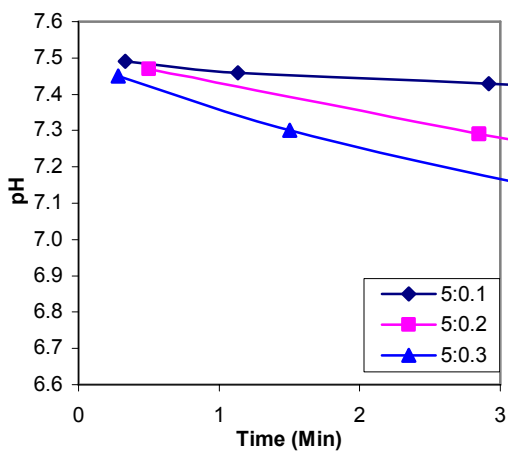


Fig. 3.3-7 pH change during the PME activity measurement at 30°C with different volume ratio of 0.2% pectin to PME

Fig. 3.3-5 shows that the pH decreased less than 0.4 in 3min with the enzyme concentration ranged from 0.17 to 0.5 units per mL. The results in Fig. 3.3-6 show that the reaction rate did not change much between pH 6.4 and 8.8. Therefore, the pH change during the assay does not affect the results much.

3.4 Conclusions and discussion

The methods for both qualitative and quantitative analysis of PME activity were established. These methods will be used to determine the PME activity through the whole project.

The ruthenium red method is convenient and fast. The pectin Petri-Dishes can be prepared and stored in advance. When the qualitative analysis is needed, just drop 5 μL of sample on the gel surface for 20min and stain the gel. One Petri-Dish can test tens of samples simultaneously.

The quantitative assay method for PME activity is better than the method by automatic titration. It is convenient since no titrator is needed, and is accurate since the cation concentration does not change, and economic since the reaction volume is small. One unit of PME is equal to the amount of PME which will catalyze the production of 1 micromole of methanol per minute at 30°C and pH 7.5. The substrate for activity assay is citrus pectin and its concentration is 0.17%. The pH is adjusted by 0.25 M Na_2HPO_4 . The sodium cation concentration is adjusted to 50mM by 1.711 M sodium chloride solution. The enzyme activity in the reaction mixture ranges from 0.16 to 0.50 unit per mL. The reaction time is 3 min. The methanol concentration is measured by potassium permanganate assay.

Chapter 4: PME Production and Characterization

4.1 Introduction

Two kinds of organisms provided by our cooperators in Hood College, CC4 and CC7, were cultured to produce pectin methyl esterase (PME). CC4 was obtained by transfer of a PME gene from *Erwinia chrysanthemi* B374 to One Shot[®] TOP10 competent *E. coli* with pBAD/TOPO[®] ThioFusion[™] Expression Kit (Invitrogen, Catalog No.K370-01). CC7 was a mutant came from a point mutation of CC4. We expected PME produced by CC7 was better than that by CC4 in terms of high temperature catalysis.

In this chapter, the productions of CC4 and CC7 were carried out on a large scale. The molecular weights of CC4 and CC7 and their concentration were measured. The effects of temperature on the reaction kinetics were studied.

4.2 PME production

Since the pBAD/TOPO[®] ThioFusion[™] expression kit has ampicillin resistance gene, CC4 and CC7 can reproduce with the existence of ampicillin while other organisms can't. The kit also has *araC* gene which requires arabinose to induce the PME production. The induction should be in the earlier exponential growth phase of the organism.

The PME was first produced in an Erlenmeyer flask and the optimum conditions were established. During the production, the LB media was prepared and autoclaved at first. The ampicillin was then added to the LB media to a concentration of 0.1 mg/mL after the LB cooled down to 37°C. The organism was inoculated and the flask was incubated at 37°C. Samples of the culture media were taken at intervals to measure the optical density at 600 nm. 0.2% arabinose was added to the media to induce the PME production once the optical density at 600nm was between 0.2 and 0.4. The organism was

cultured an additional 5-10 hours. The PME began to be produced in 30min after the induction. Finally, the cells were spun down and the PME was in the supernatant. Depending on the requirement, the PME in supernatant could be used directly or purified for further study. The following figure shows the results of ruthenium red method in the first 6 hours after induction. From this figure, both CC4 and CC7 had begun to produce PME in 30min after induction although their activities were not as strong as that after 1.6 h.

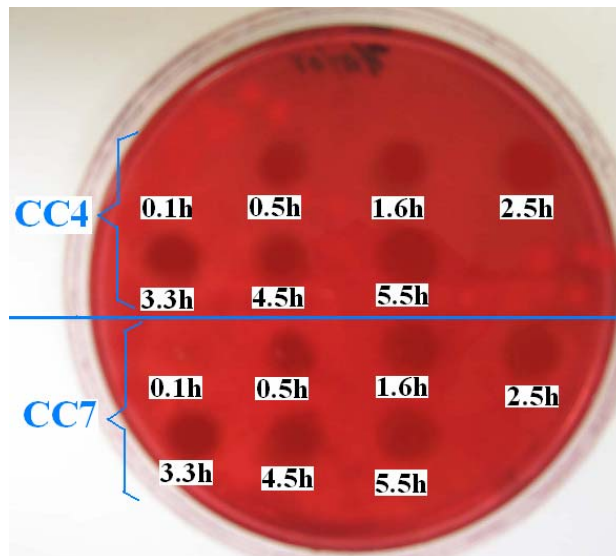


Fig. 4.2-1 The PME production after induction by ruthenium red method

According to the optimum conditions obtained from the PME production experiments in Erlenmeyer flasks, the production of PME was scaled up in fermentor. The purposes were to 1) obtain a big batch of PME so that they can be used in the future studies and the results can be comparable, 2) obtain the precious first hand data for future production in industry. The BioFlo 3000[®] bench-top fermentor was used in my study (New Brunswick Scientific Co., Inc.) as shown in Fig. 4.2-2.



Fig. 4.2-2 PME production with BioFlo 3000[®] bench-top fermentor

The first step of fermentation was to prepare the inocula. The organism was cultured in 200mL LB media at 37°C with the existence of 0.1mg/mL ampicillin in an Erlenmeyer flask. At the same time, the fermentor with 9.8L LB media was autoclaved and cooled down to 37°C (It took several hours.). After all the parameters were set to the desired value, ampicillin was added to the fermentor to a concentration of 0.1mg/mL. Once the optical density in the Erlenmeyer flask was between 0.2 and 0.4, inoculate all the 200mL inocula to the fermentor. Once the optical density in the fermentor was between 0.2 and 0.4, arabinose was added to a concentration of 0.2% to induce the PME production. After an additional 5-10 hours, the PME was harvested. Antifoam (antifoam 204 from Sigma, Lot No.A6426) could be added if necessary during the culture.

The final product, PME, was concentrated with Pellicon[™] cassette filters from Millipore (Fig. 4.2-3). The culture mixture was first pumped through a 0.22 micron cassette filter to get rid of organisms. The filtrate was then filtered by a 30k NMWL (nominal molecular weight limit) cassette filter. Since the molecular weight of PME was 36kDa (shown in next section), most of the PME should be in the retentate by 30k NMWL filter. The flow sheets of operation were shown in Fig. 4.2-4. The PME activities

of every fraction of the culture mixture were quantitatively measured by the potassium permanganate assay developed in Chapter 3 (Fig.4.2-5).

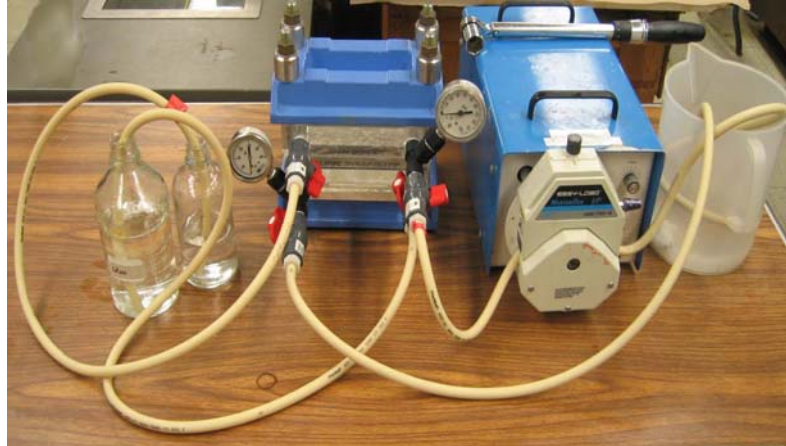


Fig. 4.2-3 Harvest PME_s with Pellicon™ cassette filters

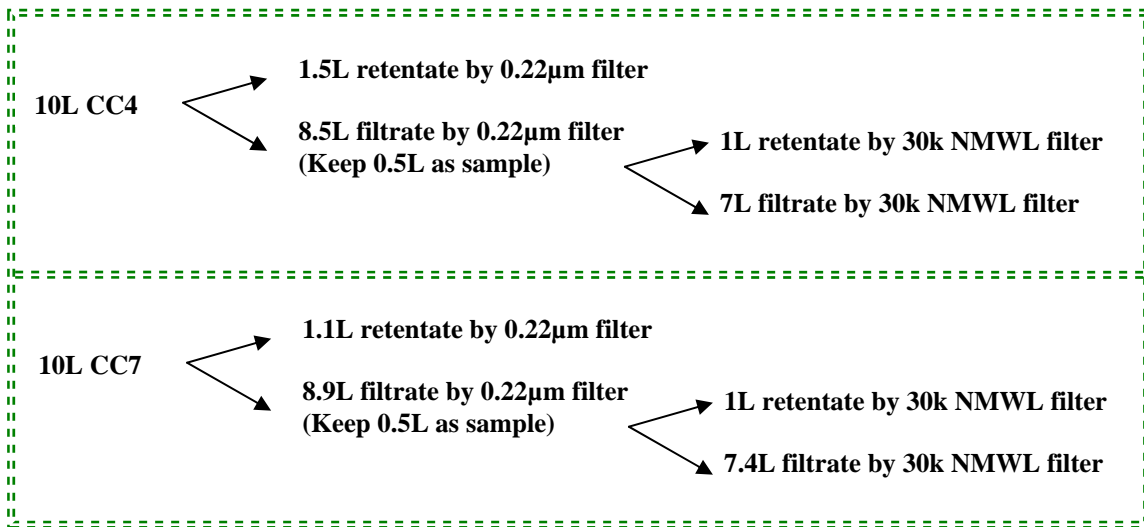


Fig. 4.2-4 Flow sheet of PME_s harvest with Pellicon™ cassette filters

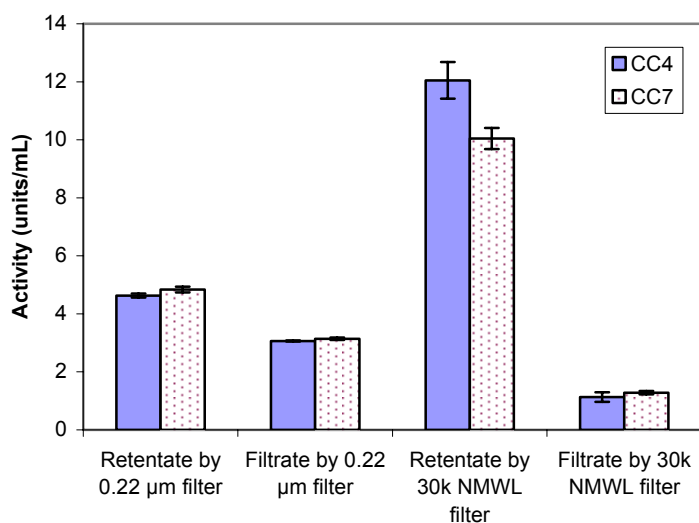


Fig. 4.2-5 PME activities of fractions of culture mixture

Fig. 4.2-5 shows that the PME can be concentrated twice to 3 times by a 30k NMWL filter. This is good for PME storage since less space is needed. In the future study, only the concentrated retentates of CC4 and CC7 by 30k NMWL filter was used.

4.3 Molecular weight and concentration of PME

The parent enzyme has a molecular weight of 36kDa (Plastow, 1988). Our enzymes have similar structure with the parent enzyme except one different amino acid. Therefore, the molecular weight should also be around 36kDa. The molecular weight was determined by Sodium dodecyl sulphate - Polyacrylamide gel electrophoresis (SDS-PAGE). Before the SDS-PAGE, 10mL of the stored PME solution was precipitated by 85% saturation of ammonium sulfate (AS). Most of the proteins were precipitated by such a high concentration of AS. The precipitated proteins were then separated by centrifugation and resolved in 1mL of sodium phosphate buffer (0.25M, pH7) for future SDS-PAGE. The gel was 1mm thick with the composition of 12% for the resolving part and 4% for stacking part. The pre-stained standard, SeeBlue Plus2 was from Invitrogen (Catalog no. LC5925).

In the SDS-PAGE, four samples, non-induced CC4, induced CC4, non-induced CC7, and induced CC7, were run. There should not have PME exist in the non-induced samples. The picture of the gel is as following.

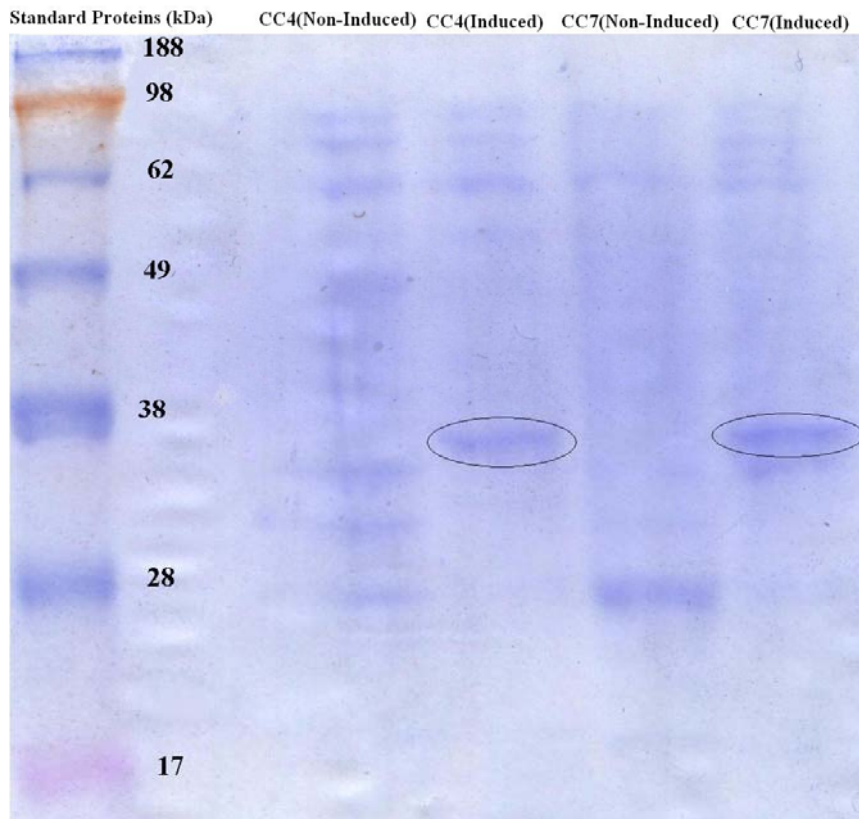


Fig. 4.3-1 SDS-PAGE of PME

From the above figure, we can clearly see that in the induced samples, two bands showed up at the position of 36kDa in induced CC4 and induced CC7 respectively. No bands showed up at the same position in the non-induced samples.

The concentration of total protein in the SDS-PAGE samples was determined by the Bradford assay according to the supplier's instruction (Sigma, Catalog No. B 6916). In details, 1.5mL of Bradford agent and 50 μ L sample were gently mixed and brought to room temperature. The absorbance at 595nm was then measured after 5 min. The protein concentration was determined by comparison of the sample to the standard curve

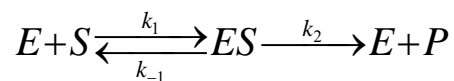
prepared using the standard proteins. The total protein concentrations were 0.22mg/mL for CC4 sample and 0.33mg/mL for CC7 sample.

The concentration of PME was obtained depending on the intensity of the color by the photo process software, ImageJ by NIH. The lane profiles of induced CC4 and induced CC7 were generated. Then, the peaks of interest were enclosed by lines and their areas were measured using the wand tool in ImageJ. The PME percentage was obtained by dividing the peak area at position 36kDa by the total area of all peaks in a lane. The final results showed that approximately 25% of the total proteins were PME in both induced CC4 and induced CC7.

From the electrophoresis results, about 25% of the total protein was PME. Since the protein had been concentrated 10 times by ammonium sulfate precipitation before electrophoresis, the PME concentrations in the initial solution should be 6µg/mL for CC4 and 8µg/mL for CC7.

4.4 Michaelis-Menten kinetics of PME

The most popular mechanistic model for simple enzyme kinetics was developed by V.C.R. Henri in 1902 and by L. Michaelis and M.L. Menten in 1913. Kinetics of simple enzyme-catalyzed reactions is often referred as Michaelis-Menten kinetics (Shuler, 2002). In this model, the single-substrate-enzyme-catalyzed reaction involves a reversible step for enzyme-substrate complex formation and a dissociation step of the enzyme-product complex.



The equation for above reaction is $v = \frac{V_m[S]}{K_m + [S]}$. The maximum reaction rate, V_m , is equal to $k_2[E_0]$ where $[E_0]$ is the initial enzyme concentration. The Michaelis-Menten

constant, K_m , is a function of k_1 , k_{-1} , and k_2 . For the rapid equilibrium assumption, K_m is equal to k_{-1}/k_1 . For the quasi-steady-state assumption, K_m is equal to $(k_{-1}+k_2)/k_1$.

Equation $v = \frac{V_m[S]}{K_m + [S]}$ can be linearized in double-reciprocal form, which is

$\frac{1}{v} = \frac{1}{V_m} + \frac{K_m}{V_m} \frac{1}{[S]}$. The determination of values for K_m and V_m can be obtained by a series

of initial-rate experiments with different initial substrate concentration. In these experiments, known amount of substrate $[S_0]$ and enzyme $[E_0]$ were mixed and the initial reaction rates were measured. Using the initial substrate concentration as $[S]$, a linear plot of $\frac{1}{v}$ versus $\frac{1}{[S]}$, named Double-reciprocal plot or Lineweaver-Burk plot can be obtained.

The intercept of the plot is $\frac{1}{V_m}$, and the slope of the plot is $\frac{K_m}{V_m}$. Once V_m is known,

$k_2 = \frac{V_m}{[E_0]}$ can be calculated.

In my experiments, the initial pectin concentrations were 0.7, 1.0, 1.4, 1.7, 2.1, 2.8, and 3.5 g/L respectively. The pH value was 7.5. The CC4 activity in the reaction mixture was 0.80units/mL. The CC7 activity in the reaction mixture was 0.67units/mL. Since the concentrations of CC4 and CC7 were 5.6 μ g/mL and 8.2 μ g/mL respectively, the specific activities of CC4 and CC7 were 143units/mg and 82units/mg, which are in the same level magnitude as orange PME (Körner, Zimmermann, and Berk, 1980). This value is ten times lower than the reported value for *Erwinia chrysanthemi* B374 PME (Pitkänen, Heikinheimo, and Pakkanen, 1992). This is because the purity of my PME was lower.

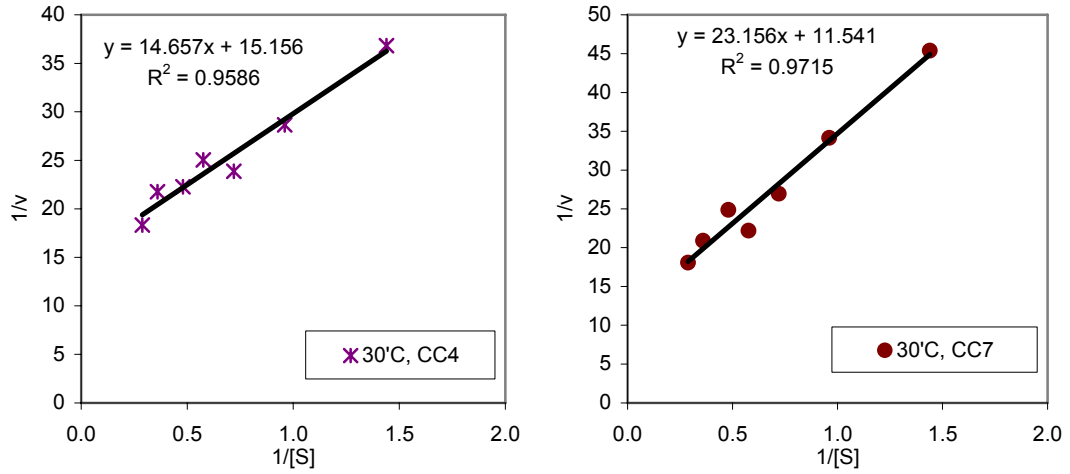


Fig. 4.4-1 Lineweaver-Burk plot of CC4 and CC7 at 30°C
(The unit of [S] is g/L. The unit of v is g/L-min.)

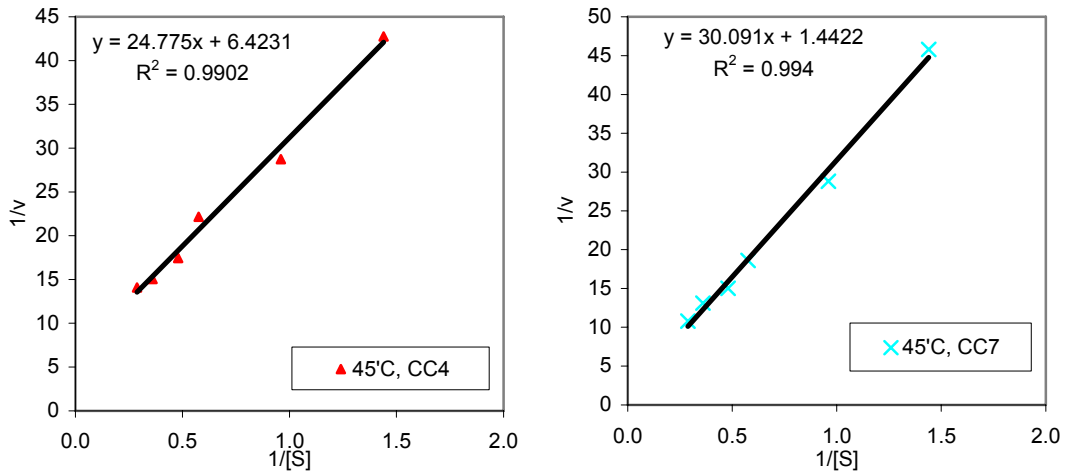


Fig. 4.4-2 Lineweaver-Burk plot of CC4 and CC7 at 45°C
(The unit of [S] is g/L. The unit of v is g/L-min.)

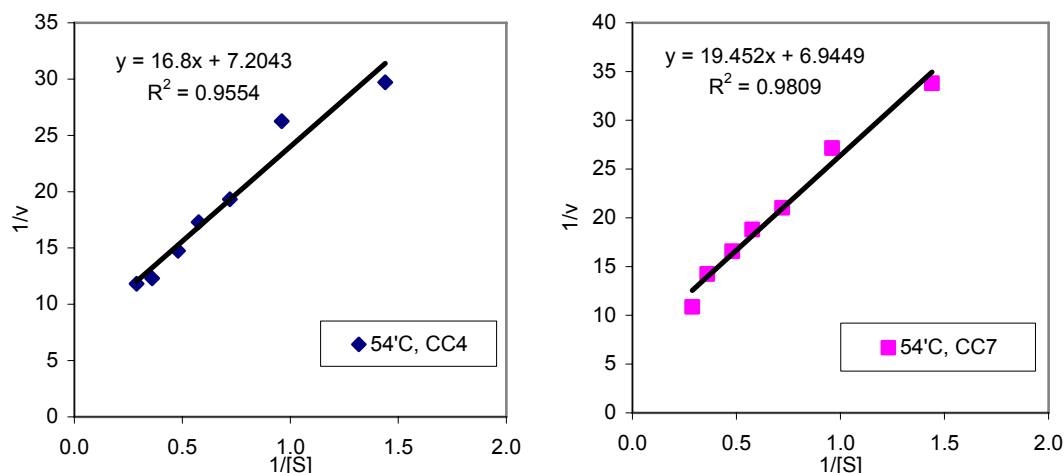


Fig. 4.4-3 Lineweaver-Burk plot of CC4 and CC7 at 54°C
(The unit of [S] is g/L. The unit of v is g/L-min.)

From the Lineweaver-Burk plots, K_m and V_m for CC4 and CC7 at different temperature can be calculated. See the following table for the results.

Table 4.4-1 V_m , K_m , and k_2 for CC4 and CC7 at different temperature

	CC4			CC7		
	30°C	45°C	54°C	30°C	45°C	54°C
V_m (g·L ⁻¹ ·min ⁻¹)	0.07	0.16	0.14	0.09	0.69	0.14
K_m (g·L ⁻¹)	0.97	3.86	2.33	2.01	20.86	2.80
k_2 (min ⁻¹)	177	417	372	158	1268	263

From Table 4.4-1, the level of magnitude of K_m value agrees with the previously report of orange PME (Hagerman and Austin, 1986; Tipson and Horton, 1976). It is also consistent well with the reported value for *Erwinia chrysanthemi* B374 (Pitkänen, Heikinheimo, and Pakkanen, 1992). Depending on this table, the reaction rate as a function of substrate concentration can be obtained by equation $v = \frac{V_m[S]}{K_m + [S]}$ as shown in the following figures.

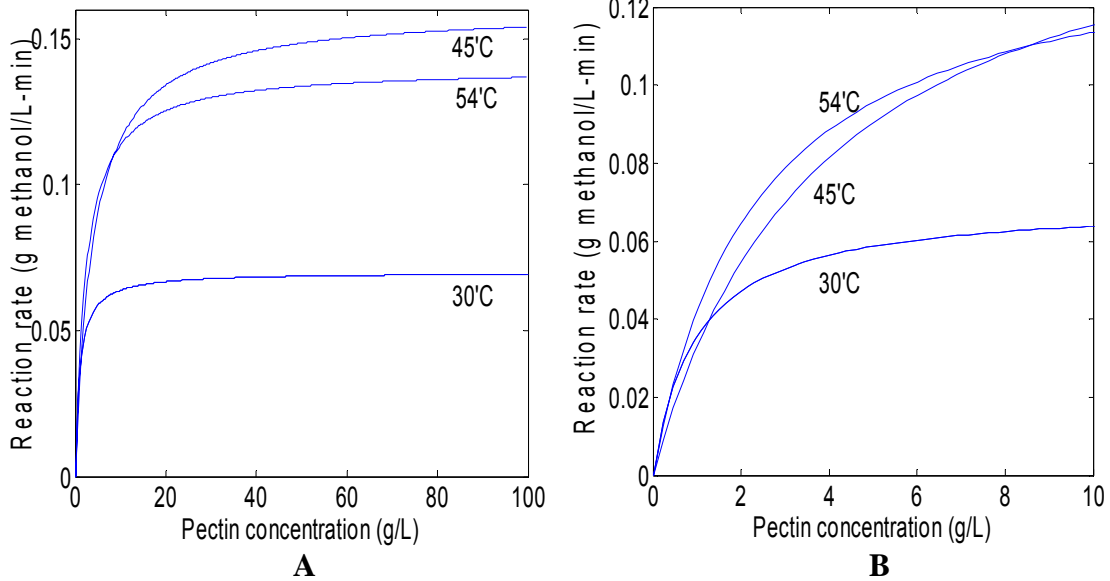


Fig. 4.4-4 Reaction rate versus pectin concentration under the catalysis of CC4 (B is the enlargement of A at low concentration)

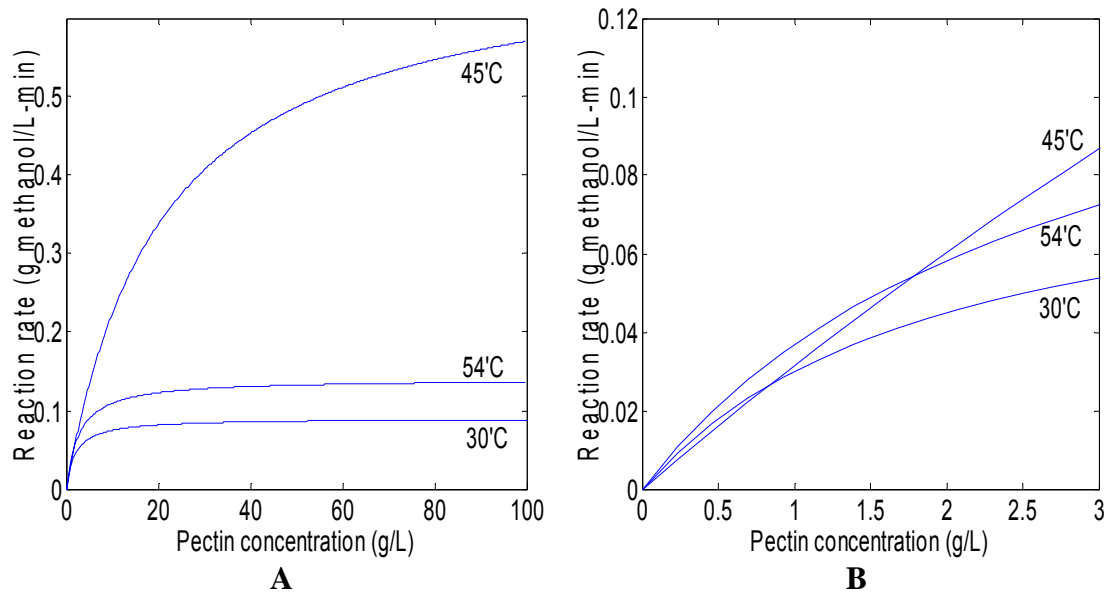


Fig. 4.4-5 Reaction rate versus pectin concentration under the catalysis of CC7 (B is the enlargement of A at low concentration)

From Fig. 4.4-4 and 4.4-5, the reaction rates at 45°C and at 54°C are similar when the pectin concentration is low. However, the reaction rate at 45°C is higher than that at 54°C when the pectin concentration is high. This result is contradictory to our understanding of the relation between reaction rate and temperature. From Table 4.4-1, when the pectin concentration is low, it is in the same order of magnitude as K_m .

Therefore, the reaction rate was controlled by both V_m and K_m . On the other hand, when the pectin concentration is high, it is in a higher order of magnitude than K_m . Therefore, the reaction rate is mainly controlled by V_m .

The results in Table 4.4-1 show that the maximum reaction rate at 45°C is higher than that at 54°C for both CC4 and CC7. This is because the deactivation speed of PME at 54°C is higher than that at 45°C. The effects of temperature on the PME activity will be discussed in details in the next section.

4.5 Effect of temperature on the activity of PME

The rate of enzyme-catalyzed reactions increases with the increase of temperature. For simple enzyme-catalyzed reactions, the reaction rate increases with temperature according to the equation $v = k[E]$, where k varies with temperature according to Arrhenius equation $k = Ae^{-E_a/RT}$ (Shuler, 2002). However, the rate of enzyme deactivation also increases with the increase of temperature. This is known as temperature inactivation or thermal deactivation. The kinetics of thermal deactivation can be expressed as $[E] = [E_0]e^{-k_d t}$, where $[E_0]$ is the initial enzyme concentration and k_d is the deactivation constant. k_d also varies with temperature according to the Arrhenius equation $k_d = A_d e^{-E_d/RT}$ (Shuler, 2002).

4.5.1 The kinetics of thermal deactivation of PME

In a reaction, if all other factors are maintained constant except the enzyme concentration, the reaction rate is proportional to the concentration of active enzyme. The deactivation constant at a certain temperature can be determined by this principle.

My experiment was carried out this way: a small amount of enzyme (to make sure the enzyme can be quickly balanced in the oven) was heated in an oven, which was pre-set to desired temperature. The enzyme activity versus heating time was then measured with the assay developed in chapter 3. Since the kinetics of thermal

deactivation of enzyme can be expressed as $[E] = [E_0]e^{-k_d t}$, the activity of enzyme under heat is proportional to $e^{-k_d t}$. Therefore, if the curve of activity versus time can be expressed as an exponential curve, the deactivation constant k_d can be obtained. Furthermore, from k_d values at different temperature, the deactivation energy E_d can be calculated by equation $k_d = A_d e^{-E_d/RT}$. The following figures show the result of residual activity versus heating time.

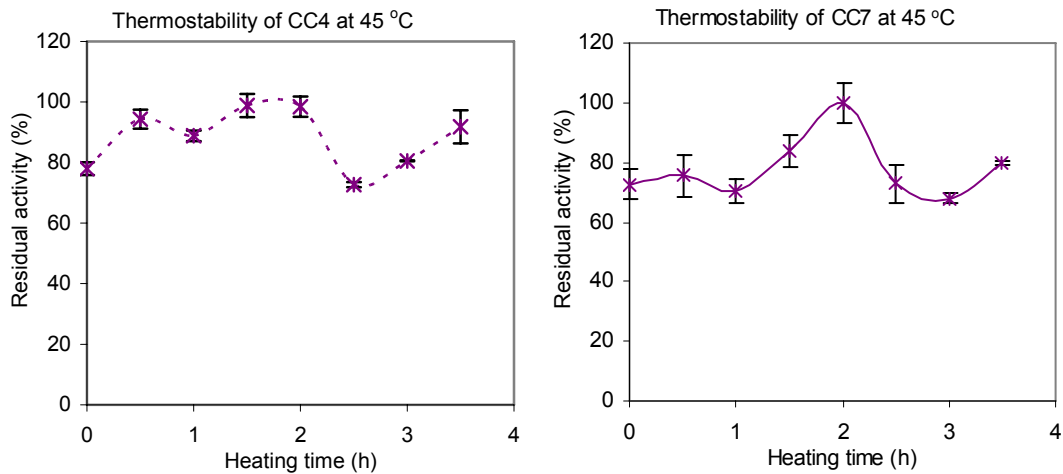


Fig. 4.5-1 Thermostability of PME at 45°C

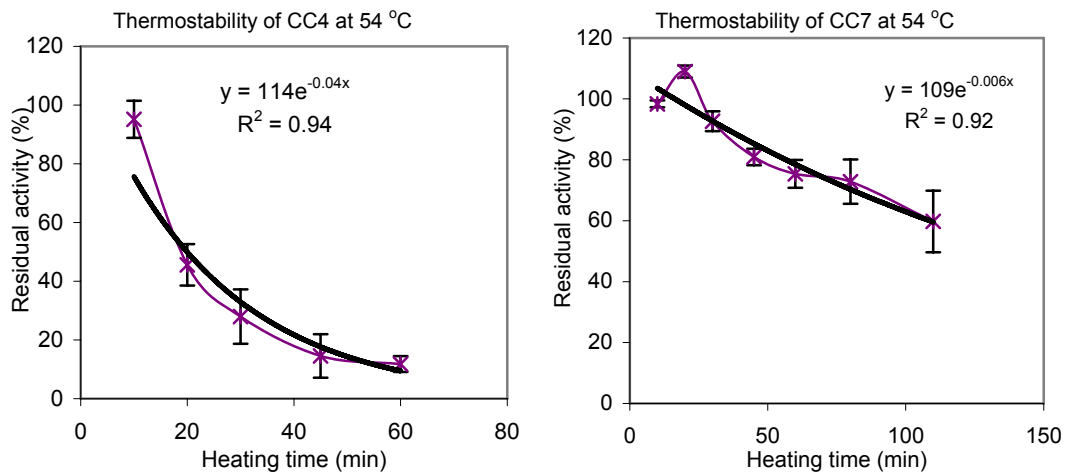


Fig. 4.5-2 Thermostability of PME at 54°C

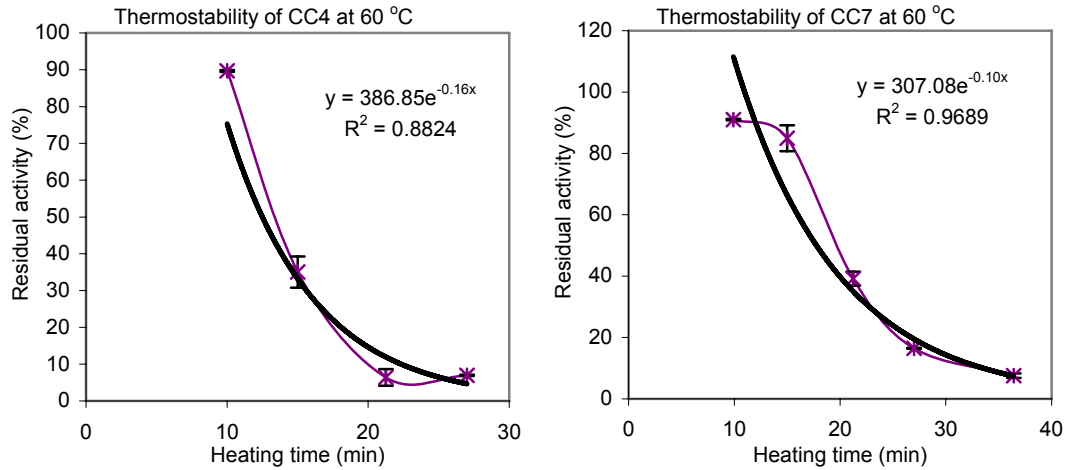


Fig. 4.5-3 Thermostability of PME at 60 °C

From the above figures, CC4 and CC7 were rather stable at 45°C. There was no significant deactivation at this temperature in 4 hours. The deactivation constants for CC4 and CC7 at 54°C and 60°C can be obtained from the curve equation in Fig. 4.5-2 and Fig. 4.5-3. From the deactivation constants of CC4 and CC7 at 54°C and 60°C, the deactivation energy of CC4 and CC7 can be calculated by equation $k_d = A_d e^{-E_d/RT}$ at different temperatures. From $k_{d,1} = A_d e^{-E_d/RT_1}$ and $k_{d,2} = A_d e^{-E_d/RT_2}$, we can get

$$\frac{k_{d,1}}{k_{d,2}} = \frac{A_d e^{-E_d/RT_1}}{A_d e^{-E_d/RT_2}} = e^{\frac{E_d}{R} \left(\frac{1}{T_2} - \frac{1}{T_1} \right)} \quad (4.5-1)$$

Therefore, the deactivation energy can be expressed as

$$E_d = R \cdot \ln \left(\frac{k_{d,1}}{k_{d,2}} \right) / \left(\frac{1}{T_2} - \frac{1}{T_1} \right) \quad (4.5-2)$$

The constant A_d can be calculated by equation $k_d = A_d e^{-E_d/RT}$ once the values of k_d and E_d have already been obtained. The deactivation constant k_d , deactivation energy E_d , and constant A_d of CC4 and CC7 are shown in following table.

Table 4.5-1 The Arrhenius equation parameters of CC4 and CC7

	CC4	CC7
k_d at 54°C (min ⁻¹)	0.04	0.006
k_d at 60°C (min ⁻¹)	0.16	0.10
E_d (kcal·mol ⁻¹)	50	101
A_d (min ⁻¹)	1.02×10^{32}	1.82×10^{65}

From Table 4.5-1, the deactivation speed of CC4 was much faster than that of CC7 at 54°C. The deactivation speed of CC4 was at the same order of magnitude as that of CC7 at 60°C although the deactivation of CC4 was a little faster than that of CC7. These results show that CC7 was much more stable than CC4 at 54°C. Once the temperature was as high as 60°C, however, both CC4 and CC7 were deactivated fast.

The deactivation energies of CC4 and CC7 were 209 kJ·mol⁻¹ and 425 kJ·mol⁻¹ respectively, or 50 kcal·mol⁻¹ and 101 kcal·mol⁻¹ respectively. These values are consistent with the data in literature which vary between 40 and 130 kcal/mol (Shuler, 2002).

According to the data in Table 4.5-1, we can actually simulate the deactivation curve by the equation. Substitution of equation $k_d = A_d e^{-E_d/RT}$ into equation $v = A e^{-E_a/RT} [E_0] e^{-k_d t}$ yields

$$v = A e^{-E_a/RT} [E_0] e^{-(A_d e^{-E_d/RT})t} \quad (4.5-3)$$

The activation energy of enzyme-catalyzed reaction, E_a , is between 4 and 20 kcal/mol (mostly about 11kcal/mol) (Shuler, 2002). The activation energy is assumed to be 11kcal/mol. Since the value of $A[E_0]$ is a constant, it can not affect the relative activity. The gas constant R is 1.987cal mol⁻¹ K⁻¹. The data for A_d and E_d can be gotten from Table 4.5-1. Therefore, the reaction rate equation for CC4 can be obtained as

$$v = A [E_0] e^{-\frac{5536}{T}} e^{-(1.0 \times 10^{32} \times e^{-\frac{25163.6}{T}})t} \quad (4.5-4)$$

and the reaction rate equation for CC7 can be obtained as

$$v = A [E_0] e^{-\frac{5536}{T}} e^{-(1.8 \times 10^{65} \times e^{-\frac{50830.4}{T}})t} \quad (4.5-5)$$

Since the reaction rate is proportional to the residue activity of enzyme, the residue activities of CC4 and CC7 as a function of time can be obtained according to Eq.(4.5-4) and Eq.(4.5-5). The simulation results (Fig. 4.5-4) can be compared with the experiment results (Fig. 4.5-4). Fig. 4.5-4 is same as Fig. 4.5-2.

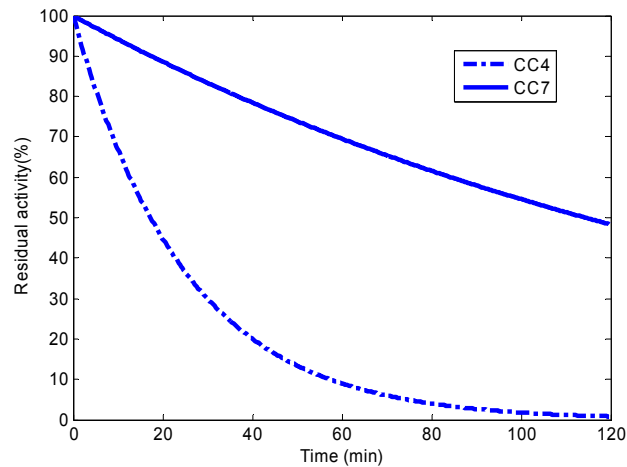


Fig. 4.5-4 Residual activity as a function of time at 54°C (Simulation)

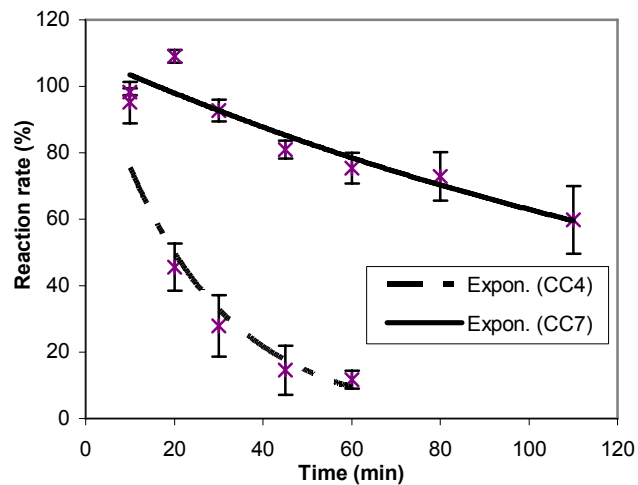


Fig. 4.5-5 Residual activity as a function of time at 54°C (Experiments)

Comparison of Fig. 4.5-4 with Fig. 4.5-5 shows that the model results and experiment results are consistent with each other. Both of these two figures show that about 50% of CC7 was denaturated after 2 hours, while almost 100% of CC4 was

denaturated after 2 hours. The deactivation of CC4 was faster than that of CC7. CC7 can work at higher temperature for a longer time.

4.5.2 The optimum reaction temperature

Because of the deactivation of enzyme as discussed above, the enzyme activity will increase with temperature to a maximum value and then decrease. Therefore, it is necessary to find the relation between reaction rate and temperature.

To test the optimal reaction temperature, the following steps were carried out at each temperature: 1) Set the oven to desired temperature; 2) In each of three tubes, mix 2.5 mL of 0.2% pectin, 78 μL of 0.25 M Na_2HPO_4 , and 222 μL of water; 3) Put the three tube in oven to preheat 20 min. At the same time, warm enzyme at 30°C incubator for 20min; 4) Add 0.2 mL of enzyme to each tube respectively; 5) Take 0.6mL of samples of each tube after 3 min to measure the methanol concentration; 6) Calculate the reaction rate and standard error. In these experiments, the enzyme and the substrate were dispersed in a molecular scale in the solution so that the enzyme could easily attack the substrate. The results are shown in the following figure.

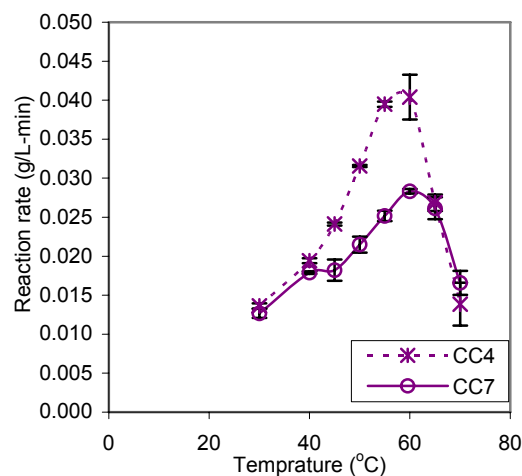


Fig. 4.5-6 Effect of temperature on the activity of PME
(The initial activity of CC4 in the mixture was 0.85 units/mL.
The initial activity of CC7 in the mixture was 0.45 units/mL.)

From the above figure, the reaction rates for CC4 and CC7 have maximum values at around 60°C. The temperature where CC7 has the maximum reaction rate is several degrees higher than that where CC4 has.

We should note that the nature of the plot will depend on the length of time the reaction mixture is exposed to the test temperature (Shuler, 2002). As shown in Eq.(4.5-3), the reaction rate keeps changing with time. Although the sample is taken in the first several minutes, the reaction rate is still an average number from the beginning to the time sample is taken. Therefore, the measured optimum reaction temperature is different depending on when the sample is taken. The average reaction rate can be calculated by integration of Eq.(4.5-3) as following

$$\begin{aligned}
 v_{ave} &= \frac{1}{t_{total}} \int v \cdot dt \\
 &= \frac{1}{t_{total}} \int A e^{-E_a/RT} [E_0] e^{-(A_d e^{-E_d/RT})t} \cdot dt \\
 &= \frac{A[E_0]}{A_d} \cdot \frac{1}{t_{total}} \cdot e^{-\frac{E_a}{RT}} \cdot e^{\frac{E_d}{RT}} \cdot e^{-(A_d e^{-E_d/RT})t_{total}} \quad (4.5-6)
 \end{aligned}$$

where t_{total} is the time when sample is taken. From this equation the average reaction rate as a function of temperature can be obtained. Since the value of $\frac{A[E_0]}{A_d}$ is a constant and

its actual temperature does not affect the results of optimal temperature, it is assumed to be 1. The figure depending on Eq.(4.5-6) can then be obtained by MATLAB. Fig. 4.5-7 shows the results for CC4 and CC7 when t_{total} is 3min and 30min respectively.

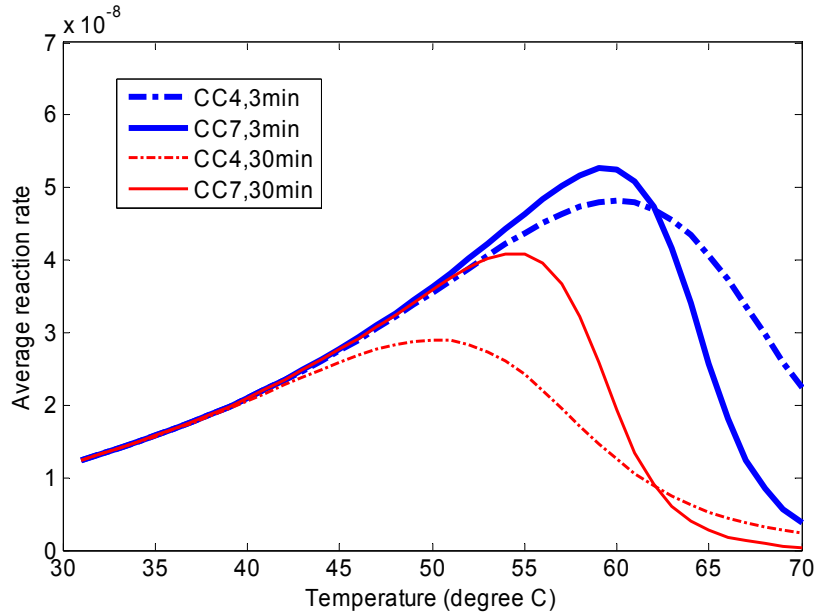


Fig. 4.5-7 Average reaction rate as a function of temperature
(The Y axis values are just relative values.)

From Fig. 4.5-7, the simulation results of CC4 and CC7 for a 3min reaction consistent well with the experiment results in Fig. 4.5-4. Both of these two figures show that the optimal temperatures for CC4 and CC7 are around 60°C. The optimal temperature shifts left and the average reaction rate decreases when the sampling time changes from 3min to 30 min. The reason is that longer exposure time can denaturize more enzyme. Therefore, to achieve maximum average reaction rate in a longer reaction time, the temperature should be lowered so that the enzyme denaturize slower. By similar figures, the optimal temperature as a function of sampling time can be obtained (Table 4.5-2, Fig. 4.5-8).

Table 4.5-2 The Arrhenius equation parameters of CC4 and CC7

Sampling time (min)	CC4 (°C)	CC7 (°C)
3	60	59
10	55	57
20	52	55
30	50	54
60	47	53
120	44	52
180	43	51
240	42	50
300	41	50
360	40	49

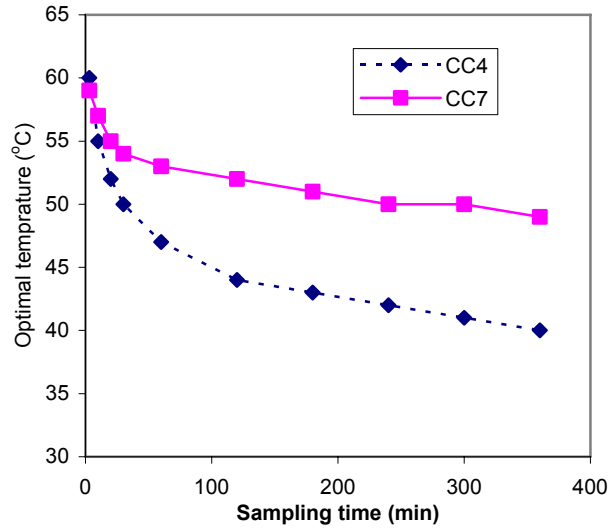


Fig. 4.5-8 Optimal temperature as a function of sampling time

Table 4.5-2 and Fig. 4.5-8 are useful to determine the optimum reaction temperature for a batch reactor. Assume substrate and enzyme are added to a batch reactor. If we do not add new enzyme during the reaction and the total reaction time is fixed, what is the optimal reaction temperature? The answer can be obtained directly from Table 4.5-2 or Fig. 4.5-8.

4.6 PME stability during storage

In real production, the PME should be produced in advance. The produced PME will then be stored for future production. Depending on the actual condition, the storage

time can be shorter or longer. Therefore, we want to know if the PME activity will change during storage.

A batch of PMEs, CC4 and CC7, were produced on July 14, 2005. The enzymes were then stored in a refrigerator at 4°C for several months. Their activities were tracked by the method developed in Chapter 4. The results were shown bellow.

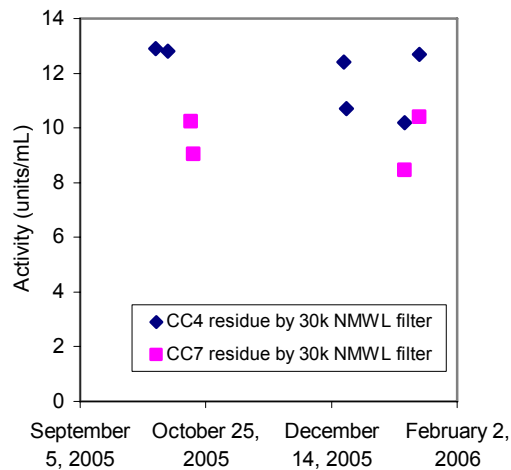


Fig. 4.6-1 PME stability during storage

From Fig. 4.6-1, the enzyme activity almost did not change between October 5, 2005 and January 18, 2006. Both CC4 and CC7 were rather stable.

Chapter 5: Produce Methanol from Beet Pulp

5.1 Introduction

Till now, the quantitative analysis of methanol, the assay of PME activity, and the PME kinetics study have been finished. However, our goal is to produce methanol from sugar beet pulp, not pectin.

In this chapter, the pectin in sugar beet pulp was characterized at first. The methoxyl groups' content in beet pulp was measured and the theoretical yield of methanol from beet pulp was calculated. The effects of pH value, organisms, temperature, etc on the methanol production from sugar beet were then studied.

5.2 Characterization of pectin in sugar beet pulp

Sugar beet is abundant in pectin and pectin in turn is abundant in methoxyl groups. If the content of methoxyl groups in beet pulp is known, the theoretical yield of methanol from beet pulp can be obtained. To measure the content of methoxyl groups, the pectin was extracted from the beet pulp at first. The methoxyl groups in the pectin were then totally hydrolyzed and the amount of methanol was assayed, depending on which the content of methoxyl groups was calculated.

5.2.1 Extraction of pectin from sugar beet pulp

Pectins are a group of closely associated polysaccharides from the primary cell walls and intercellular regions of higher plants. Pectins have a relative solubility in water and no solubility in ethanol (Ujejski, 1957). The extraction of pectins from different plants has been studied for decades. Depending on the size of beginning material, the first step of pectin extraction is usually grinding the material in ethanol or acetone, following by washing with methanol to inactivate endogenous enzyme instantaneously and removal of alcohol-soluble solids. The alcohol-insoluble residue (AIR) is then treated sequentially

with water, chelating agents (ammonium oxalate, sodium hexametaphosphate, ethylene diamine tetraacetate(EDTA), cyclohexane diamine tetraacetate(CDTA)), acid, and alkali(Stephen, 1995). Among these steps, the highest amount of pectin is generally extracted by hot acid. The pectin extracted account 59% of the total pectin extracted (Thibault, 1988; Rombouts, Thibault, 1986). Alkaline extraction can also extract lots of pectin. However, it decreases the degree of methylation (DM). Water and chelating agents only extract minor amount of pectin.

Extraction of Alcohol-insoluble residues (AIR) from sugar beet

A widely used procedure for sugar beet pectin extraction was developed by Rombouts and Thibault (Rombouts and Thibault, 1986). Since only a small amount of pectin can be extracted by water and chelating, only acidic extraction followed by alkaline extraction was applied in my experiments.

AIR was extracted from drip-dry pulp (14.43% dry weight). The mixture of 850mL of 95% ethanol and 200g of drip-dry pulp was added into a 2L flask with a condenser installed. The flask was heated to boiling and maintained boiling for 30 min. The mixture was filtered and the filtrate was discarded. The insoluble material was washed with 250mL of 95% ethanol and then with 250mL of acetone. The insoluble material was separated and dried. The results are shown in the following table.

Table 5.2-1 Results of AIR extraction

Mass of Wet Pulp (g)	Mass of Dry Pulp (g)	Mass of AIR (g)	AIR Fraction in Dry Pulp
200	28.86	27.48	95.2%

Extraction of pectin from AIR

The mixture of 1750mL of 0.05M HCl and 27.48 g of dry AIR was added into a flask with a condenser. After 40 min of soaking, the mixture was heated to 85±5 °C and

maintained for 1h. When the mixture was cooled down, it was filtered and the filtrate was collected. The filtrate was then neutralized to pH 4.5 with 1.5M NaOH to obtain solution A. Continuously, 1750mL of 0.05M NaOH was added to the residue from filtration and the mixture was maintained at 18°C for 1h. The mixture was then filtered and the filtrate was collected. The filtrate was neutralized to pH 4.5 with 6M HCl to obtain solution B. Solution A and B were lyophilized to obtain acid-soluble pectin and alkali-soluble pectin. The masses of acid-soluble pectin and alkali-soluble pectin are shown bellow.

Table 5.2-2 Results of pectin extraction from AIR

Mass of AIR (g)	Acid-soluble pectin		Alkali-soluble pectin	
	Mass (g)	Fraction in AIR (%)	Mass (g)	Fraction in AIR (%)
27.48	12.2	42.4%	4.5	15.7%

5.2.2 Measurement of methoxyl group content in sugar beet pectin

The methoxyl group content in pectins is usually measured by alkaline deesterification followed by methanol assay. The details of the alkaline deesterification condition in different paper are different. Rombouts and Thibault dialyzed pectin solution (4mg/mL) against sodium hydroxide (0.05M) at 2°C for 6 h (Rombouts & Thibault, 1986). Levigne et al. released the methanol by sodium hydroxide (0.5M) at 4°C for 1 h (Levigne, Ralet, & thibault, 2002). Kravtchenko et al. hydrolyze the pectin by potassium hydroxide (0.5M) at 5°C for 1 h.

In my experiments, 0.25mL of 1.5 M sodium hydroxide was added to 0.5mL of 0.2% pectin. After 1 h at 4°C, the samples were acidified by 0.25mL of 5.5N H₂SO₄. The methanol concentration was then assayed by continuing step 2 in the potassium permanganate assay developed in Chapter 2.

Finally, 27 mg methanol was obtained from 1 gram of acid-soluble pectin and 7 mg methanol was obtained from 1 gram of alkali-soluble pectin. Together with the results in Table 5.2-2, 13mg methanol can be obtained from 1g dry beet theoretically.

The methoxyl group content in commercial citrus pectin and apple pectin from Sigma were also assayed in the same way. 87mg of methanol and 90mg of methanol were obtained from 1g of commercial citrus pectin and 1g of commercial apple pectin respectively. The methoxyl group contents in citrus pectin and apple pectin were higher than that in sugar beet pectin. The result for citrus pectin is consistent with the results in literature (Klavons & Bennett, 1986).

5.3 Effects of pH value on methanol production from sugar beet pulp

The pH value is an important factor for the reaction. In Chapter 4, the results showed that PME work more effectively on pectin at neutral or a little alkaline pH value than at acidic pH value. In this chapter, I will only discuss the effect of pH value on the hydrolysis of beet pulp.

Ester bond can be hydrolyzed in alkaline condition. At different pH values and different temperatures, the hydrolysis rate is different. In Chapter 3, the PME activity assay was carried out at pH 7.5 and 30°C and the hydrolysis of pectin in this condition was studied. The results showed no significant hydrolysis within 20 min. However, since our production process of methanol from pulp will be carried on in several hours at higher temperature, the hydrolysis of pectin at higher temperature for a longer time could happen. The experiments were carried out in the same way as in Chapter 3. The control experiments at pH 4.2 were also carried out at the same time. The results are shown below.

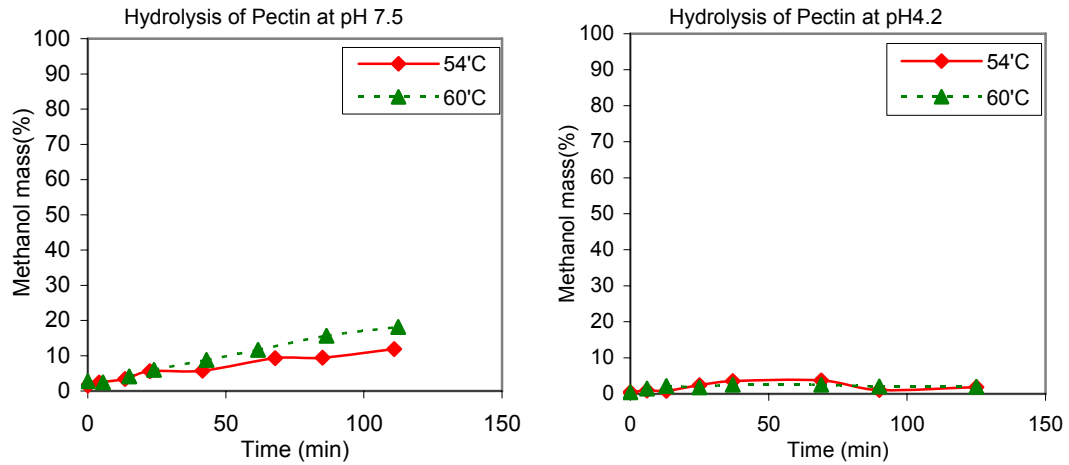


Fig. 5.3-1 Pectin hydrolysis at different temperatures and pH values

From above figures, the hydrolysis at pH 7.5 was significant while that at pH 4.2 was ignorable. Depending on these results, we wonder if the hydrolysis of sugar beet pulp is also significant at pH 7.5. Experiments were carried on to find the answer.

The beet pulp and water were added into a sealed Erlenmeyer flask. The pH value was adjusted by 0.25M of Na_2HPO_4 buffer every 30min to maintain the value between 7 and 7.5. The dry weight of the wet pulp was 12%. The reaction was at 54°C. A syringe was used to take samples at intervals. Samples were centrifuged to measure methanol concentration by potassium permanganate assay. The results are shown bellow.

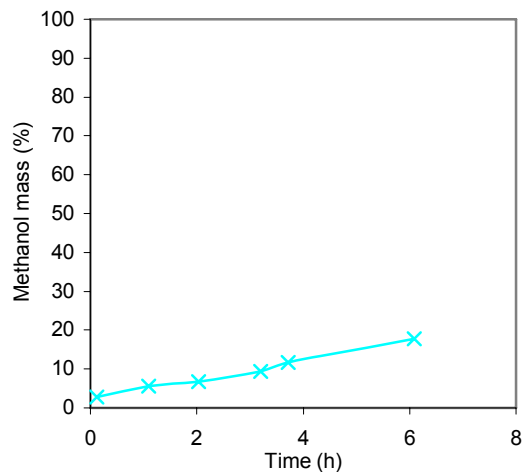
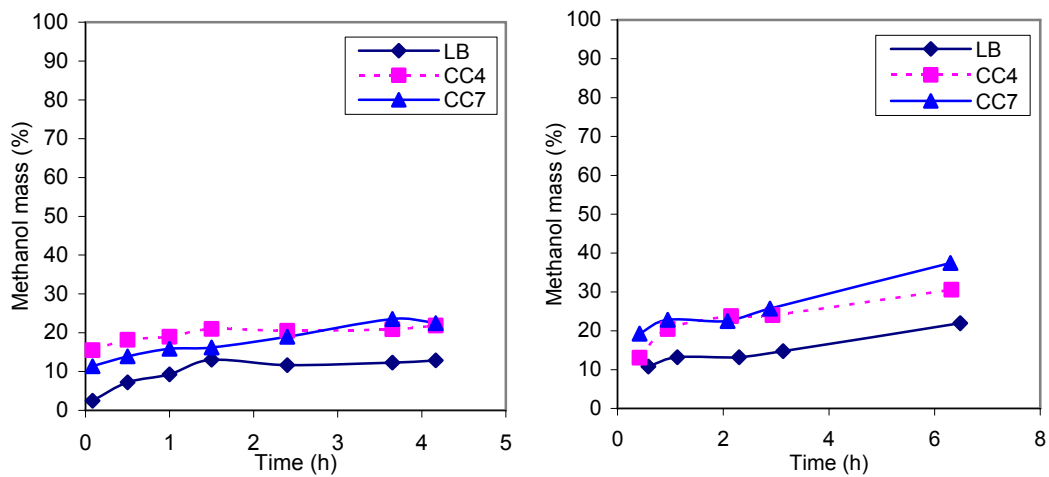


Fig. 5.3-2 Hydrolysis of pulp at pH 7~7.5 at 54°C

Fig. 5.3-2 shows a significant hydrolysis by buffer. Similar experiments were repeated. This time, LB, CC4 and CC7 were added respectively. The control experiments in which no buffer was added were also carried out. The methanol mass as a function of time is shown in Fig. 5.3-3. The methanol mass is expressed as a relative mass (actual mass divided by the theoretical maximum mass). Furthermore, the decrease of PME activity in these experiments was also measured (Fig. 5.3-4) by the assay developed in Chapter 3.



A. No buffer added

B. Maintain neutral pH by buffer

Fig. 5.3-3 Produce methanol from pulp at 54°C

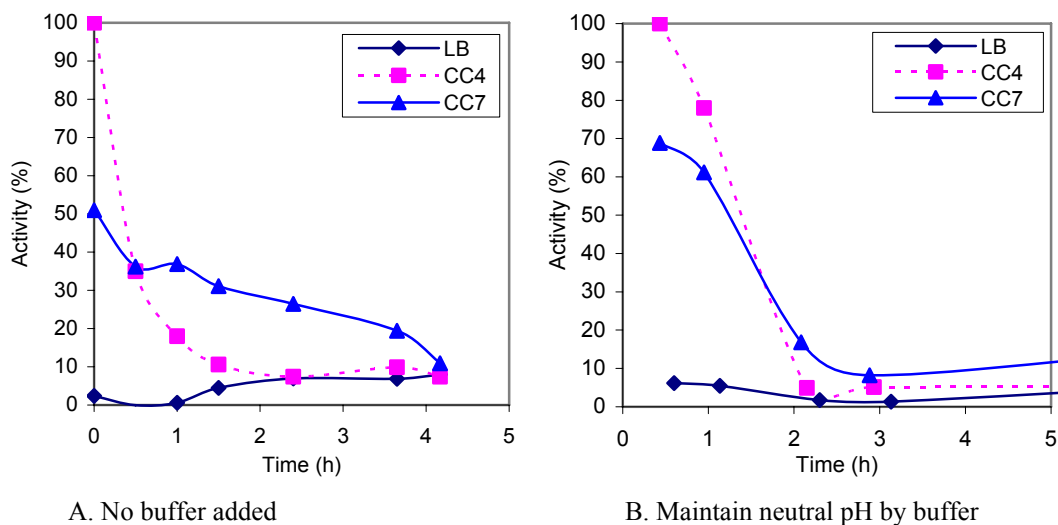


Fig. 5.3-4 PME activity versus time at 54°C

From Fig. 5.3-3 (1), the methanol amount obtained by LB, CC4 and CC7 in 4 hours were about 10%, 20%, and 20% of the maximum amount respectively when no buffer was added. During the reaction, the pH decreased from 6 to 4. From Fig. 5.2-4 (2), the methanol amount obtained by LB, CC4 and CC7 in 4 hours were about 15%, 25%, and 30% of the maximum amount respectively when buffer was added to maintain the pH value between 7 and 7.5. The result by LB (Fig. 5.3-3 B) is similar with the result by just buffer (Fig. 5.3-2).

From Fig. 5.2-4, the activity of CC4 was higher initially. However, the deactivation speed of CC4 was faster than that of CC7 at 54°C. CC4 was almost totally deactivated within 2 hours. These results are consistent with the results in Chapter 4. However, Fig. 5.3-3 shows that the methanol production was still going on even after the PME was totally deactivated. The reasons will be discussed later.

Experiments in this section and in Chapter 4 show that pH buffer is not only important to the enzyme activity but also to the hydrolysis of pectin. The pH buffer plays a comparable role as enzyme during the reaction.

One disputation from these results is that: why we should use enzyme since the pH buffer can do a similar job? We are considering the future. The hydrolysis by pH buffer has been fully studied. On the other hand, the PME study is just in its infancy. Our

goal is to develop a robust organism that can reproduce in beet pulp directly and continuously produce PME. In this way, the cost for enzyme can be zero. Of course, the ideal enzyme should be effective in acidic condition.

5.4 Effects of organisms on the methanol production

From Fig. 5.4-3 A, methanol could still be produced even if there was no PME and no buffer added. Since the reaction mixture is acidic, the hydrolysis by water was ignored. One of the possible reasons for the methanol production comes from the organisms. Organisms exist everywhere, on the reaction flask, in pulp, in PME solution. Lots of them can digest the organic stuffs which include sugar beet. It is possible that some bacteria can produce some enzyme that can either degrade the pulp or hydrolyze the methoxyl group directly.

To test the action of organisms, experiments should be done with the bacteria inhibited. Autoclave is a common method to kill the bacteria. However, the pulp structure will be changed during autoclave. Another method is to use antibiotic in the reaction flask.

Sodium azide is a widely used bacteriostatic agent which can prevent the bacteria from using oxygen by binding irreversibly to the heme cofactor and thus the function of cytochrome oxidase is inhibited. Because of the diversity of organism, the sodium azide concentration as an inhibitor varies from 0.01% to 0.25% (Lichstein, 1944). A concentration of 0.05% can inhibit most organisms. Therefore, 0.05% sodium azide was used in my experiments.

5.4.1 Effect of sodium azide on potassium permanganate assay

To use sodium azide, its effect on the methanol assay should be studied at first. The standard curves of methanol concentration were obtained following the procedure in Chapter 2. For the standard curve that had no sodium azide, 182 μ L of sulfuric acid

(5.5N), 310 μL of water, 500 μL of 0.2% pectin, and 8 μL of standard solution were mixed together. The concentrations of standard solution were 0%, 0.2%, 0.4%, 0.6%, 0.8%, and 1.0% respectively. The mixtures were then assayed following the second step of methanol assay in Chapter 2. For the standard curve that have 0.05% sodium azide, the 310 μL of water was replaced by 305 μL of water and 5 μL of 10% sodium azide. The results are shown in Fig. 5.4-1.

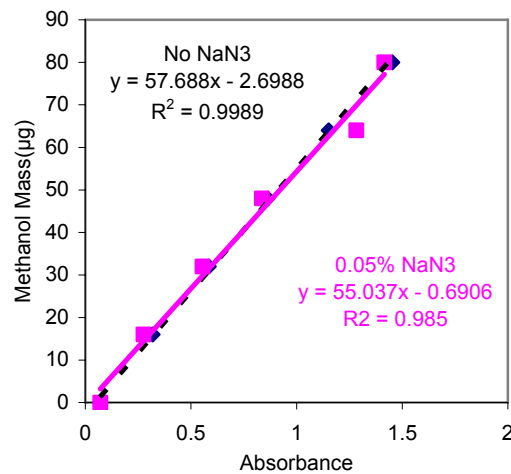


Fig. 5.4-1 Effect of sodium azide on the methanol assay

From Fig. 5.4-1, the standard curves of with and without sodium azide match well with each other. That means 0.05% sodium azide had no effect on the methanol assay.

5.4.2 Effect of sodium azide on PME activity

Our purpose is to inhibit organisms in reaction, not the enzyme. Therefore, it is important to make sure 0.05% sodium azide does inhibit the PME activity. The activities of CC4 and CC7 were measured in pectin solution at 30°C and 54°C respectively. The procedure developed in Chapter 4 was followed. The results for CC4 and CC7 at different temperatures are shown bellow.

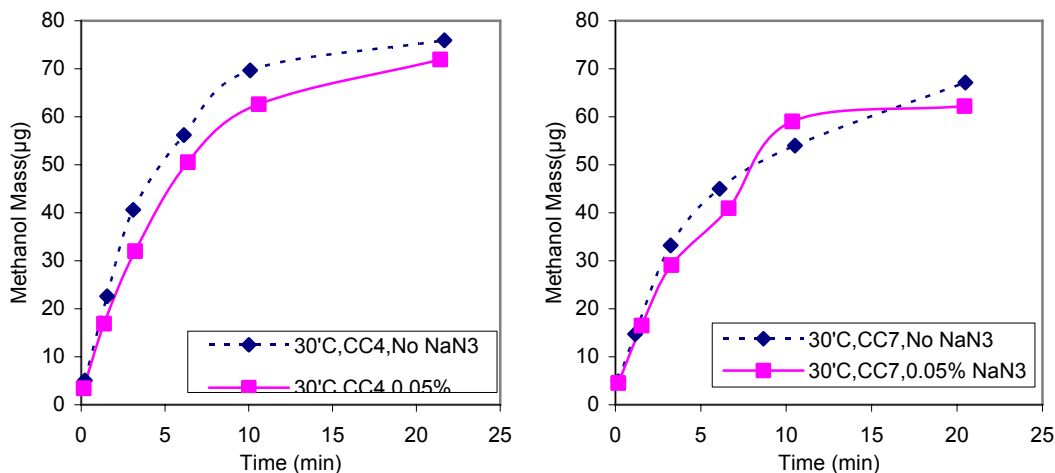


Fig. 5.4-2 Effect of sodium azide on PME activity at 30°C

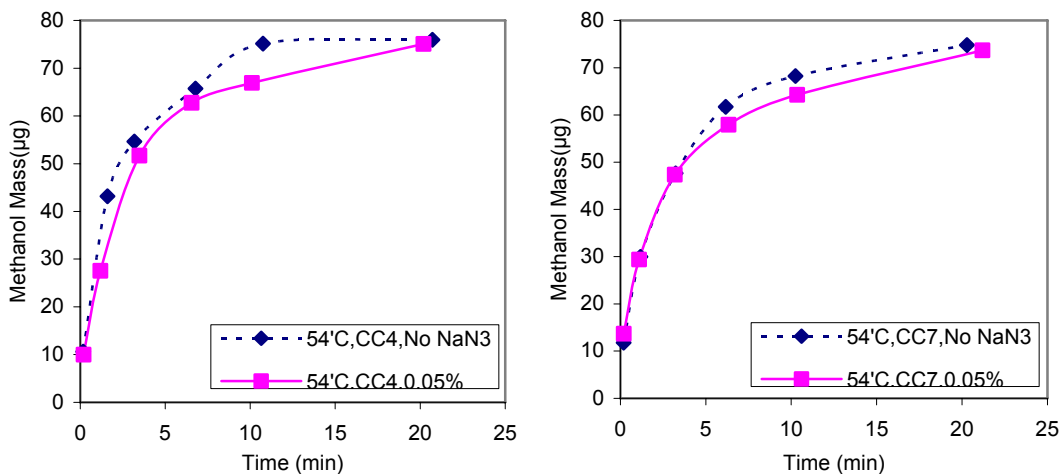


Fig. 5.4-3 Effect of sodium azide on PME activity at 54°C

Above figures show no significant effect by 0.05% sodium azide on the activities of CC4 and CC7 at 30°C and 54°C. Therefore, 0.05% sodium azide can be used to study the effect of organism on methanol production from pulp.

5.4.3 Effect of organisms on methanol production

Since 0.05% sodium azide had no significant effects on methanol assay and PME activity, it was used to study the organisms' effect during methanol production from pulp. In the experiments, pulp, water, sodium azide and PME (or water, LB as controls) were added into a sealed Erlenmeyer flask. The final sodium azide

concentration was 0.05%. The pH value, adjusted by 0.25M of Na_2HPO_4 buffer every 30min, was maintain between 7 and 7.5. New enzyme was added every 2 hours in the first 6 hours. Samples were taken and centrifuged to measure methanol concentration at intervals by potassium permanganate assay developed before. The reaction was at 54°C . A series of control experiments that had no sodium azide added were also carried out.

The dry weight of pulp was about 11%. The maximum amount of methanol production was 1.3% of the dry weight. Therefore, the percentage of methanol produced can be calculated. The results are shown bellow.

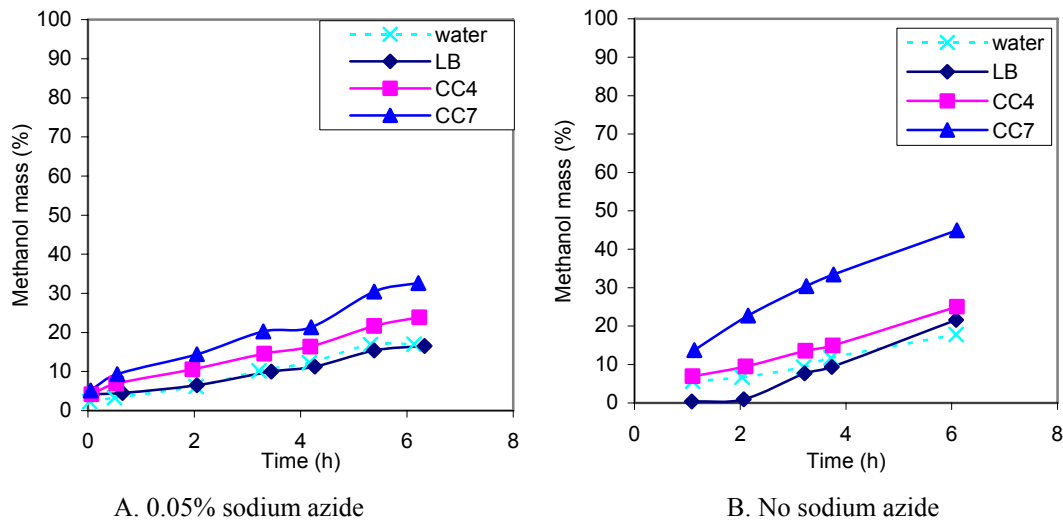


Fig. 5.4-4 Effect of organisms on methanol production from pulp at 54°C

From Fig. 5.4-4, the reaction rate for methanol production was decreased when sodium azide was added. That means the organism can promote the reaction rate probably by digesting the pulp.

Te test the organisms amount in the experiments, the samples from each flasks were spread on Petri-Dish. The results showed that the order of magnitude for the number of organisms was 10 if 0.05% sodium azide was added and 10^3 if no sodium azide was added.

Another proof for the effect of organisms came from the continuous experiments of those in Fig. 5.3-3 B. After those experiments, the flasks were sealed at room temperature overnight. The methanol concentration in the flasks was measured the second day. The results were shown in the following figure.

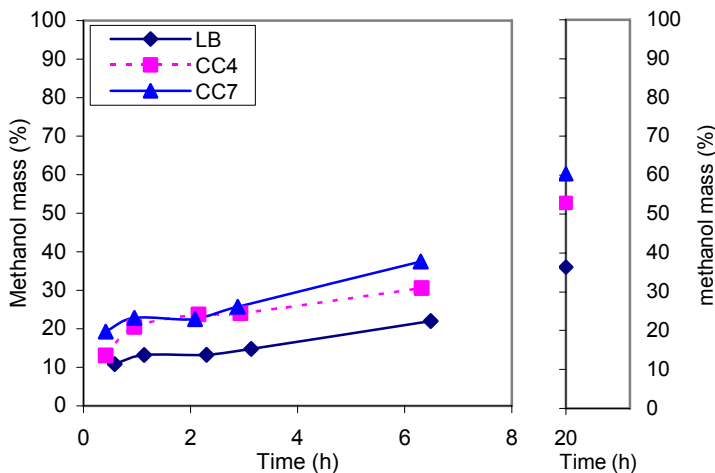


Fig. 5.4-5 Methanol produced by organisms

From Fig. 5.4-5, the methanol concentration in the second day jumped to a significant higher value in the night. From the results in Fig. 5.3-4, the PME had already been denaturated at the end of experiments in the first day. The pH value would decrease to around 4 with the hydrolysis going on and the temperature was low during the night. In these conditions, the hydrolysis of pulp at low pH value and low temperature was very slow. Therefore, the hydrolysis mainly came from the bacteria.

5.5 Effects of temperature on the methanol production

For an enzyme catalyzed reaction, the reaction rate increases exponential with the increase of temperature if the inactivation of enzyme is not considered. In Chapter 4, the temperature effect on the PME activity was studied. In this section, the direct relation between the methanol production and heat, in other words, the thermal decomposition of pectin will be studied.

The thermal decomposition of pectin has been studied for more than half a century. In 1945, Merrill and Weeks find that the viscosity of pectin solution decreased rapidly and irreversibly when the pectin solution was heated because of the degradation of pectin (Merrill and Weeks, 1945). Lots of papers about the thermal decomposition were published since then on (Sajjaanantakul, T., Van Buren, J. P., and Downing, D. L., 1989 & 1993; Sajjaanantakul, T., 1989). However, these papers seldom discussed the decomposition of methoxyl groups.

Experiments were designed to study the thermal decomposition of the methoxyl groups on beet pectin at 60°C, 80°C, 100°C, and 120°C respectively. For the experiments at 60°C, 80°C and 100°C, the mixture of pulp in D.I. water was maintained constant in an Erlenmeyer flask with condenser in water bath. The methanol concentration was measured with the time going on. The experiment at 120°C was carried out by autoclave. A series of small flasks with the same composition of beet pulp and D.I. water were prepared. Each flask was sealed by a big piece of thin elastic rubber. These flasks were then autoclaved for different lengths. The methanol concentration in each flask was measured after autoclave. The experiments results are shown below.

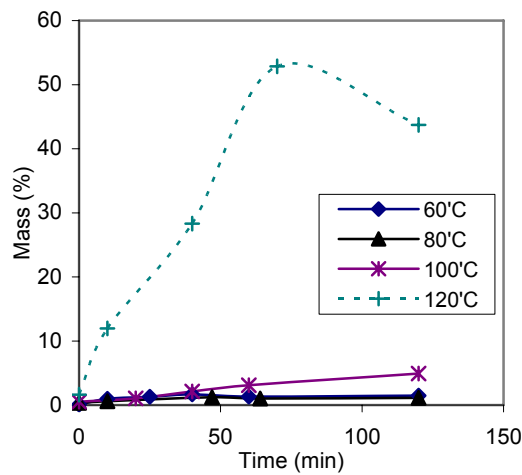


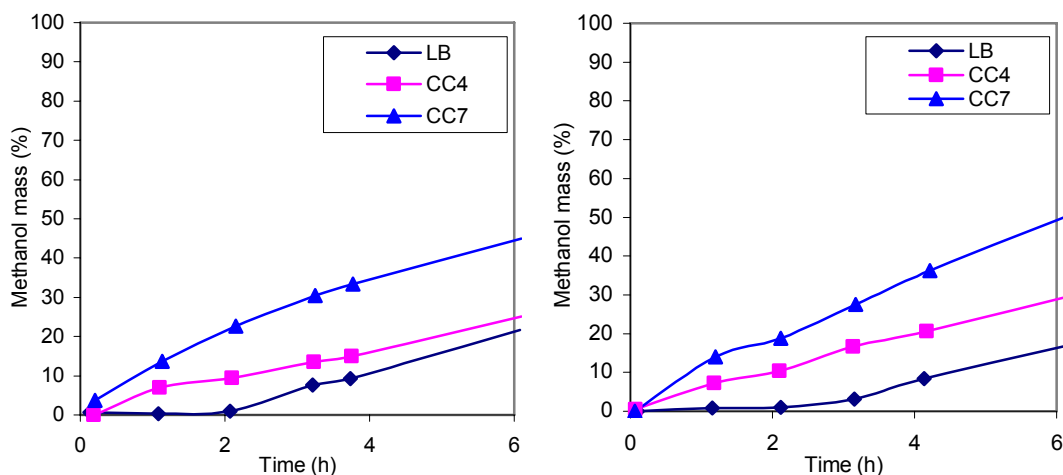
Fig. 5.5-1 Thermal hydrolysis of pulp

Since the temperature was high in the experiments, the proteins were denaturated soon after the experiments began. The bacteria would soon be killed or at least their growth was inhibited. Also, the experiments were carried out at natural pH (about pH 5) with no pH buffer added. Hydrolysis from buffer was ignorable. Therefore, the decomposition was mainly caused by heat, not enzymes, buffer or bacteria. Fig. 5.5-1 shows that there was no significant thermal decomposition of methoxyl group bellow 80 °C. However, the decomposition was huge at 120 °C. More than 50% methanol was obtained after 70min by autoclave. Since our reaction temperature is bellow 60 °C, the heat decomposition is not significant. The effects of heat are on the PME activity, organisms' growth, and other factors, not directly on pulp.

5.6 Inhibition of PME activity

5.6.1 Effect of methanol on the PME activity

Product inhibition is common in enzyme-catalyzed reaction. If there is product inhibition, the product should be removed regularly during the reaction. To test the methanol inhibition on PME activity, two sets of experiments, three experiments in every set, were carried out simultaneously. In the first series of experiments, 15 g wet pulp, 15mL PME (CC4, CC7 and LB in three experiments respectively) and 10mL water were mixed together and put in 54°C oven. The pH value, adjusted every 0.5h with 0.25M Na₂HPO₄, was maintained between 7.0 and 7.5. Samples were taken and centrifuged to measure methanol. 10mL of new enzyme was added every 2 hours in the first 6 hours. Methanol concentration and PME activity were measured by potassium permanganate assays developed in Chapter 2 and Chapter3. The second series of experiments were carried out in similar ways as the first series. The only difference was that the same volume of liquid was taken out before adding new enzyme. The results are shown as following figures.



(1) Do not remove liquid from reactor (2) Remove liquid from reactor intermittently

Fig. 5.6-1 Methanol inhibition on PME activity at 54°C

Comparison of figures (1) and (2) in Fig. 5.6-1 shows no significant difference, which means there was no significant inhibition by methanol under this condition.

5.6.2 Inhibition of the PME activity by foreign matter in pulp

Another possible inhibition could come from foreign matter in pulp. To find out the results, two sets of experiments, four in each set, were designed at 30°C and 54°C respectively. The composition of each experiment is shown in Table 5.6-1. In each experiment, 5 g wet pulp (or 5mL water), 12.5mL 0.2% pectin were mixed and the pH value was adjusted to around 7.3 with 0.25M Na₂HPO₄ (about 0.5mL). The mixture was then preheated at the designed temperature for 30min. After that, 525 μL of CC4 (or CC7) was added and the methanol concentration was monitored with the time going on. The methanol concentration was measured by potassium permanganate assay developed before. The results are shown in Fig. 5.6-2.

Table 5.6-1 Experiments compositions

	Experiment #1	Experiment #2	Experiment #3	Experiment #4
Wet pulp (g)	5	5	0	0
Water (mL)	0	0	5	5
0.2% pectin (mL)	12.5	12.5	12.5	12.5
CC4 (μL)	525	0	525	0
CC7 (μL)	0	525	0	525

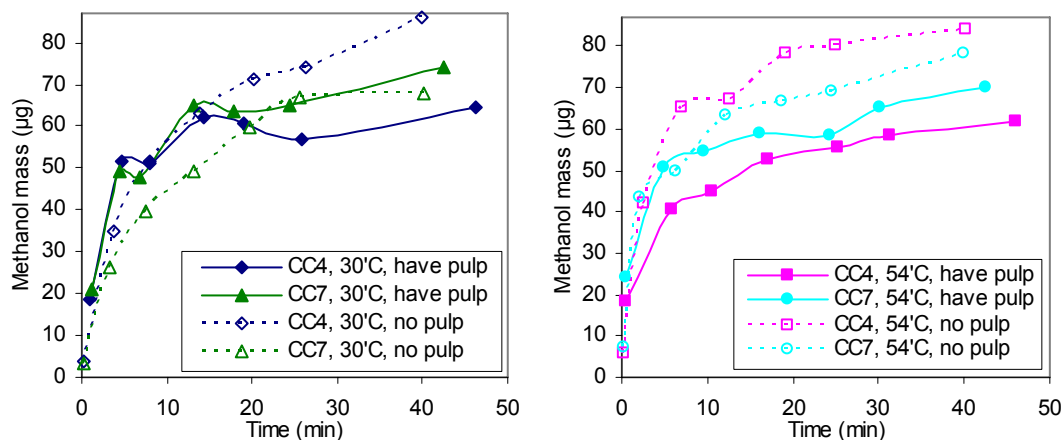


Fig. 5.6-2 Inhibition of PME activity from pulp

From former results, the amount of methanol produced from pulp within the first 40 min was neglectable. Therefore, the methanol can be assumed to come from pectin. At 30°C, there was no significant change for the amount of methanol produced by CC7 when pulp was added. The amount of methanol produced by CC4 was a little lower after 20 min when pulp was added. At 54°C, the results show that the amount of methanol produced by both CC4 and CC7 decrease a little if pulp exist.

It seems that there was inhibition from pulp. However, we can not make a conclusion that the inhibition came from the chemicals in pulp. It could only because that pulp in the reaction prohibited the diffusion of PME and some PME was adsorbed on the surface of pulp.

Further experiments were carried on to find out the real reason. In these experiments, 30g wet pulp was soaked in 80mL D.I. water for 100min at 40°C. The steep was then taken out by filtration to prepare 0.2% pectin solution. Anything that will

inhibit the PME activity, if there are some, should be in the steep. The activity of CC4 and CC7 at 30°C and 54°C in the pectin solution was then measured following the similar procedure as before. The results are shown below.

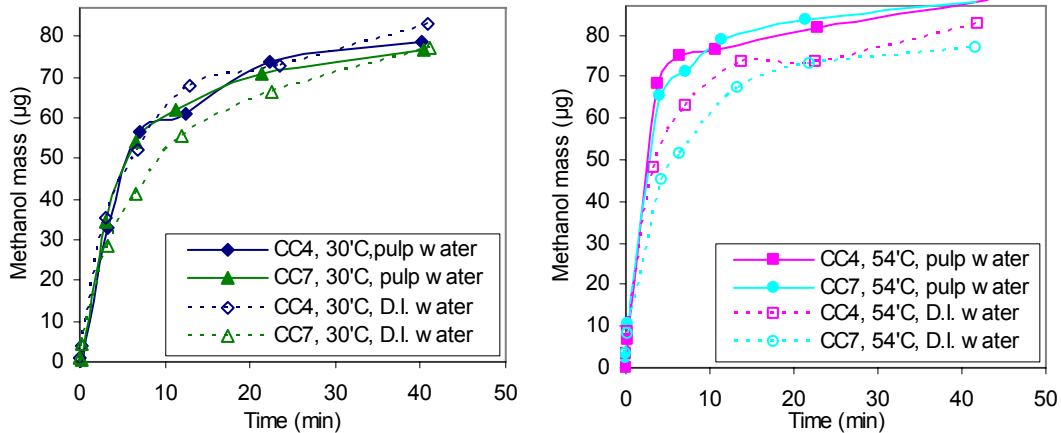


Fig. 5.6-3 Inhibition of PME activity from pulp steep

From Fig. 6.5-3, there was no significant difference between the steep water prepared pectin and D.I. water prepared pectin at 30°C. At 54°C, the reaction rate from the steep water prepared pectin was even a little faster than that from the D.I. water prepared pectin. Future study can be carried on to see if there is something that can accelerate the reaction rate in the pulp. Here, I will only make a conclusion that nothing in the pulp inhibited the PME activity.

5.7 Methods to help the PME access to the methoxyl groups in pulp

Fig. 5.6-1 shows that only 50% methanol was obtained from sugar beet pulp in a 6 hours reaction. However, the enzyme kinetics results in Chapter 4 show that the methanol production from pectin solution was fast. Therefore, the PME activity in the pulp was possibly reduced because the structure of the pulp obstructed the PME from entering the beet pulp.

To help the enzyme access the methoxyl groups, we can cut the pulp to smaller pieces to shorten the diffusion distance. Two sets of experiments were carried out using the initial pulp and the grinded pulp respectively. In each set of experiments, 15 g wet pulp, 15mL PME (or water, LB as a control) and 10mL water were mixed together and maintained at 54°C. Dry weight of the wet pulp was 12.2%. Theoretically maximum methanol amount was 1.3 % of dry weight. The initial activities of CC4 and CC7 were 12 units per mL and 10 units per mL respectively. The pH value was adjusted every 0.5h with 0.25M Na₂HPO₄ and maintained between 7.0 and 7.5. Samples were taken and centrifuged to measure methanol concentration and PME activity intermittently. Methanol concentration was measured by the potassium permanganate assay developed in Chapter 2. The results are shown in the following figures.

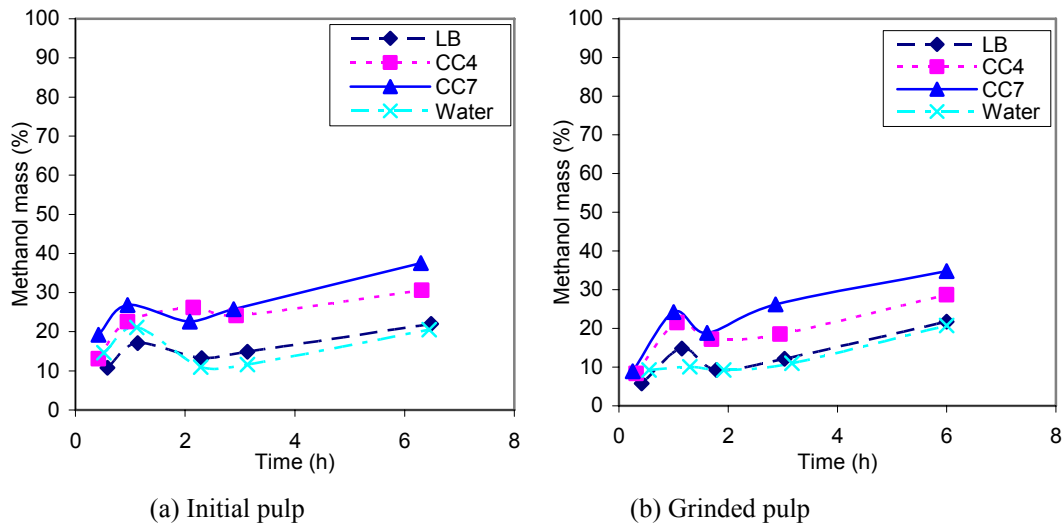


Fig. 5.7-1 Produce methanol from pulp at 54°C

Theoretically, the methanol production rate should be higher since more pectin is exposed to PME and the diffusion distance of PME is shorter. From the results, however, smaller pulp size did not help in the improvement of reaction rate. The reason could be that the size of grinded pulp was still in the same order of magnitude as the size of initial pulp that the PME did not see the size change of pulp.

The experiments results show that grinding the pulp does not improve the reaction rate of methanol production. Other methods should be considered. For example, another enzyme such as polygalacturonanase (PG), which can help to break the cell wall so that PME can access the pectin inside easily, can be added into pulp together with PME. Our cooperators are still engaged in the study of enzymes. It is quite possible this problem can be solved one day.

5.8 Modeling the methanol production from pulp

The main issue here is to figure out the reaction time and the amount of enzyme to obtain 100% methanol at designed temperature. The results in Fig.5.4-4B were used here (Fig. 5.8-1B). Another set of experiments following the same procedure were carried out at 45°C (Fig. 5.8-1A). During the reaction, the PME (or LB, water as a control) was added as an average rate of 5.6 ml per hour. Since the activities of initial CC4 and CC7 were 12 units per mL and 10 units per mL respectively, the enzyme adding rate of CC4 and CC7 can be converted to 67 units per hour and 56 units per hour. The methanol production as a function of time is shown in following figures.

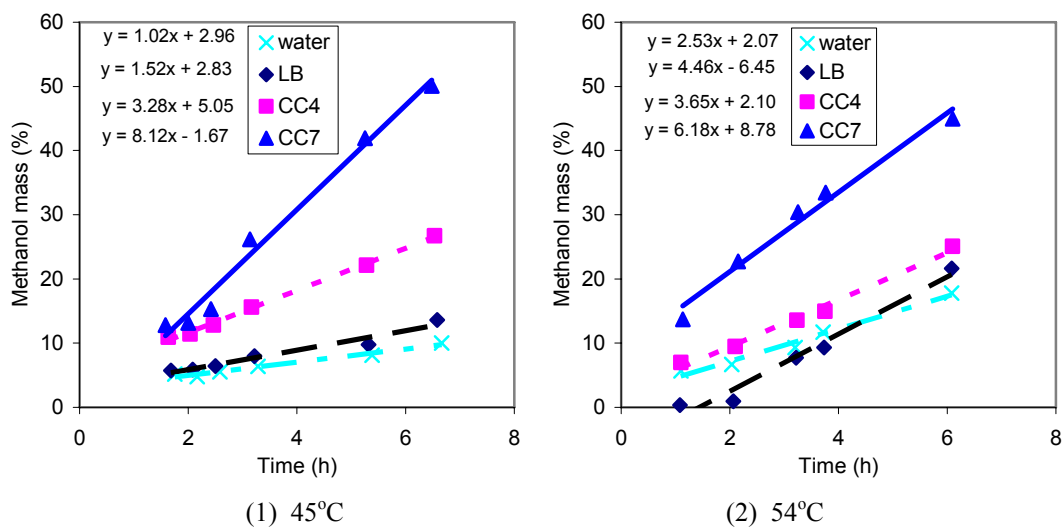


Fig. 5.8-1 Produce methanol at different temperature

The trend lines of the data as well as their equations are shown in the figures. We assume the reaction will keep the same rate with time going on if the condition is kept constant. Therefore, we can calculate the total time and total amount of PME to obtain 100% methanol (Table 5.8-1).

Table 5.8-1 Reaction time and enzyme amount needed to obtain 100% methanol

Reaction temperature (°C)		45°C	54°C
Time to obtain 100% methanol (h)	by water	95	39
	by LB	64	24
	by CC4	29	27
	by CC7	13	15
Total enzyme to obtain 100% methanol from 1g dry beet pulp (units)	by CC4	1295	1206
	by CC7	485	560

From Table 5.8-1, the following conclusion can be obtained:

- (1) The reaction rate was not proportional to the amount of enzyme added.
The reaction was zero order reaction.
- (2) Methanol can still be produced by the hydrolysis of buffer or digestion of organisms even if no enzyme is added.
- (3) When only water was added in the reaction, the methanol production was mainly through the hydrolysis by buffer assisted by small amount of organism. Therefore, the reaction rate at higher temperature is faster. 100% methanol can be obtained in 40h at 54 °C and in 100h at 45 °C.
- (4) When only LB was added in the reaction, the organisms grown faster in LB than in water. Therefore, the methanol production was mainly through the hydrolysis by buffer and large amount of organisms. Still, the reaction rate at 54 °C was faster than that at 45 °C.
- (5) The amount of CC4 needed was about twice of the amount of CC7 at both 45 °C and 54 °C. That was because the deactivation speed of CC4 was faster than that of CC7

5.9 Conclusions and discussion

Till now, some of the most important factors that can affect the methanol production have been studied. These factors include pH buffer, organisms, and heat. The results show that all of these factors are important.

pH buffer can promote the hydrolysis of methoxyl group directly. Organisms can digest the pulp which will help the PME attack on pectin. The organism may also produce some enzyme to catalyze the hydrolysis of the methoxyl group directly. Heat itself can degrade the pulp. However, at our reaction temperature, this will not happen. The effects of heat are on the PME activity, organisms' growth, and the buffer hydrolysis, not directly on pulp. The reaction rate at higher temperature is faster. Therefore, if no enzyme deactivation is considered, higher temperature is better. On the other hand, the enzyme may be denaturated faster at higher temperature. Therefore, there is an optimal temperature for PME activity. Fig. 5.8-1 shows that 45°C is better than 54°C.

Chapter 6: Methanol Separation

6.1 Introduction

The initial concentration of methanol produced from sugar beet pulp is low. The highest concentration for one batch of production is only 0.1%. However, the required concentration for commercial utility is usually above 90% depending on the purposes. Therefore, the methanol produced from sugar beet should be separated and concentrated.

The methanol can be separated either during the reaction or after the reaction. In this chapter, three different separation methods, stripping, distillation, and pervaporation were studied to obtain the first hand data for future process design.

6.2 Modeling of methanol stripping

Stripping is a unit operation in which one or more components of a liquid stream are removed by being vaporized into an insoluble gas stream. To strip methanol out of water, hot air can be purged into the reactor. Since the vapor pressure of methanol is higher than that of water, the methanol concentration in the vapor phase is higher than that in the liquid phase. The air saturated with methanol and water is then condensed by a condenser at low temperature. Most of the methanol and water in vapor will be condensed.

6.2.1 Methanol stripping after reaction

In this section, a model for methanol stripping was established to see if purging air through the reactor was an effective method to strip out methanol. Parameters in the model can be adjusted to simulate the actual production. The model follow sheet is at Fig.6.2-1.

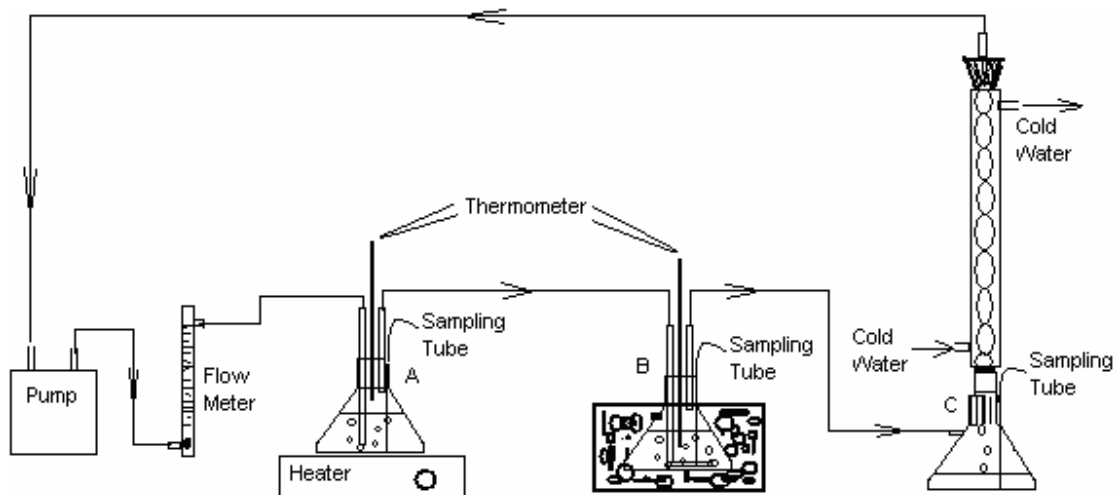


Fig. 6.2-1 Methanol stripping from the reactor

In this flow sheet, a pump, a flow meter, a heater, three flasks and a condenser are connected by pipes. Air is forced to go through the flow meter, flask A, flask B, flask C, and the condenser in turn by pump. Flask A is filled with water that is maintained at a constant high temperature. Flask B, a simulation of the actual reactor, contains low concentration of methanol. The purposes of purging air into flask A are 1) to pre-warm the air so that it will not decrease the temperature in flask B, and 2) to saturate the air by water so that air will not bring too much water out of flask B. Gas flowing out of flask B is then condensed in flask C. The assumptions of 1) the equilibration state between the gas phase and liquid phase is quickly established in every flask and 2) the pressure of gas phase does not change much in the flow sheet are made.

The vapor pressures of pure water and methanol can be calculated by the Antoine equation which was suggested by Antoine in 1888. In the pressure range of 1 to 200kPa, this equation is highly accurate. The Antoine equation is expressed as $P = 10^{A - \frac{B}{T+C}}$, where A, B and C are Antoine coefficients. Antoine coefficients, which vary from substance to substance, are tabulated in *Lange's Handbook of Chemistry* (12th ed., McGraw-Hill, New York, 1979) or other data base.

The total pressure of methanol and water mixture can be calculated by the Raoult's law with the assumption that the physical properties of water and methanol are

identical. The total vapor pressure P_t above the methanol and water mixture is equal to the sum of the vapor pressures of methanol and water, P_1 and P_2 . Since methanol and water are similar, the vapor pressure of each one will be equal to the vapor pressure of the pure substance P^0 times the mole fraction in the solution. Thus the total pressure above methanol and water mixture is $P_t = P_1^0 x_1 + P_2^0 x_2$.

Assume the mole flow rates of methanol between flask A and B, B and C, and C and A are $N_{AB,1}$, $N_{BC,1}$ and $N_{CA,1}$ respectively and the mole flow rates of water between flask A and B, B and C, and C and A are $N_{AB,2}$, $N_{BC,2}$ and $N_{CA,2}$ respectively. These parameters can be expressed by combining the ideal gas law, Raoult's law, and Antoine equation as following.

$$N_{AB,1} = \frac{P_{A1} \cdot x_A \cdot V_A}{R \cdot T_A} \quad (6.2-1)$$

$$N_{AB,2} = \frac{P_{A2} \cdot (1 - x_A) \cdot V_A}{R \cdot T_A} \quad (6.2-2)$$

$$N_{BC,1} = \frac{P_{B1} \cdot x_B \cdot V_B}{R \cdot T_B} \quad (6.2-3)$$

$$N_{BC,2} = \frac{P_{B2} \cdot (1 - x_B) \cdot V_B}{R \cdot T_B} \quad (6.2-4)$$

$$N_{CA,1} = \frac{P_{C1} \cdot x_C \cdot V_C}{R \cdot T_C} \quad (6.2-5)$$

$$N_{CA,2} = \frac{P_{C2} \cdot (1 - x_C) \cdot V_C}{R \cdot T_C} \quad (6.2-6)$$

where R is the ideal gas constant, V_A , V_B and V_C the volume flow rates between flask A and B, B and C, and C and A respectively, T_A , T_B and T_C the temperature in flask A, B, and C respectively, P_{A1} , P_{B1} and P_{C1} the vapor pressures of pure methanol at the temperatures same as in flask A, B, and C respectively, P_{A2} , P_{B2} and P_{C2} the vapor pressures of pure water at the temperatures same as in flask A, B, and C respectively, x_A , x_B and x_C the mole fraction of methanol in flask A, B, and C respectively. x_A , x_B and x_C can be expressed as

$$x_A = \frac{N_{A1}}{N_{A1} + N_{A2}} \quad (6.2-7)$$

$$x_B = \frac{N_{B1}}{N_{B1} + N_{B2}} \quad (6.2-8)$$

$$x_C = \frac{N_{C1}}{N_{C1} + N_{C2}} \quad (6.2-9)$$

where N_{A1} , N_{B1} , N_{C1} are the mole number of methanol in liquid phase in flask A, B, and C respectively.

Assume the gas is ideal gas. Since the total mole number of methanol and water in gas is small, we assume the total mole number of gas in the flow sheet does not change. Therefore, V_A , V_B and V_C can be obtain by ideal gas law as following.

$$V_A = \frac{V_0 P_0}{P_0 + P_A} \quad (6.2-10)$$

$$V_B = \frac{V_0 P_0}{P_0 + P_B} \quad (6.2-11)$$

$$V_C = \frac{V_0 P_0}{P_0 + P_C} \quad (6.2-12)$$

where V_0 is the volume flow rate of air, P_0 the pressure of air, P_A , P_B and P_C the vapor pressures of methanol and water in air in flask A, B, and C respectively. P_A , P_B and P_C can be calculated by the Raoult's law.

$$P_A = P_{A1} \cdot x_A + P_{A2}(1 - x_A) \quad (6.2-13)$$

$$P_B = P_{B1} \cdot x_B + P_{B2}(1 - x_B) \quad (6.2-14)$$

$$P_C = P_{C1} \cdot x_C + P_{C2}(1 - x_C) \quad (6.2-15)$$

Assume the gas in and out every flask has the same temperature as the liquid in flask. The material balance equation in every flask can then be established. The molar increasing rates of methanol and water in every flask are

$$\frac{dN_{A1}}{dt} = N_{CA,1} - N_{AB,1}, \quad \frac{dN_{A2}}{dt} = N_{CA,2} - N_{AB,2}$$

$$\frac{dN_{B1}}{dt} = N_{AB,1} - N_{BC,1}, \quad \frac{dN_{B2}}{dt} = N_{AB,2} - N_{BC,2}$$

$$\frac{dN_{C1}}{dt} = N_{BC,1} - N_{CA,1}, \quad \frac{dN_{C2}}{dt} = N_{BC,2} - N_{CA,2}$$

If the gas phase and liquid phase can equilibrate quickly in flasks, the variable in above equations can then be converted to the total volume of gas passed (V) instead of the time (t). Assume the flow rate from the flow meter is V_0 and the flow rate does not change much in the whole flow sheet. The dt can then be represented by $d(\frac{V}{V_0})$.

Therefore, the material balance equations can be converted to the following forms

$$\frac{dN_{A1}}{dV} = \frac{1}{V_0} (N_{CA,1} - N_{AB,1}) \quad (6.2-16)$$

$$\frac{dN_{A2}}{dV} = \frac{1}{V_0} (N_{CA,2} - N_{AB,2}) \quad (6.2-17)$$

$$\frac{dN_{B1}}{dV} = \frac{1}{V_0} (N_{AB,1} - N_{BC,1}) \quad (6.2-18)$$

$$\frac{dN_{B2}}{dV} = \frac{1}{V_0} (N_{AB,2} - N_{BC,2}) \quad (6.2-19)$$

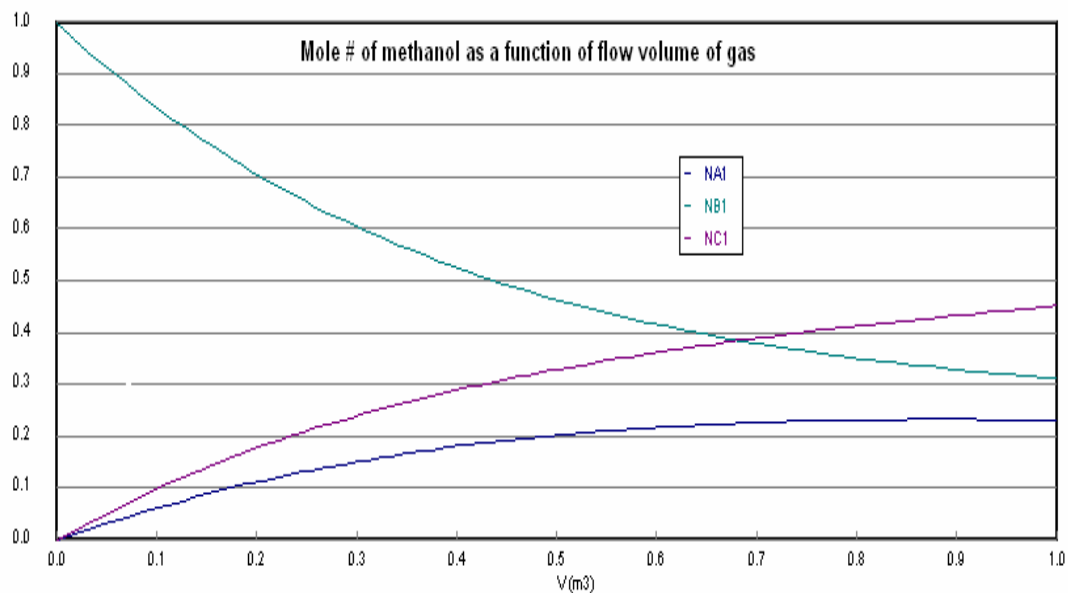
$$\frac{dN_{C1}}{dV} = \frac{1}{V_0} (N_{BC,1} - N_{CA,1}) \quad (6.2-20)$$

$$\frac{dN_{C2}}{dV} = \frac{1}{V_0} (N_{BC,2} - N_{CA,2}) \quad (6.2-21)$$

From all of these equations, the plots of mole number change of methanol/water as a function of total gas volume purged were obtained by software Polymath. Fig.6.2-2 is one of the simulation results. The initial condition for the simulation is shown in Table 6.2-1.

Table 6.2-1 Initial conditions in flasks

Flask Number	Composition	Mole Number of Methanol	Temperature (oC)
A	500mL water	0	67
B	250mL water, 40.5mL MeOH	1	54
C	empty	-	10



condition was carried out. The flow rate of air was 0.115 m^3 per hour. The temperature of flask A, B, and C was maintained constant as in Table 6.2-1. Samples from the flasks were taken at intervals and their concentrations were analyzed by Bioanalyzer YSI 2700. The volume changes of liquid in flasks were also measured. From the changes of methanol concentration and liquid volume, the changes of methanol mole number in every flask were calculated. The mole number changes in flask A, B, and C are shown in following figure.

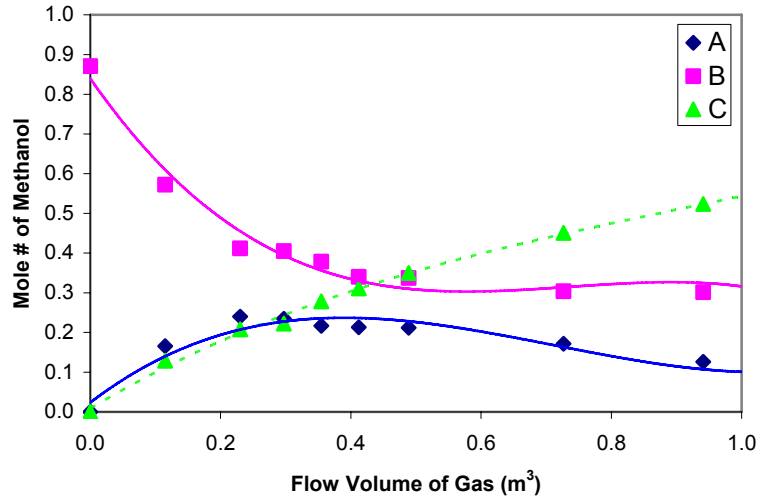


Fig. 6.2-3 Experiment results of methanol stripping

Fig.6.2-2 and Fig.6.2-3 show similar results. That means the simulation equations were reliable. Both the simulation results and experiment results show that methanol in flask B can be transferred into flask C effectively. From these results, more than half of methanol in flask B was transferred into flask C after 0.3m³ of air pass through flask B. Therefore, purging hot air through the reactor is an effective method for methanol-water separation.

6.2.2 Methanol stripping during reaction

The above study is a simulation of methanol stripping after reaction. In a continuous reactor, methanol can be stripped out during the reaction. Since methanol will be continuously produced in flask B, one more term, methanol production rate, can be added to Eq.(6.2-18). The equation then becomes

$$\frac{dN_{B1}}{dV} = \frac{1}{V_0} (N_{A1} - N_{B1} + N_p) \quad (6.2-22)$$

where N_p is the production rate. The whole process can then be simulated in the same way as above. The following figure shows the simulation results of methanol stripping from a continuous reactor. The methanol producing rate was assumed to be 0.0006 moles per hour in the simulation.

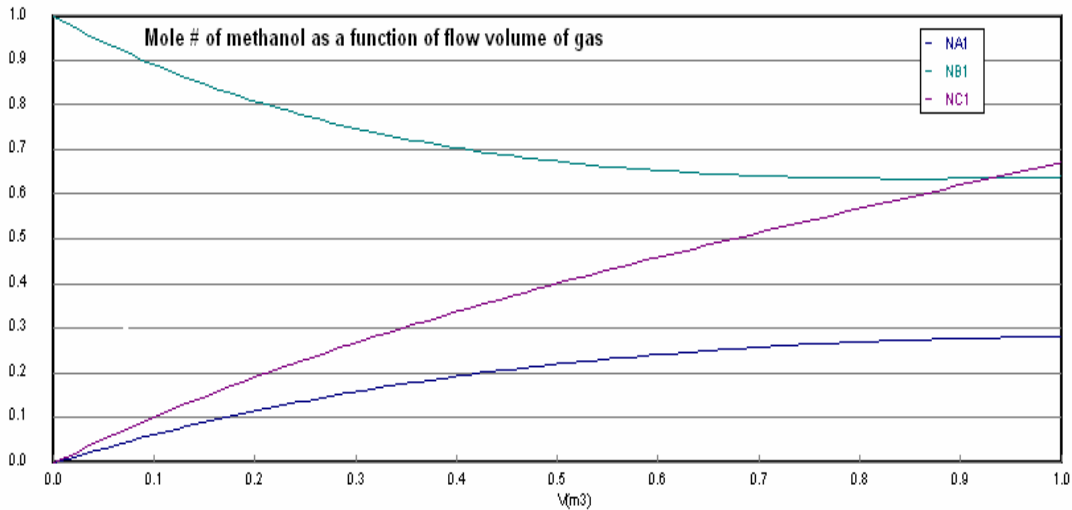


Fig. 6.2-4 Simulation result of methanol stripping from a continuous reactor

6.3 Distillation

One method to separate methanol and water is to separate the liquid mixture from pulp after reaction followed by column distillation. Distillation is the most common separation technique. It is a process in which a liquid or vapor mixture of two or more substances is separated into a component of desired purity, by the application and removal of heat. The principle of distillation is that the vapor of a boiling mixture will be richer in the components that have lower boiling points. Better separation can be obtained if the volatilities (markedly, boiling points) difference between the components is bigger. A vertical condenser (or column), in which a gradient of temperatures exists, is used in distillation. More complete separation can be obtained by more plates or greater distance over which the temperature gradient in the column is applied.

It is difficult to study a distillation column in a lab since there are so many parameters to control. To find an economic way to obtain a high concentration of methanol, simulation of the distillation process with CHEMCAD software is a good approach. However, only this software is not enough. To make sure the simulation results are useful, experiments with the same operating condition as in CHEMCAD should also

be done. The experiments' results can be used either to test the accuracy of CHEMCAD or to establish a small scale bench-top production line in the near future.

In this section, the distillation experiments were done and their results were compared with the simulation results by CHEMCAD. The experiments were carried out in a small distillation tower with a diameter of 5cm and height of 46cm. The plate number was 10. The total setups included the distillation tower, two pumps for feed-in and pump-out, and a heating pan to maintain the feed-in temperature. The picture of the tower is shown in Fig. 6.3-1.

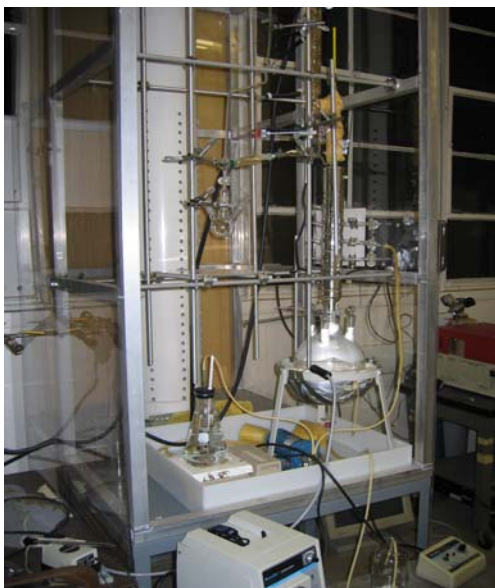


Fig. 6.3-1 Distillation tower

The pre-heated methanol was fed at a constant rate of 5.0 g/min. At bottom, the residue was pumped out at a rate of 4.7 g/min. The distillate was collected at a rate of 0.3 g/min. The reflux ratio, R , was 1.67. After the whole system was at a steady state, samples were taken and their concentrations were analyzed by the NIRSystems (NIRSystems, Inc. Silver Spring, MD 20904). The results were shown in the following table. The simulation results based on the same operation parameters by CHEMCAD were listed together.

Table 6.3-1 Experiments and simulation results

		30°C Feed		70°C Feed	
		Experiment	Simulation	Experiment	Simulation
Feed	Temperature (°C)	30	30	70	70
	Methanol concentration (w/w%)	1	1	1	1
Top	Temperature (°C)	97	92	98	92
	Methanol concentration (w/w%)	13	16	12	15
Bottom	Temperature (°C)	102	103	103	103
	Methanol concentration (w/w%)	0.3	0.05	0.3	0.1

From the above table, the results from experiments match quite well with those from the simulation by CHEMCAD. CHEMCAD can well simulate the actual distillation tower.

6.4 Pervaporation

The word pervaporation is derived from two steps, firstly the permeation of permeate through the membrane, then the evaporation of permeate into the vapor phase. The membrane, acting as a selective barrier between the liquid phase feed and the vapor phase permeate, is the most important part for pervaporation. Unlike distillation whose fractionation process is due to the volatility difference of the components in the feed, pervaporation is mainly due to polarity difference. For instance, a hydrophobic membrane can let hydrophobic component(s) transfer through it while it bars the hydrophilic component(s).

Pervaporation is considered an attractive alternative to other separation methods for some processes. It is typically suited to separating a minor component of a liquid mixture. For example, it has emerged as a good choice for the dehydration of organic solvents and the removal of organics from water. Some heat sensitive products can also be separated by pervaporation. Pervaporation may have cost and performance advantages for the separation of constant-boiling azeotropes.

High selectivity through the membrane is essential for pervaporation. The research about pervaporation was flourishing in the past several years (Veen & Delft, 2004; Kita, Inoue, Asamura, Tanaka & Okamoto, 1997; Maus & Brüsckhe, 2002; Molina, Vatai & Bekassy-Molnar, 2002; Won, Feng, & Lawless, 2003; Zhang, Zheng, & Shevade et al. 2002; Hwang, 2004). Some membranes have been commercially available. My purpose here is not to develop a new membrane, but to find a commercial one to separate methanol. However, no specific membrane for the separation of methanol and water was found. A decent PDMS hydrophobic pervaporation membrane was found from *Pervatech BV* (Rondweg 48, 7468 MC Enter, The Netherlands). The company had a fair separation result of water-ethanol mixture. No results about water-methanol were available.

Set up as shown in Fig.6.4-1 and Fig.6.4-2 was used to separate methanol from water with the PDMS hydrophobic membrane. During the pervaporation, the feed mixture, which was first heated to a designed temperature, then was pumped into the membrane chamber. In the chamber, more methanols permeated the membrane than water. The permeate was then evaporated because of the high degree of vacuum on the other side of the membrane. When the permeate vapor passed the sample collector which was immersed into liquid nitrogen, it condensed and became solid. After the experiment, the sample was melted and its mass and methanol concentration were measured.

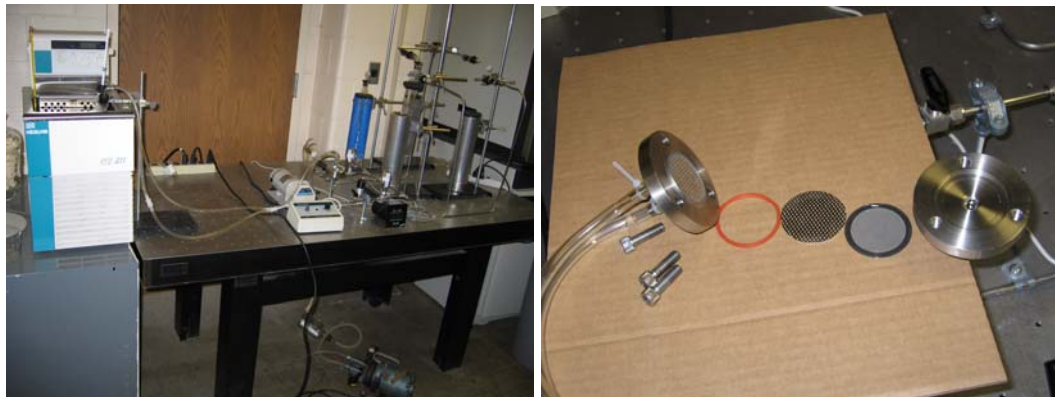


Fig. 6.4-1 Pervaporation setup (Right figure was the membrane chamber)

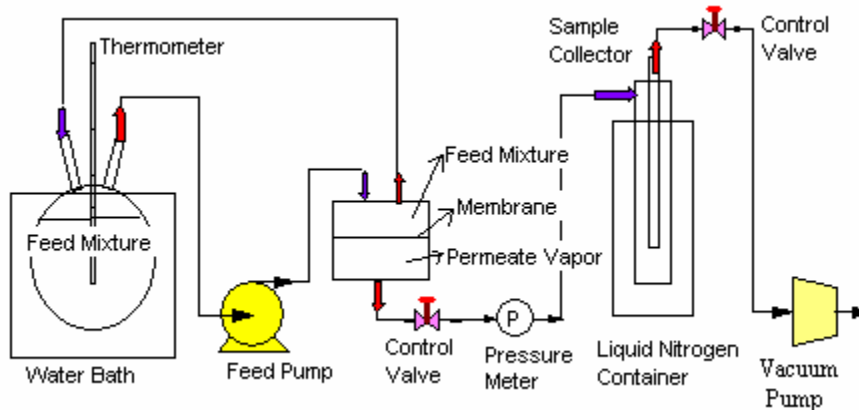


Fig. 6.4-2 The sketch map of pervaporation

Since the sample composition was sample, the refractive index was used to measure the methanol concentration. The refractive index is the ratio of speeds of light in two different materials. It is a constant for a given pair of materials. The measure of refractive index is simple, fast, and it only needs a small drop of the sample. Like other assay methods, it needs a standard curve. The standard curve of refractive index of methanol-water mixture is shown bellow.

Table 6.4-1 Refractive index of methanol-water mixture at 20°C

Methanol Concentration (w/w%)	Refractive Index	Methanol Concentration (w/w%)	Refractive Index
0	1.3330	40	1.3423
1	1.3332	50	1.3424
2	1.3335	60	1.3421
4	1.3339	70	1.3405
6	1.3348	80	1.3385
8	1.3354	90	1.3338
10	1.3362	100	1.3290
20	1.3388		
30	1.3414		
40	1.3423		
50	1.3424		

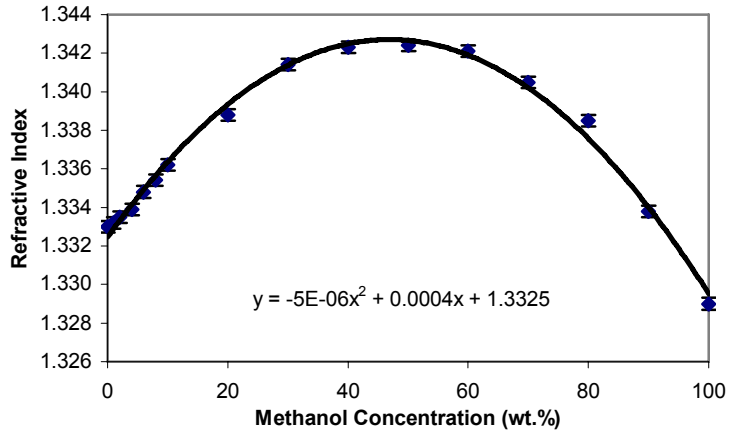


Fig. 6.4-3 Standard curve of refractive index versus methanol concentration at 20°C

From the above figure, the whole curve is not monotonous. Since the methanol concentration in experiments was low, only the left part of the whole curve was used. Since we want to read methanol concentration according to the refractive index, we make the refractive index the x coordinate (Fig. 6.4-4).

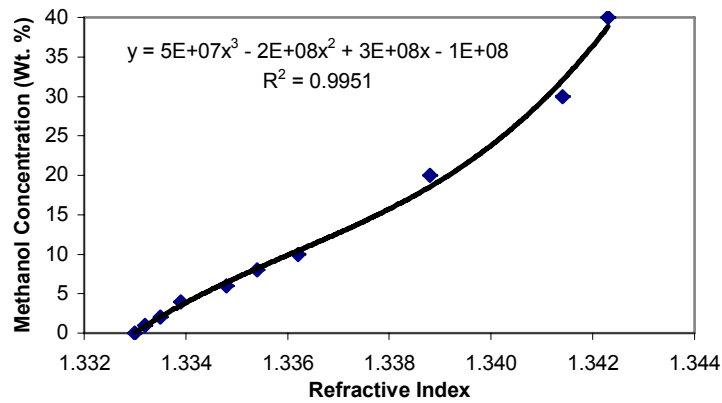


Fig. 6.4-4 Standard curve of refractive index versus methanol concentration (0-40%) at 20°C

The experiments were carried out at 47°C. The feed-in pressure was under 1 atm. The pressure on the permeate side was 7-11kPa. The membrane area was 11.6 cm². Three different feed-in concentrations were tried. Their permeate fluxes and concentrations were shown in the following figure. The separation factors, defined as the mole ratio of light component to heavy component in the gas passing through the membrane at a given

point divided by a similar mole ratio on the high pressure surface of the membrane at the same point, were calculated.

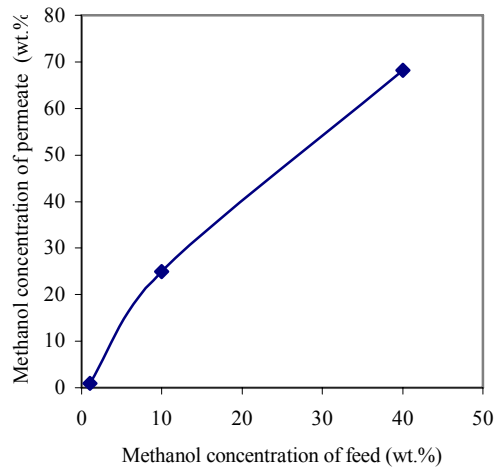


Fig. 6.4-5 Permeate concentration versus feed concentration

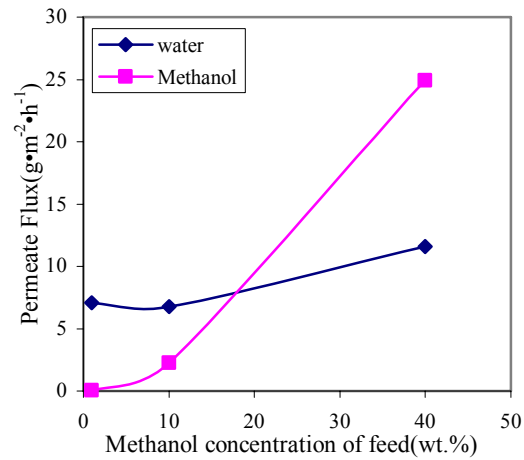


Fig. 6.4-6 Permeate flux versus feed concentration

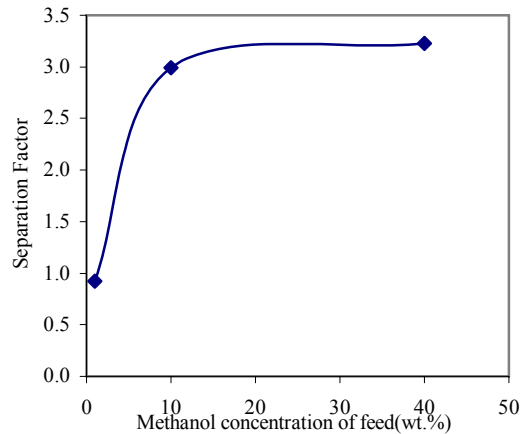


Fig. 6.4-7 Separation factor versus feed concentration

From above figures, we can see that the separation factor could reach 3 when the feed concentration was 10%. That means the separation effect was fine. However, the permeate flux was slow. Therefore, it was not applicable to the separation of methanol from water. With more and more new membrane available, it is possible to find a good one for the separation of methanol and water mixture in the near future.

6.5 Conclusions and discussion

Several different separation methods were studied. Among these methods, column distillation was powerful. However, one important aspect about distillation is that it consumes enormous amounts of energy, both in terms of cooling and heating requirements. Also, the tower itself is very expensive. It can totally contribute to more than 50% of plant operation cost.

Since our goal is to produce a renewable energy, we do not want to consume too much energy to produce another kind of energy. A good way to reduce the operating costs is to improve the efficiency of operation via process optimization. The combination of different separation methods can be considered. For example, the methanol can be extracted by stripping or vacuum distillation during reaction at first, followed by the column distillation. Pervaporation can be used at the last step to dehydrate the high concentration methanol from the distillation column.

In a word, the study for the separation of methanol is not finished yet. To increase the separation speed, improve the product quality and lower the cost, the whole separation process should continue to be optimized.

Chapter 7: Methanol Recovery from Sugar Beet Pulp

7.1 Introduction

Sugar beet pulp from a bioreactor should be separated from the methanol-water mixture by filtration, centrifuge or twin-screw machine at first. Since the separated pulp contain methanol, which is harmful both to environment during the drying process and to cattle if some methanol is left in the beet, it should be washed before drying. Hopefully, some methanol in pulp can also be recovered by washing the pulp.

In a continuous process, the pulp can be washed in two different ways, direct rinse and counter-current flow washing. For the direct rinse, the pulp is transferred slowly from one side to the other by a porous transfer belt. At the same time, water sprinkles over the pulp. The schematic is shown in Fig. 7.1-1. For the counter-current flow washing, a screw machine is used. An auger transfers the pulp from bottom to top and water flows from top to bottom. The schematic is shown in Fig.7.1-2.

To fully understand the washing process and to obtain some useful parameters for the future design, the mass transfer models of pulp washing were established and the mass transfer coefficients were measured by experiments.

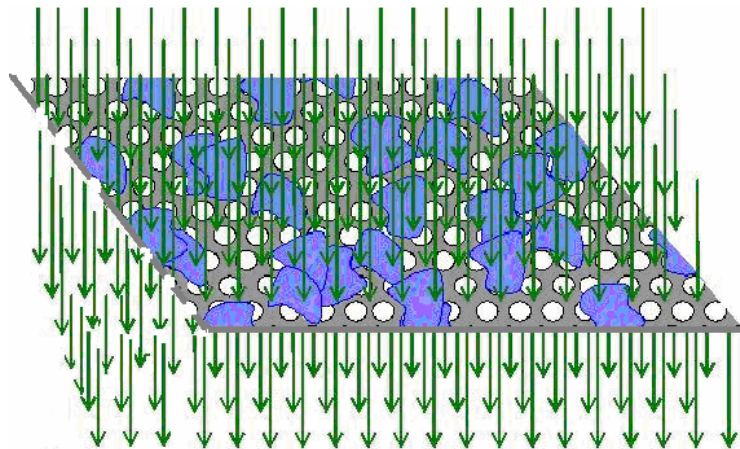


Fig. 7.1-1 Wash pulp by direct rinse

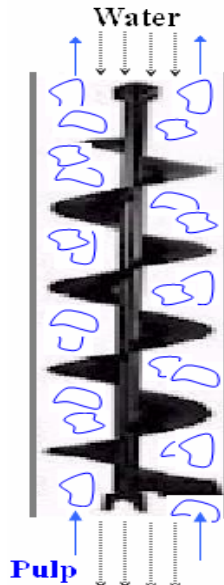


Fig. 7.1-2 Wash pulp by counter-current flow

7.2 Wash pulp by direct rinse

The direct rinse of pulp can be described by a simple model. In this model, small pieces of beet pulp saturated by methanol-water solution are continuously rinsed by water as shown in Fig. 7.2-1.

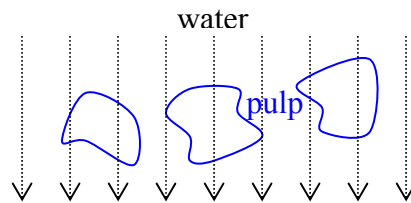


Fig. 7.2-1 Rinse beet pulp with water continuously

In this model, we assume the methanol concentration inside pulp and in water is homogeneous and mass transfer happens at interfaces (Deen, 1998). The mass transfer at interfaces can then be written as

$$\frac{dC_B}{dt} = -k(C_B - C_W) \quad (7.2-1)$$

where C_B and C_W are the bulk concentration of methanol in beet pulp and water phase respectively, k the mass transfer coefficient. If the water amount is big enough, the bulk concentration of methanol in water is zero. Eq. (7.2-1) can be simplified as

$$\frac{dC_B}{dt} = -kC_B \quad (7.2-2)$$

$$k = -\frac{1}{C_B} \frac{dC_B}{dt} \quad (7.2-3)$$

The mass transfer coefficient can be calculated by measuring the change of methanol concentration in beet pulp. Experiments were designed. In the experiments, 100 g of drop-dry sugar beet pulp was emerged into 500ml of 5% methanol solution for one day. The saturated beet pulp was press to drop-dry and then put on a porous surface as a thin layer. The pulp was then rinsed continuously using a shower spray. Pulp samples were taken at intervals. Liquid in sample was squeezed out by pliers and the methanol concentration was analyzed. The curve of methanol concentration in pulp versus time was generated as shown in Fig.7.2-2. The equations of trend line for each curve were obtained and the mass transfer coefficient was calculated from the trend line equation. The derivatives, dy/dx , divided by the methanol concentration, y , give us the k value. The average result of the k value was $0.013s^{-1}$.

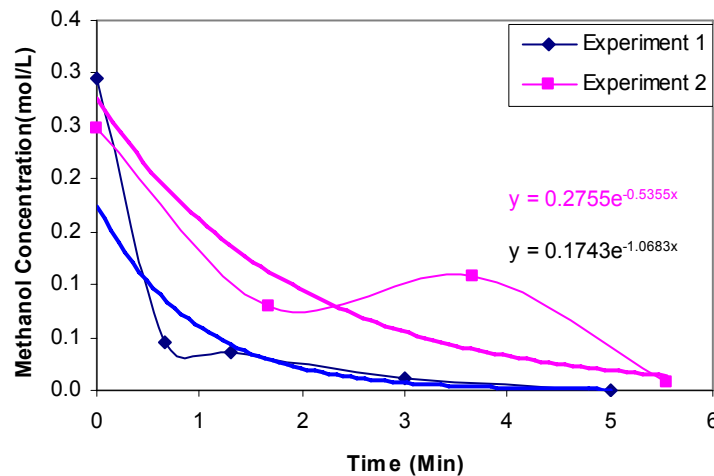


Fig. 7.2-2 Methanol concentration in beet pulp as a function of time

7.3 Wash pulp by counter-current flow

The flow direction of pulp and water can be the same or different. Therefore, we can have two types of flow, co-current and counter-current. Since the design goal is to remove the largest amount of methanol in each pass, counter-current exchange is superior to co-current exchange. With co-current exchange, the exit concentration in water is slightly less than the exit concentration in pulp and much less than the inlet concentration in pulp. On the contrary, the exit concentration with counter-current in water can exceed the exit concentration in pulp and approach the inlet concentration in pulp. Therefore, only counter-current flow was studied in this section. As for the co-current flow, the model equations can be derived in the same way as counter-current flow since both co-current and counter-current share the same mass transfer principles and similar deduction process (Truskey, Yuan, and Katz, 2003). The following figures demonstrate the concentration changes in co-current flow and counter-current flow.

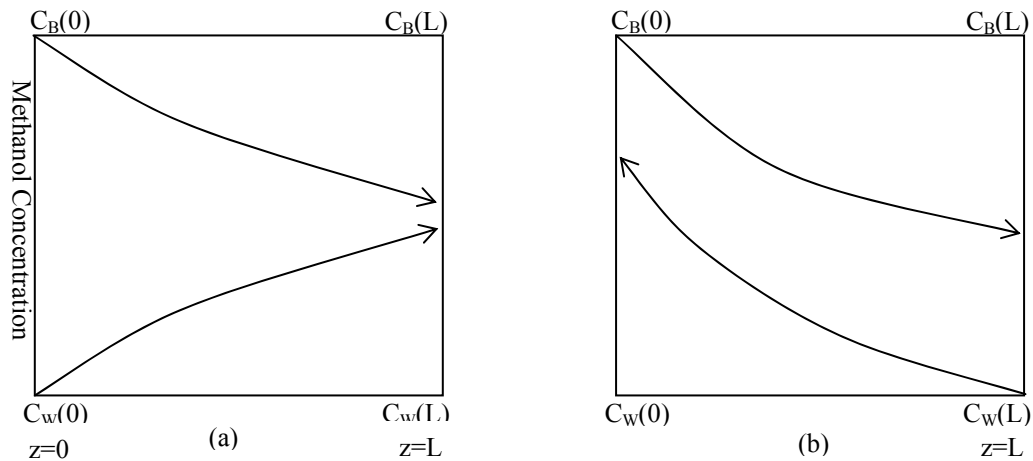


Fig. 7.3-1 Schematics of methanol concentration change in a screw machine
(a) co-current flow; (b) counter-current flow

The idea of washing pulp by a counter-current flow screw machine has been demonstrated in Fig. 7.1-2. With the assumption that the pulp is in a continuous solid phase and water is in a continuous liquid phase, the model can be simplified as Fig. 7.3-2. Between these two phases, is the membrane, whose area is equal to the total surface area

of all the pulps. The mass transfer happens at interface and is controlled by the bulk concentration of methanol in solid phase and in water phase.

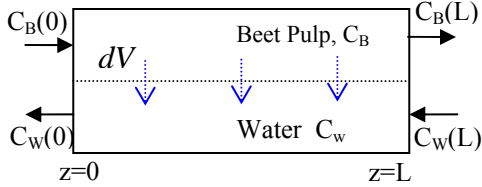


Fig. 7.3-2 Schematic of pulp washing by counter-current flow

In this model, $C_B(0)$ and $C_B(L)$ are the bulk concentrations of methanol in beet pulp at $z=0$ and $z=L$ respectively, $C_w(0)$ and $C_w(L)$ the bulk concentrations of methanol in water at $z=0$ and $z=L$ respectively. Molar flow rate of methanol in beet pulp is

$$\frac{dM_B}{dt} = Q_B dC_B \quad (7.3-1)$$

Molar flow rate of methanol in water is

$$\frac{dM_w}{dt} = -Q_w dC_w \quad (7.3-2)$$

where Q_B and Q_w are the volume flow rate of the beet pulp and water respectively, C_B and C_w the molar concentration of methanol in the beet pulp and water respectively, M_B and M_w the molar number of methanol in beet pulp and water respectively, t the time. Q_B and Q_w are scalars. The loss of methanol from beet pulp is equal to the gain of methanol in water. The material balance equation is

$$\frac{dM_B}{dt} = -\frac{dM_w}{dt} \quad (7.3-3)$$

Substituting Eq.(7.3-3) into Eq.(7.3-2) yields

$$\frac{dM_B}{dt} = Q_w dC_w \quad (7.3-4)$$

The mass exchange of methanol across the membrane can be described with a mass transfer coefficient

$$\frac{dM_B}{dt} = -k_0(C_B - C_w)dA_m \quad (7.3-5)$$

where A_m is the area of membrane.

Subtract Eq.(7.3-4) from Eq. (7.3-1), we can obtain:

$$dC_B - dC_W = \frac{dM_B}{dt} \left(\frac{1}{Q_B} - \frac{1}{Q_W} \right) \quad (7.3-6)$$

Replace $\frac{dM_B}{dt}$ in Eq. (7.3-6) with Eq.(7.3-5), yielding

$$dC_B - dC_W = -k_0 dA_m \left(\frac{1}{Q_B} - \frac{1}{Q_W} \right) (C_B - C_W) \quad (7.3-7)$$

Integrating from the inlet to the outlet results in the following expression:

$$\ln \left(\frac{C_B(0) - C_W(0)}{C_B(L) - C_W(L)} \right) = k_0 A_m \left(\frac{1}{Q_B} - \frac{1}{Q_W} \right) \quad (7.3-8)$$

Integrating of Eq. (7.3-1) and (7.3-4) from the inlet to the outlet results in the following expression:

$$\frac{dM_B}{dt} = Q_B (C_B(L) - C_B(0)) = Q_W (C_W(L) - C_W(0)) \quad (7.3-9)$$

or

$$Q_B = \frac{dM_B / dt}{C_B(L) - C_B(0)} \quad (7.3-10)$$

$$Q_W = \frac{dM_B / dt}{C_W(L) - C_W(0)} \quad (7.3-11)$$

Substituting Eq.(7.3-10) and (7.3-11) into Eq. (7.3-8) and solving for the molar flow rate yields

$$\frac{dM_B}{dt} = k_0 A_m \frac{(C_B(L) - C_W(L)) - (C_B(0) - C_W(0))}{\ln \left(\frac{C_B(0) - C_W(0)}{C_B(L) - C_W(L)} \right)} \quad (7.3-12)$$

Combining Eq. (7.3-9) and (7.3-12) obtain

$$Q_W (C_W(L) - C_W(0)) = k_0 A_m \frac{(C_B(L) - C_W(L)) - (C_B(0) - C_W(0))}{\ln \left(\frac{C_B(0) - C_W(0)}{C_B(L) - C_W(L)} \right)} \quad (7.3-13)$$

$$Q_B (C_B(L) - C_B(0)) = k_0 A_m \frac{(C_B(L) - C_W(L)) - (C_B(0) - C_W(0))}{\ln \left(\frac{C_B(0) - C_W(0)}{C_B(L) - C_W(L)} \right)} \quad (7.3-14)$$

Since the membrane area is proportional to the total volume of beet pulp in the mass transfer unit, let $A_m = k_l V_B$, Eq.(7.3-13) and Eq.(7.3-14) can be rearranged as

$$Q_W(C_W(L) - C_W(0)) = k_0 k_1 V_B \frac{(C_B(L) - C_W(L)) - (C_B(0) - C_W(0))}{\ln\left(\frac{C_B(0) - C_W(0)}{C_B(L) - C_W(L)}\right)} \quad (7.3-15)$$

$$Q_B(C_B(L) - C_B(0)) = k_0 k_1 V_B \frac{(C_B(L) - C_W(L)) - (C_B(0) - C_W(0))}{\ln\left(\frac{C_B(0) - C_W(0)}{C_B(L) - C_W(L)}\right)} \quad (7.3-16)$$

Let $k = k_0 k_1$, the rearrangement of Eq. (7.3-15) and (7.3-16) yield

$$(C_W(L) - C_W(0)) = k \frac{V_B}{Q_W} \frac{(C_B(L) - C_W(L)) - (C_B(0) - C_W(0))}{\ln\left(\frac{C_B(0) - C_W(0)}{C_B(L) - C_W(L)}\right)} \quad (7.3-17)$$

$$(C_B(L) - C_B(0)) = k \frac{V_B}{Q_B} \frac{(C_B(L) - C_W(L)) - (C_B(0) - C_W(0))}{\ln\left(\frac{C_B(0) - C_W(0)}{C_B(L) - C_W(L)}\right)} \quad (7.3-18)$$

Therefore, by measuring the methanol concentration in beet pulp and water at the positions of both inlet and outlet, k can be calculated from Eq. (7.3-17) or (7.3-18) if V_B and the volume flow rate are given. In these equations, $C_B(0)$, $C_B(L)$, $C_W(0)$, $C_W(L)$, V_B , Q_B , Q_W , and k are all the parameters. Usually, the methanol concentrations in pulp ($C_B(0)$) and water ($C_W(0)$) at the inlet position are known. Our goal is to decrease the methanol concentration in pulp at the exit to $C_B(L)$. $C_W(L)$ can be calculated by the material balance from Eq. (7.3-9). Therefore, we can easily derive the relationship in V_B , Q_B , and Q_W , which can be used for future design, once k is known.

According to the above modeling results, a model of a counter-current flow screw machine was designed to find out the k value (Fig.7.3-3). In this setup, the angle of auger can be adjusted so that all the beet pulp can be immersed in water, which can make sure of the highest interface area. Before experiment, 100g drop-dry beet pulp was submerged in 500 mL of 1% (or 5%) methanol for 1 day. The pulp was then pressed to drop dry by hand and added into the funnel of the setup. The auger motor and water-feed pump were turned on. The flow rates of water (Q_W) and beet pulp (Q_B) were 31.3mL/min and 4.7mL/min respectively. The volume of pulp in the unit (V_B) was 13mL. The methanol concentration in water at the inlet position $C_W(0)$ was zero. After the

system was stable, the pulp samples in the funnel and at the outlet, and the water sample at the outlet were taken. The methanol concentration in the water sample was measured by potassium permanganate assay directly. The pulp samples were squeezed by a pliers and the methanol concentration in the liquid squeezed out were measured by potassium permanganate assay. The k value was calculated with equation

$$k = \frac{Q_B}{V_B} \cdot \frac{(C_B(L) - C_B(0)) \cdot \ln\left(\frac{C_B(0) - C_W(0)}{C_B(L) - C_W(L)}\right)}{(C_B(L) - C_W(L)) - (C_B(0) - C_W(0))} \quad (7.3-19)$$

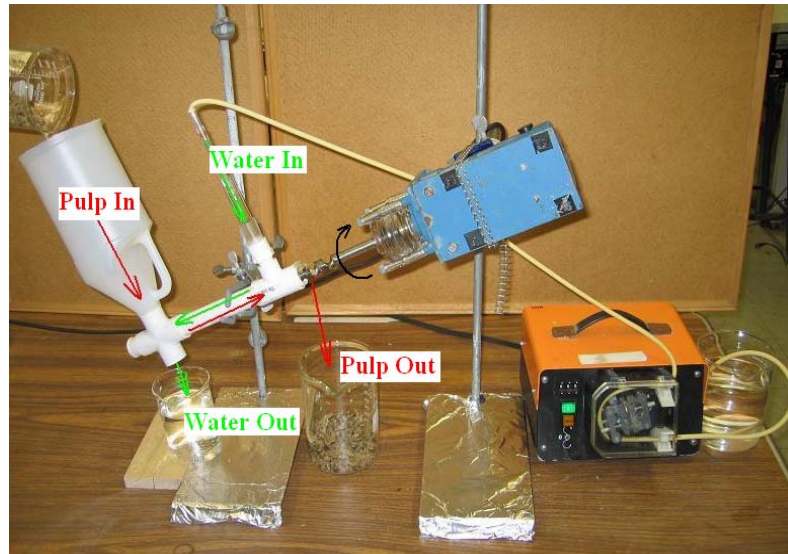


Fig. 7.3-3 Screw machine model

Two sets of experiments with different methanol concentrations in feed pulp were carried out. In the first experiment, the methanol concentration in feed pulp was 1%. In the second experiment, the methanol concentration in feed pulp was 5%. The average k value of two experiments was $0.017s^{-1}$.

7.4 Compare the k values from direct rinse and counter-current flow

Since the k value is an intrinsic property of pulp, it should be a constant number under different mass transfer conditions. The k value from direct rinse has exactly the

same meaning as that from counter-current flow, which can be proved by following derivation.

Considering one piece of beet pulp, whose volume is V_B and surface area is A_B , the mass transfer across the surface can be described with a mass transfer coefficient as following.

$$\frac{dM_B}{dt} = -k_0(C_B - C_W)A_B \quad (7.4-1)$$

Eq.(7.4-1) is same as Eq. (7.3-5). k_0 has the exactly same meaning in these two equations. Substitution of $dM = V_B dC_B$ into Eq. (7.4-1) yields

$$V_B \frac{dC_B}{dt} = -k_0(C_B - C_W)A_B \quad (7.4-2)$$

Rearrangement of Eq. (7.4-2) results the following expression:

$$\frac{dC_B}{dt} = -\left(\frac{A_B}{V_B} k_0\right)(C_B - C_W) \quad (7.4-3)$$

Compare of Eq. (7.2-1) and (7.4-3) yields the same result as the counter-current mass transfer, $k = \frac{A_B}{V_B} k_0$. Therefore, the average k value from direct rinse and from counter-

current flow, $0.015s^{-1}$ can be used for future design.

Chapter 8: Process Design and Economic Estimation

8.1 Introduction

A main task of the leader of a biochemical company is to show the investor the profitability. Although some essential data have been obtained, the project of biomethanol conversion from sugar beet pulp is still at its beginning and needs further financial support. Therefore, it is necessary to do the profitability analysis of investment.

Generally, pulp from sugar factory gets a temperature as high as about 60°C. The methanol production was hence designed at this temperature. The main reason was to use the heat in the pulp so that the reaction could be faster and the cost for energy in the process of methanol purification could be reduced.

To use the heat in pulp, the methanol production process should be combined to the process of sugar production. The flow sheet for sugar production is illustrated in Fig. 8.1-1. The methanol production process is added between the pulp press (point A) and pulp dryer (point B). The process of methanol production is schematically illustrated in Fig. 8.1-2.

From Fig. 8.1-2, the reactor, flash unit and distillation tower are the main equipment for the methanol production. The mixture of wet pulp, enzyme and water is fed into the reactor where the methoxyl group in pulp will be hydrolyzed by PME to produce methanol. The mixture after reaction is then pumped to a flash unit in which most of the methanol is vaporized together with water. The pulp from flash unit is then sent to a compressor. The vaporized methanol-water mixture is sent to the distillation tower where the desired purity of methanol is obtained.

In this chapter, the flow sheet of methanol conversion from sugar beet pulp was developed with the aid of CHEMCAD and the production process was simulated. The simulation data were from *American Crystal Sugar Company* (101 North Third St., Moorhead, MN-56560). The bioreactor and distillation tower in Fig. 8.1-2 were designed

either with the aid of computer or manually and the cost for the equipment and its operation energy was estimated. The cost for other equipment, such as pumps, compressors, heat exchangers, pipes, and valves, was not considered. Therefore, the economic estimation results show the minimum cost for a sugar factory to produce methanol. The actual cost for the equipment will be higher.

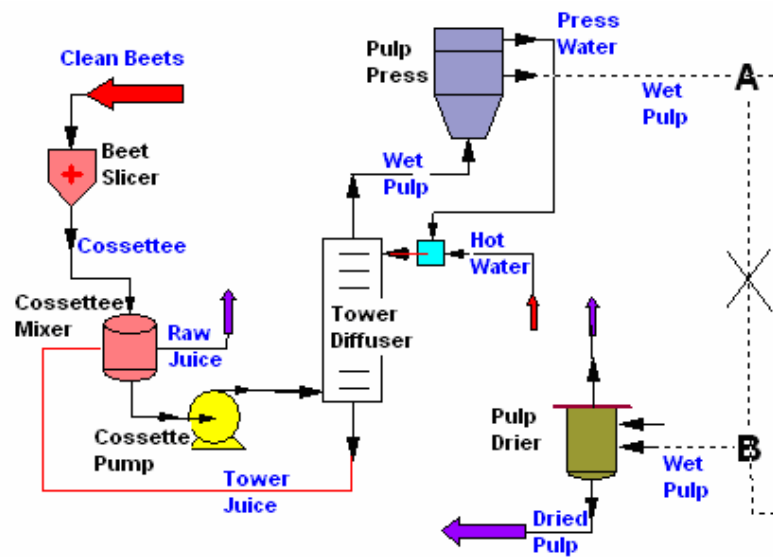


Fig. 8.1-1 Flow sheet of sugar production

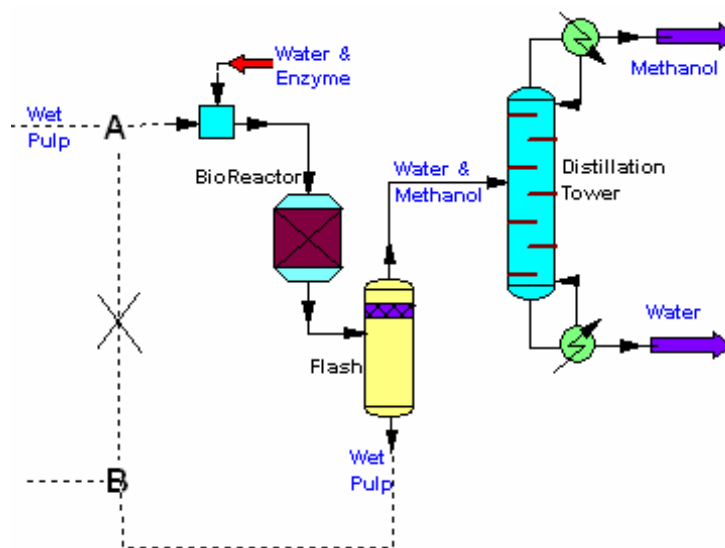


Fig. 8.1-2 Flow sheet of methanol production

8.2 Simulation of reactor

Most reactors can be classified as one or a combination of the following types: 1) Batch reactor-no material flowing into or out of the reactor; 2) Fed batch reactor-has material flowing into the reactor; 3) Continuous flow reactor-has material flowing into and out of the reactor. There are two sub-types of continuous flow reactors, the Continuous Stirred Tank Reactor (CSTR) and the Plug Flow Reactor (PFR). A CSTR typically is a big tank with continuous stirring. A PFR is much simpler. It can just be a pipe through which material flows. The mixing in CSTR is much better than that in PFR. Since the reactor will be connected to a distillation tower in my design and the reaction need stirring, only CSTR will be considered in the design.

8.2.1 Theoretical equations for the calculation of volume and residence time

The material balance equation is described as
[accumulation] = [in] -[out] +[generation] (8.2-1)

The material balance for reactor with the reactant A is

$$F_{A0} - F_A + G_A = \frac{dN_A}{dt} \quad (8.2-2)$$

Where F_{A0} is the inlet flow rate of species A, F_A the outlet flow rate of species A, G_A the generation rate of species A, N_A the total amount of species A in reactor. G_A can be expressed as $G_A = r_A \cdot V$, where V is volume of the reactor and r_A the reaction rate based on species A. G_A can be obtained by integrating the generation rate in the whole reactor, as expressed as Eq. (8.2-3), if r_A varies with position in a reactor:

$$G_A = \int_0^V r_A dV \quad (8.2-3)$$

Substituting Eq.(8.2-3) into the material balance equation above yields the generalized design equation for reactors:

$$F_{A0} - F_A + \int_0^V r_A dV = \frac{dN_A}{dt} \quad (8.2-4)$$

Since $F_{A0} - F_A = F_{A0} \cdot X_A$ where X_A is the fractional conversion, the equation above can be modified as

$$F_{A0} \cdot X_A + \int^V r_A dV = \frac{dN_A}{dt} \quad (8.2-5)$$

An important parameter for a continuous reactor is the residence time τ which means the average amount of time a discrete quantity of reagent spends inside the reactor. It is calculated from the volume of the reactor and the volumetric flow rate

$$\tau = \frac{V}{v} \quad (8.2-6)$$

For steady state CSTR, conditions will not change over time, that is, $\frac{dN_A}{dt} = 0$. If the

mixture is homogenous in the reactor, then

$$\int^V r_A dV = Vr_A \quad (8.2-7)$$

Eq.(8.2-5) can thus be simplified to Eq.(8.2-8)

$$F_{A0} \cdot X_A + r_A \cdot V = 0 \quad (8.2-8)$$

Since F_{A0} is equal to $C_{A0} \cdot v$, where C_{A0} is the initial concentration of A, the equation

above can be conformed to

$$C_{A0}v \cdot X_A + r_A \cdot V = 0 \quad (8.2-9)$$

From the equations above, the residence time and reactor volume can be obtained.

$$\tau = -\frac{C_{A0}X_A}{r_A} \quad (8.2-10)$$

$$V = \frac{F_{A0}X_A}{-r_A} = \frac{F_{A0} - F_A}{-r_A} \quad (8.2-11)$$

From Eq.(8.2-10) and (8.2-11), the value and residence time depend on the reaction rate. In my simulation, the actual data of reaction rate from Chapter 5 were used. From Fig.5.8-1, the reaction can be looked as a zero order reaction whose reaction rate is constant.

8.2.2 Cost estimation of CSTR

1. Simulation of reactor by CHEMCAD

The main purpose of the simulation is to obtain the feed to distillation tower so that the whole flow sheet can be run as a system. We can calculate the material balance;

define the fractional conversion, and so on in the simulation. However, the software can not do cost estimation for the reactor. Therefore, the cost estimation will be calculated manually.

To begin the CHEMCAD simulation, beet pulp and PME should be defined at first. The beet was named as 'Beet1' and 'Beet2' before and after reaction respectively. The PME was named as 'PME'. Essential data for the simulation were molecular weight, melting point, density and heat capacity. The melting points of beet and PME were both assumed to be 330°C. The actual value is not important if only they are in solid state during reaction. Since density and heat capacity for beet and PME are not available, they are assumed to have the same values as that of liquid water. This assumption should not cause significant error since the total mass of dry beet and enzyme is small compared with that of water. From Chapter 4, the molecular weight of PME was 36kDa. Sugar beet has quite complex compositions. However, only pectin is involved in the reaction. Therefore, the sugar beet was assumed to be composed of only one component, Beet 1 before reaction or Beet 2 after reaction. The molecular weight of Beet 1 is assumed to be similar to the molecular weight of commercial citrus pectin ranging from 20 to 400 kDa, with the majority of the molecules ranging from 50 to 150 kDa. According to this, molecular weight of 'Beet1' was assumed to be 200 kDa. Again, the actual value is not important.

The simulations were based on the experimental results in Chapter 5. Since the reaction catalyzed by CC7 at 45°C was the fastest, its results were chosen for the simulation. From Chapter 5, the dry weight of pulp was about 11% and the maximum amount of methanol production was 1.3% of the dry weight. During the reaction, 15g wet pulp and 10ml water was mixed. The enzyme was added as an average rate of 5.6 ml per hour or 56 units per hour (the activity of CC7 was 10 units per mL). The concentration of CC7 was 0.33mg/mL. To simplify the simulation, the volume of buffer was ignored. The

reaction mixture was assumed to be neutral. From all the assumptions and results above, the reaction equation can be described as following.

	PME			
	Beet1 + water		Beet2 + methanol	
Molecular weight:	200000	18	198863	32
Stoichiometric coefficient:	0.01231	1	0.01231	1
Material balance (mass):	2462	18	2448	32

Fig. 8.2-1 Reaction equation for reactor simulation

2. Reactor volume

Type, size, materials, and wall thickness are critical items in the design of reactor. The volume of reactor depends on the volumetric flow rate and residence time. The residence time in turn depends on the reaction rate.

Since the enzyme was still under developing and the residence time could still be reduced, I assumed the residence time was 4 h. Also, I assumed the total volumetric flow rate of water and enzyme solution was the same as that of wet pulp.

The data from *American Crystal Sugar Company* were adopted in simulation. This factory only ran six months in one year. When it was running, 2961 tons of wet beet pulps were produced per day or 123 m³ per hour (assume the density of pulp is same as that of water). The moisture content in wet pulps was 89%.

The total volume of reaction mixture was calculated by timing the total volumetric flow rate of feed with the residence time. The volume of the reactor was the sum of the volume of reaction mixture and the surge volume. The surge volume was assumed to be 20% of the reaction mixture.

Table 8.2-1 Volume calculation of the reactor

Items	Symbols and equations	Values
Flow rate of wet pulp (m ³ /h)	F _p	123
Total flow rate of water and enzyme solution(m ³ /h)	F _w	123
Total volumetric flow rate (m ³ /h)	F=F _p +F _w	246
Residence time (h)	τ	4
Volume of reaction mixturer (m ³)	V _r = F · τ	984
Surge volume (m ³)	V _s	197
Reactor volume (m ³)	V = V _r + V _s	1181

Note: the bold numbers were the numbers than can be initialized depending on the actual condition.

3. Cost estimation of reactor

The reactor can be designed as one reactor or a number of connected reactors. A number of connected reactors are sometimes more economical than a single reactor for achieving the same conversion especially when designing a new process using existing equipment. Here, I will only consider a single reactor.

The cost for a bioreactor is very expensive. The purchased cost of a 10m³ jacketed and stirred reactor made of carbon steel is \$42,000 in January 2002 (Peters, Timmerhaus, & West, 2003). Since the reaction of producing methanol from beet pulp is rather robust and does not generate heat, a mixing tank can be used as the reactor and its cost can be reduced in half.

From last section, the volume of the reactor was 1181m³. From Fig. 12-52 in the book of *Plant Design and Economics for Chemical Engineers* (Peters, Timmerhaus, and West, 2003), the purchased cost of a 1181m³ mixing tank made of carbon steel is about \$420,000. This value is based on the data in 2002. The present purchased cost can be obtained by the following equation.

$$Present\ cost = original\ cost \times \left(\frac{index\ value\ at\ present}{index\ value\ at\ time\ original\ cost\ was\ obtained} \right)$$

The *chemical engineering plant cost indexes* for January 2002 and October 2005 are 390 (Peters, Timmerhaus, and West, 2003) and 473 (*Chemical Engineering*) respectively. The nonmanufacturing capital such as building, service, and land is typically 40% of the purchased cost. The fixed capital includes the purchased cost and

the nonmanufacturing capital. The working capital, which is necessary for the operation of the plant, was ignored. The life of the reactor was assumed to be 20 years. If there is no heat input or removal, the main power consumption in the reactor is from the agitator whose power input is between 0.1kW/m^3 and 0.3kW/m^3 (the chemical engineers' resource page, 2002). With the assumption that the power input is 0.2kW/m^3 and the electric rate is \$0.01 per kwh, \$11.4 per hour is needed to make the agitator run. The energy cost for six months is approximate \$49,000. From all the information above, the cost for the reactor is summarized in following table.

Table 8.2-2 Cost estimation of the reactor

Purchased cost in Jan. 2002, \$1000	420
Index Value in Jan. 2002	390
Index Value in Oct. 2005	473
Purchased cost in Oct. 2005, \$1000	509
Nonmanufacturing Capital, \$1000	204
Fixed capitals, \$1000	713
Annual cost for the reactor depreciation, \$1000	36
Annual cost for the energy, \$1000	49
Total annual cost, \$1000	85

8.3 Simulation of flash

Flash unit in the flow sheet is to separate the liquid from solid. In a factory, this unit may not be necessary. A centrifuge or a press can be used for this purpose. Since the factory has press ready to use, the cost will not be estimated. The simulation of flash together with the simulation of reactor is to obtain the composition of the feed for distillation tower. The flow sheet is shown in Fig.8.3-1. The parameters for simulation are listed in Table 8.3-1. The compositions of the streams are shown in Table 8.3-2.

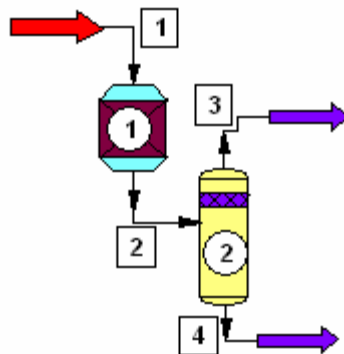


Fig. 8.3-1 Simulation of flash after reactor

Table 8.3-1 Parameters during simulation of flash and reactor

	Parameters	Settings
Reactor	Number of reactions	1
	Reactor Model	General equilibrium reactor
	Thermal Mode	Isothermal at 60°C
	Specify calculation mode	Reaction conversion (Parallel reaction)
	Base component	Beet1
	Fractional conversion	1
Flash	Flash Mode	Specify V/F and T; calculate P and Heat
	Mole Vapor Fraction	0.5
	Temperature	60°C

Table 8.3-2 Compositions of streams in simulation of flash and reactor

	Stream 1	Stream 2	Stream 3	Stream 4
Beet 1 (kg/min)	226.0	0.0	0.0	0.0
Water (kg/min)	3883.0	3881.3	1940.2	1941.2
Beet2 (kg/min)	0.0	224.7	0.0	224.7
Methanol (kg/min)	0.0	2.9	2.4	0.6
PME (kg/min)	3.5	3.5	0.0	3.5

From Table 8.3-2, the dry weight of beet pulp in Stream 4 was 10%. By material balance from Stream 2, 3, and 4, 83% of the total methanol was collected in Stream 3 which would be sent to the distillation tower.

8.4 Cost estimation of distillation tower

There are several models to simulate the distillation process in CHEMCAD. For the simulation of a simple distillation column with one input and two product streams, the

shortcut model is a good choice. In this section, the distillation was simulated with a shortcut to find out the relations among reflux ratio, heat removed in condenser, and heat added in reboiler. Then, the number of trays, height of tower, and diameter of tower were calculated by hand base on the simulation results. Finally, the optimum reflux ratio was found and the total cost for the tower was estimated.

8.4.1 Simulation of distillation by a shortcut

The flow sheet of simulation is shown in Fig. 8.4-1. In the simulation, I assumed the methanol split was 90% and the methanol concentration in distillate was 95%. The water split, $6e-5$, was calculated with material balance equation. The composition of feed was same as the composition in stream 3 in the flash simulation. The parameters for simulation are shown in Table 8.4-1. The compositions of streams after simulation are shown in Table 8.4-2.

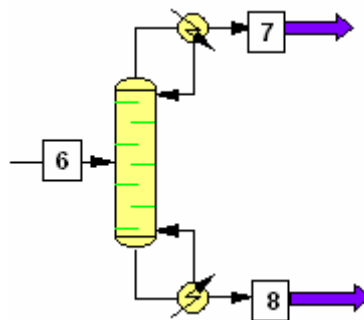


Fig. 8.4-1 Simulation of distillation tower

Table 8.4-1 Parameters during simulation of distillation tower

	Parameters	Settings
Stream 6	Temperature	60°C
	Pressure	1 atm
	Water Flow	1940.2kg/min
	Methanol Flow	2.4kg/min
Shortcut	Mode	2 Design
	Condenser Type	Partial
	Column Pressure	1 atm

	Column Pressure drop	0.5 atm
	Light Key Component	Methanol
	Light Key Split	0.95
	Heavy Key Component	Water
	Heavy Key Split	2.75e-5

Table 8.4-2 Compositions of streams in simulation of distillation tower

	Stream 6	Stream 7	Stream 8
Water (kg/min)	1940.2	0.1	1940.1
Methanol (kg/min)	2.4	2.1	0.2

The *case study* function in a shortcut was used to find out the relations among reflux ratio, number of stages, feed stage, heat removal in condenser, and heat input in reboiler. The results are shown in Table 8.4-3. The same results are also shown in Fig.8.4-2 and Fig.8.4-3.

Table 8.4-3 Compositions of streams in simulation of distillation tower

R/Rmin	Reflux ratio	No. of stages	Feed stage	$Q_{\text{condenser}}/\text{MJ}\cdot\text{min}^{-1}$	$Q_{\text{reboiler}}/\text{MJ}\cdot\text{min}^{-1}$
10.69	4111	9.6	7.8	11940	12360
6.23	2397	10.0	8.1	6958	7385
3.26	1254	10.9	8.8	3640	4065
3.10	1193	11.0	8.9	3462	3890
2.87	1104	11.2	9.1	3206	3631
2.64	1016	11.5	9.3	2949	3374
2.52	968	11.6	9.4	2810	3236
2.41	927	11.8	9.5	2692	3118
2.18	839	12.2	9.8	2435	2861
1.95	750	12.7	10.3	2179	2604
1.77	682	13.4	10.8	1980	2406
1.72	662	13.6	10.9	1922	2348
1.49	573	15.0	12.1	1664	2091
1.26	485	17.8	14.3	1407	1834
1.03	396	27.3	22.0	1151	1577
1.00	386	57.4	46.3	1121	1547
0.95	366	203.3	164.0	1062	1488

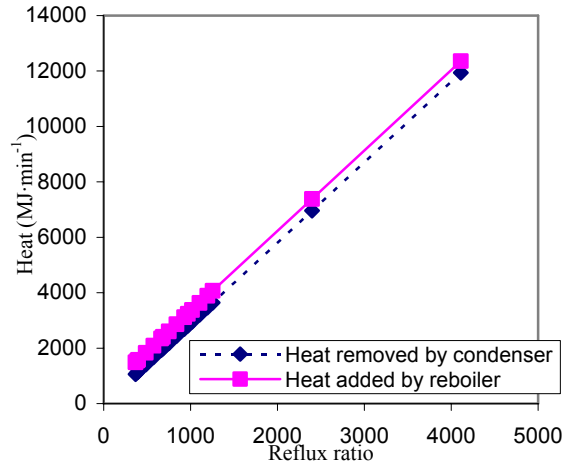


Fig. 8.4-2 Heat exchange as a function of reflux ratio

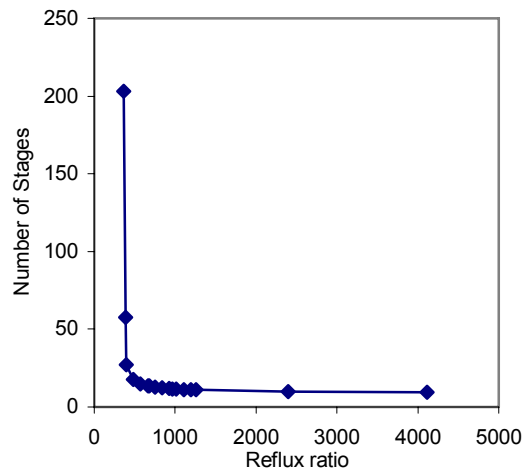


Fig. 8.4-3 Number of stages as a function of reflux ratio

From above figures, energy consumption in both condenser and reboiler increased linearly with the increase of reflux ratio. On the other hand, the number of stages decreased sharply when the reflux ratio increased, especially from 366 to 1254. The optimum reflux ratio occurs where the sum of fixed charges and operating cost is a minimum.

8.4.2 Tower height and diameter

Tower diameter

To calculate the diameter of a tower, the cross sectional area should be calculated at first with the following equation

$$A = \frac{v}{0.8U_{nf}\varepsilon\rho_g} \quad (8.4-1)$$

where v is the gas mass flow rate, U_{nf} the flooding velocity, ε the fraction of the area available for vapor flow (about 0.6 for bubble cap trays, 0.75 for sieve trays), and ρ_g the gas mass density. The number 0.8 means the column runs at 80% of the flooding velocity.

U_{nf} is given by

$$U_{nf} = C_{sb,f} \left(\frac{\rho_l - \rho_g}{\rho_g} \right)^{0.5} \left(\frac{20}{\sigma} \right)^{0.2} \quad (8.4-2)$$

where $C_{sb,f}$ is the Souders and Brown factor at flood conditions which can be obtained from handbook (Biegler, Grossmann, & Westerberg, 1997), σ the liquid surface tension, ρ_l the liquid mass density.

The cross sectional area above the feed tray and below the feed tray is usually different. The bigger value should be used for the design. Assume the sieve tray was used. The calculated cross sectional area was 10.1m² and the diameter of tower was 3.2m.

Tower height

The tower height depends on the number of trays, which is the quotient of the stage number over the efficiency factor. The optimum stage number can be obtained from Table 8.4-3 where the reflux ratio is also an optimum. In my calculation, the efficiency factor was assumed to be 0.8. The tray spacing was assumed to be 0.61m and the additional space for tower was 4m. The heights of towers with different stages as shown in Table 8.4-3 were then calculated. The results are shown in Table 8.4-4.

8.4.3 The optimum reflux ratio and annual cost of distillation tower

The costs of towers were calculated with the following equation

$$\text{BMC} = \text{BC} \cdot (\text{MPF} + \text{MF} - 1) \cdot \text{UF} \quad (8.4-3)$$

where BMC was the updated bare module cost, BC the base cost, MPF the material and pressure factor, MF the module factor, and UF the update factor. The basic costs were calculated with equation

$$\text{BC} = C_0 \left(\frac{L}{L_0}\right)^\alpha \left(\frac{D}{D_0}\right)^\beta \quad (8.4-4)$$

where C_0 was nominal cost, L the actual tower height, L_0 the nominal tower height, D the actual diameter, D_0 the nominal diameter, α and β the exponents. D and L came from the design. The update factor was found from *Chemical Engineering*. All other parameters in Eq.(8.4-3) and (8.4-4) were from *Systematic Methods of Chemical Process Design* (Biegler, Grossmann, and Westerberg, 1997).

The Fixed capital included the bare module cost and the nonmanufacturing capital such as building, service, and land which is typically 40% of the bare module cost. The working capital, which is necessary for the operation of the plant, was ignored. The annual cost for the tower depreciation was calculated with the assumption that the life of the distillation tower was 20 years.

The energy cost in distillation tower mainly came from the condenser and reboiler. Since *American Crystal Sugar Company* locates in North America where the cold water was available at almost zero cost, only the energy cost for the reboiler was considered. With the assumption that the electric rate was \$0.01 per kwhr, the energy costs for the reboiler were calculated base on Table 8.4-3.

The relations among reflux ratio, tray number, tower height, annual fixed charge on tower, the annual energy cost, and annual total cost are shown in Table 8.4-4. Fig. 8.4-4 is from Table 8.4-4. The results show that the minimum total cost per year occurs at

reflux ratio of 396. Thus, the optimum reflux ratio is 396 where the annual cost is \$1,175,000.

Table 8.4-4 Annual cost of distillation tower

Reflux ratio	No. of trays	Tower Height, m	Annual fixed charge on tower, \$1000	Annual cost of energy, \$1000	Annual cost, \$1000
573	19	15.4	39	1506	1533
485	23	17.6	43	1320	1351
396	35	24.8	56	1135	1175
386	72	47.8	92	1114	1179
366	255	159.0	237	1071	1241

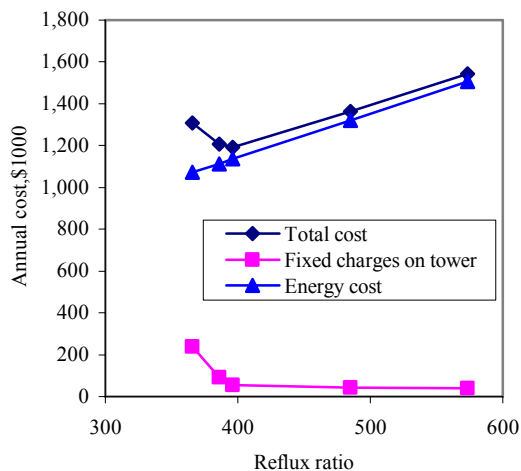


Fig. 8.4-4 Annual cost as a function of reflux ratio

8.5 Conclusions and discussion

If 2961 tons of wet beet pulps are produced per day and the factory only run 6 months per year. Then 5.86×10^5 kg (2.0×10^5 gallons) of methanol can be produced (assume 100% of the methanol is obtained) per year. Today's market price for methanol is around \$1.1 /gal(ICIS, <http://www.icislor.com>). Then \$200,000 can be earned per year.

The annual costs for the depreciation of a reactor and the energy cost by the reactor are \$85,000 per year. The annual costs for the depreciation of a distillation tower

and the energy cost by the distillation tower are **\$1,175,000** per year. Therefore, the total cost by the reactor and distillation tower is **\$1,260,000** per year. Besides above cost, the cost for water and enzyme should also be considered. Since new enzyme is still being developed, the cost for enzyme is ignored here.

From the cost estimation, producing methanol from sugar beet can not earn money at this time. However, it could be profitable in the future if the methanol price increases more than seven times or the cost decreases sharply.

The evaluation results show that the cost mainly comes from the distillation tower which is very high at this time. However, the cost can be decrease on a large scale when a new separation method is available. One prospective method is the pervaporation by membrane. If an effective hydrophobic membrane that only allows methanol in the methanol-water mixture pass through can be developed in the future, the separation will be more economic.

REFERENCES

- Anthon, G.E., & Barrett, D.M. (2004). Comparison of three colorimetric reagents in the determination of methanol with alcohol oxidase. Application to the assay of pectin methylesterase. *Journal of Agriculture and Food Chemistry*, 52, 3749-3753.
- Babel, U.B.F., & Reinbeck, H. (1964). Thin-layer studies of the decomposition of lignified tissue in soil. *Proc. Intern. Working-Meeting Soil Micromorphol.*, 2nd, Arnhem, Neth.
- Bateman D.F. (1963). Pectolytic activities of culture filtrates of *Rhizoctonia solani* and extracts of *Rhizoctonia*-infected tissues of bean. *Phytopathology*, 53, 197-&.
- Biegler, L.T., Grossmann, I.E., & Westerberg, A.W. (1997). *Systematic Methods of Chemical Process Design*. NJ: Prentice-Hall.
- Boyle, G. (2004). *Renewable Energy*. Oxford University Press in association with The Open University.
- Brummell, D.A., Cin, V.D., Crisosto, C.H., & Labavitch, J.M. (2004). Cell wall metabolism during maturation, ripening and senescence of peach fruit. *Journal of Experimental Botany*, 55, 2029-2039.
- Collins, J.L. (1970). Pectin methyl esterase activity in southern peas (*Vigna sinensis*). *Journal of Food Science*, 35, 1-4.
- Deen, W.M. (1998). *Analysis of Transport Phenomena*. New York: New York 10016.
- Endo, A. (1964). Studies on pectolytic enzymes of molds Part XII. Purification and properties of pectinesterase. *Agricultural and Biological Chemistry*, 28, 757-764.
- Fares, K., Renard, C.M.G.C., R'zina, Q., & Thibault, J.F. (2001). Extraction and composition of pectins and hemicelluloses of cell walls of sugar beet roots grown in Morocco. *International Journal of Food Science and Technology*, 36, 35-46.
- Fish, V.B., & Dustman, R.B. (1945). The enzyme activities of pectinol A on pectin and other substances. *Journal of the American Chemical Society*, 67, 1155-1157.
- Hagerman, A.E. & Austin, P.J. (1986). Continuous spectrophotometric assay for plant pectin methyl esterase. *Journal of Agriculture and Food Chemistry*, 34, 440-444.
- Hasunuma, T., Fukusaki E. & Kobayashi A. (2003). Methanol production is enhanced by expression of an *Aspergillus niger* pectin methylesterase in tobacco cells. *Journal of Biotechnology*, 106, 45-52.
- Hildebrand, F.B.(1976). *Advanced Calculus for Applications*. Englewood Cliffs, NJ: Prentice-Hall.

- Hou, W.C., Chang, W.H., & Jiang, C.M. (1999). Quantitative distinction of carboxyl group distributions in pectins with ruthenium red. *Botanical Bulletin of Academia Sinica*, 40, 115-119.
- Huisman, M.M.H., Oosterveld, A., & Schols, H.A. (2004). Fast determination of the degree of methyl esterification of pectins by head-space GC. *Food Hydrocolloids*, 18, 665-668.
- Hwang, S.T. (2004). Nonequilibrium thermodynamics of membrane transport. *AICHE Journal*, 50, 862-870.
- Iwai, H., Kikuchi, A., Kobayashi, T., & Kamada, H. (1999). High levels of non-methylesterified pectins and low levels of peripherally located pectins in loosely attached non-embryogenic callus of carrot. *Plant Cell Reports*, 18, 561-566.
- Jiang, C.M., Hou, W.C., & Chang, W.H. (1998). A rapid method for pectinesterase activity staining. *Shipin Kexue*, 25, 46-58.
- Kimura, H., Uchino, F., & Mizushima, S. (1973). Purification and properties of pectinesterase from *Acrocylindrium*. *Agricultural and Biological Chemistry*, 37, 1209-1210.
- Kita, H., Inoue, T., Asamura, H., Tanaka, K., & Okamoto, K. (1997). NaY zeolite membrane for the pervaporation separation of methanol-methyl *tert*-butyl ether mixtures. *Chemical Communications*, 1, 45-46.
- Klavons, J.A., & Bennett, R.D. (1986). Determination of methanol using alcohol oxidase and its application to methyl ester content of pectins. *Journal of Agriculture and Food Chemistry*, 34, 597-599.
- Körner, B., Zimmermann, G., & Berk, Z. (1980). Orange pectinesterase: purification, properties, and effect on cloud stability. *Journal of Food Science*, 45, 1203-1206.
- Kravtchenko, T.P., Voragen, A.G.J., & Pilnik, W. (1992). Analytical comparison of three industrial pectin preparations. *Carbohydrate Polymers*, 18, 17-25.
- Kuo, C.C., Wen, Y.H., Huang, C.M., Wu, H.L., & Wu, S.S. (2002). A removable derivatization HPLC for analysis of methanol in Chinese liquor medicine. *Journal of Food and Drug Analysis*, 10, 101-106.
- Lee, M., & Macmillan, J.D. (1968). Mode of action of pectic enzymes. I. Purification and certain properties of tomato pectinesterase. *Biochemistry*, 7, 4005-4010.

- Levigne, S., Ralet, M.C., & Thibault, J.F.(2002). Characterization of pectins extracted from fresh sugar beet under different conditions using an experimental design. *Carbohydrate Polymers*, 49, 145-153.
- Lichstein, H.C., & Soule, M.H. (1944). Studies on the effect of sodium azide on microbic growth and respiration. I. The action of sodium azide on microbic growth. *Journal of Bacteriology*, 47, 221-230.
- Lieberman, B. (2005). America Is Not Facing an Unavoidable Energy Shortage. Available at http://www.cei.org/gencon/019_04373.cfm [accessed September 26, 2005].
- Lineweaver, H., & Ballou, G.A. (1945). The effect of cations on the activity of Alfalfa pectinesterase(pectase). *Archives of Biochemistry*, 6, 373-387.
- MacDonnell, L.R., Jansen, E.F., & Lineweaver, H. (1945). The properties of orange pectinesterase. *Archives of Biochemistry*, 6, 389-401.
- Manabe, M. (1973). Purification and properties of Citrus natsudaikai pectinesterase. *Agricultural and Biological Chemistry*, 37, 1487-1491.
- Mangos, T.J., & Haas, M.J. (1997). A spectrophotometric assay for the enzymatic demethoxylation of pectins and the determination of pectinesterase activity. *Analytical Biochemistry*, 244, 357-366.
- Maus, E., & Brüscke, H.E.A. (2002). Separation of methanol from methylesters by vapour permeation: experiences of industrial applications. *Desalination*, 148, 315-319.
- Merrill, R.C., & Weeks, M. (1945). The thermal degradation of pectin. *Journal of the American Chemical Society*, 67, 2244-2247.
- Molina, J.M., Vatai, G., & Bekassy-Molnar, E. (2002). Comparison of pervaporation of different alcohols from water on CMG-OM-010 and 1060-SULZER membranes. *Desalination*, 149, 89-94.
- Nakagawa, H., Yanagawa, Y., & Takehana, H. (1970). Studies on the pectolytic enzyme. Part V. Some properties of the purified tomato pectinesterase. *Agricultural and Biological Chemistry*, 34, 998-1003.
- Ohlström, M., Mäkinen, T., Laurikko, J., & Pipatti, R. (2001). New concepts for biofuels in transportation. Biomass-based methanol production and reduced emissions in advanced vehicles. VTT Research Notes 2074.
- Ovodova, R.G., Bushneva, O.A. & Shashkov, A.S. et al. (2005). Structure studies on pectin from marsh cinquefoil *Comarum palustre* L. *Biochemistry-Moscow*, 70, 867-877.

- Peters, M.S., Timmerhaus, K.D. & West, R.E. (2003). *Plant Design and Economics for Chemical Engineers*. New York: McGraw-Hill.
- Pitkänen, K., Heikinheima, R., & Pakkanen, R. (1992). Purification and characterization of *Erwinia chrysanthemi* B374 pectin methylesterase produced by *Bacillus subtilis*. *Enzyme and Microbial Technology*, 14, 832-836.
- Plastow, G.S. (1988). Molecular cloning and nucleotide sequence of the pectin methyl esterase gene of *Erwinia chrysanthemi* B374. *Molecular Microbiology*, 2, 247-254.
- Rombouts, F.M., & Thibault, J.F. (1986). Sugar beet pectins: chemical structure and gelation through oxidative coupling. *Chemistry and Function of Pectins*. Washington, DC: American Chemical Society.
- Rombouts, F.M., & Thibault, J.F. (1986). Feruloylated pectic substances from sugar-beet pulp. *Carbohydrate research*, 154, 177-187.
- Rose, R. (2003). Fuel Cells and Hydrogen: The Path Forward. Available at <http://www.methanol.org/pdfFrame.cfm?pdf=PathForward.pdf> [accessed September 26, 2005].
- Sajjaanantakul, T., Van Buren, J. P., & Downing, D. L. (1993). Effect of cations on heat degradation of chelator-soluble carrot pectin. *Carbohydrate Polymers*, 20, 207-214.
- Sajjaanantakul, T. (1989). A study on heat degradation of carrot chelator-soluble pectin in a model system. *Dissertation abstracts international B 1990*, 50, 3782-3783.
- Sajjaanantakul, T., Van Buren, J. P., & Downing, D. L. (1989). Effect of methyl ester content on heat degradation of chelator-soluble carrot pectin. *Journal of Food Science*, 54, 1272-1277.
- Savary, B.J., & Nunez, A. (2003). Gas chromatography- mass spectrometry method for determining the methanol and acetic acid contents of pectin using headspace solid-phase microextraction and stable isotope dilution. *Journal of Chromatography A*, 1017, 151-159
- Shuler, M.L., Kargi, K. (2002). *Bioprocess Engineering*. Upper Saddle River, NJ: Prentice Hall PTR.
- Slezárik, A., & Rexová, L'. (1967). Characterization of extracellular pectolytic enzymes of *Monilia Laxa*. *Biologia (Bratislava)*, 22, 407-13.
- Stephen, A.M. (1995). *Food Polysaccharides and Their Applications*. New York: Marcel Dekker, Inc.

Sterling, C. (1970). Crystal structure of ruthenium red and stereochemistry of its pectic stain. *American Journal of Botany*, 57, 172-175.

The chemical engineers' resource page. (2002). Available at <http://www.cheresources.com/exprules.shtml> [accessed March 17, 2006].

Thibault, J.F. (1988). Characterization and oxidative crosslinking of sugar-beet pectins extracted from cossettes and pulps under different conditions. *Carbohydrate Polymers*, 8, 209-223.

Tipson, R.S., & Horton, D. (1976). *Advances in Carbohydrate Chemistry and Biochemistry*. New York: Academic Press, Inc.

Truskey, G.A., Yuan, F., & Katz, D.F. (2003). *Transport Phenomena in Biological Systems*. Upper Saddle River, New Jersey: Pearson Prentice Hall.

Twidell, J., & Weir, A. (1986). *Renewable Energy Resources*. London: E & FN Spon.

Ujejski, L. (1957). The detection and separation of pectic substances by paper chromatography and paper electrophoresis. *The Ohio Journal of Science*, 57, 212.

U.S. Department of Energy. (2005). Available at <http://www.eere.energy.gov/biomass/> [accessed September 26, 2005].

U.S. Department of Energy. (2005). Available at <http://www.eere.energy.gov/hydrogenandfuelcells/fuelcells/basics.html> [accessed September 26, 2005].

Van Buren, J.P., Moyer, J.C., & Robinson, W.B. (1962). Pectin methylesterase in snap beans. *Journal of Food Science*, 27, 291-294.

Van Den Berg, F.W.J., Van Osenbruggen, W.A., & Smilde, A.K. (1997). Process analytical chemistry in the distillation industry using near-infrared spectroscopy. *Process Control and Quality*, 9, 51-57.

Veen, H.M., & Delft, Y.C. (2004). Methanol separation from organics by pervaporation with modified silica membranes. *The Eighth International Conference on Inorganic Membranes*. Cincinnati, Ohio, USA July 18-22, 2004 ICIM8 2004

Voragen, A.G.J., Schols, H.A., & Pilnik, W. (1986). Determination of the degree of methylation and acetylation of pectins by HPLC. *Food Hydrocolloids*, 1, 65-70.

Wang, M.L., Wang, J.T. & Choong, Y.M. (2004). Simultaneous quantification of methanol and ethanol in alcoholic beverage using a rapid gas chromatographic method coupling with dual internal standards. *Food Chemistry*, 86, 609-615.

Wang, S.C., & Pinckard, J.A. (1971). Pectic enzymes produced by *diplodia gossypina* in vitro and in infected cotton bolls. *Phytopathology*, 61, 1118-1124.

Weiss, W. (2001). Current development of the market and the potential of solar thermal systems in the medium-term, Arbeitsgemeinschaft Erneuerbare Energie, <http://www.aee.at/verz/english/therm11e.html> [accessed 14 March 2003].

Wiens, B. (2005). The Future of Fuel Cells. Available at <http://www.benwiens.com/energy4.html#energy1.14> [accessed September 26, 2005].

Won, W., Feng, X., & Lawless, D. (2003). Separation of dimethyl carbonate/methanol/water mixtures by pervaporation using crosslinked chitosan membranes. *Separation and purification Technology*, 31, 129-140.

Wood, P.J. & Siddiqui, I.R. (1971). Determination of Methanol and Its Application to Measurement of Pectin Ester Content and Pectin Methyl Esterase Activity. *Analytical Biochemistry*, 39, 418-428.

Zhang, Q., Zheng, J., Shevade, A., Zhang, L., Gehrke, S.H., Heffelfinger, G.S., Jiang, S. (2002). Transport diffusion of liquid water and methanol through membranes. *Journal of Chemical Physics*, 117, 808-818.